Wright State University

CORE Scholar

2021

ALS-induced Excitability Changes in Individual Motorneurons and the Spinal Motorneuron Network in SOD1-G93A Mice at Symptom Onset

Christiana S.I. Draper
Wright State University

Follow this and additional works at: https://corescholar.libraries.wright.edu/etd_all

Part of the Biomedical Engineering and Bioengineering Commons

ALS-INDUCED EXCITABILITY CHANGES IN INDIVIDUAL MOTORNEURONS AND THE SPINAL MOTORNEURON NETWORK IN SOD1-G93A MICE AT SYMPTOM ONSET

A dissertation submitted in partial fulfillment of the
requirements for the degree of
Doctor of Philosophy

by

CHRISTIANA S. I. DRAPER

B.A., Spelman College, 2015

2021

Wright State University

WRIGHT STATE UNIVERSITY

GRADUATE SCHOOL

April 26, 2021

I HEREBY RECOMMEND THAT THE DISSERTATION PREPARED UNDER MY SUPERVISION BY Christiana S. I. Draper ENTITLED ALS-induced Excitability Changes in Individual Motorneurons and the Spinal Motorneuron Network in SOD1-G93A Mice at Symptom Onset BE ACCEPTED IN PARTIAL FULFILLMENT OF THE REQUIREMENTS FOR THE DEGREE OF Doctor of Philosophy.

_____
Sherif M. Elbasiouny, Ph.D.
Dissertation Director

_____
David R. Ladle, Ph.D.
Director, BMS Ph.D. Program

_____
Barry Milligan, Ph.D.
Vice Provost for Academic Affairs
Dean of the Graduate School

Committee on Final Examination:

_____
Sherif M. Elbasiouny, Ph.D.

_____
Khalid M. Elased, Pharm.D., Ph.D.

_____
Lynn K. Hartzler, Ph.D.

_____
Mark M. Rich, M.D., Ph.D.

_____
Keiichiro Susuki, M.D., Ph.D.

ABSTRACT

Draper, Christiana S. I. Ph.D., Biomedical Sciences Ph.D. Program, Wright State University, 2021. ALS-induced Excitability Changes in Individual Motorneurons and the Spinal Motorneuron Network in SOD1-G93A Mice at Symptom Onset.

Amyotrophic lateral sclerosis (ALS) is the most common motorneuron (MN) disease in adulthood. ALS is hallmarked by the progressive loss of MNs in the brain, brainstem, and spinal cord. Many hypotheses to explain the pathogenesis of ALS have been explored, but the exact mechanisms underlying the development of this disease remain unknown. However, abnormalities in MN excitability and glutamate excitotoxicity are the most widely studied. For decades, researchers have examined MN excitability in ALS, but the current literature is inconsistent, showing evidence of hyperexcitability, hypoexcitability, or no change in excitability of MNs in ALS. Many of these studies also focus solely on the excitability of individual MNs, rather than the spinal MN network, whose output collectively drives muscle activity. Using electrophysiology intracellular and ventral root recordings in SOD1-G93A$^{\text{High-Copy}}$ (SOD) mice, the standard rodent model of ALS, at symptom onset, we demonstrate evidence of both hypo- and hyperexcitability in ALS, whereby disease mechanisms change MN excitability in one direction and compensatory mechanisms alter MN excitability in the opposite direction. Additionally, we show evidence of a novel mechanism contributing to the development of motor dysfunction in ALS at symptom onset, impaired sensorimotor

integration.

We also studied the effects of a novel treatment for ALS on MN excitability. In recent years, small-conductance calcium-activated potassium (SK) channels have been implicated in the pathogenesis of ALS. In MNs, these channels mediate the afterhyperpolarization (AHP) and synaptic transmission and plasticity and subsequently regulate MN excitability at the individual and network levels. In SOD mice, these channels are significantly reduced throughout disease progression and early treatment with an SK channel activator, CyPPA, restores these deficits. Early treatment with CyPPA also prolongs the survival and motor function of SOD mice. Our results demonstrate that the long-term therapeutic benefits of CyPPA in SOD mice are not due to alterations in MN excitability. SK channels are also implicated in neuroinflammation and microglia activation, mitochondrial dysfunction, and many other putative mechanisms related to ALS. Thus, deficits in one of these alternative molecular pathways is likely restored with early CyPPA treatment in SOD mice.

TABLE OF CONTENTS

LIST OF FIGURES

vii

LIST OF TABLES

LIST OF ABBREVIATIONS

ALS	Amyotrophic lateral sclerosis
MN	Motorneuron
SOD mice	SOD1-G93A$^{\text{High-Copy}}$ mice
SK channel	Small-conductance calcium-activated potassium channel
CyPPA	SK channel activator
G_{SK} density	SK channel conductance
AHP	Afterhyperpolarization
F-type MNs	Fast-type motorneurons
S-type MNs	Slow-type motorneurons
sALS	Sporadic amyotrophic lateral sclerosis
fALS	Familial amyotrophic lateral sclerosis
SOD1	Superoxide dismutase 1
TDP-43	TAR-DNA binding protein 43
FUS	Fused in sarcoma
C9ORF72	Chromosome 9 open reading frame 72
FDA	Food and Drug Administration
MOA	Mechanism of action
CSF	Cerebrospinal fluid
AP	Action potential
NAPIC	Voltage-gated sodium persistent inward current
CAPIC	Voltage-gated calcium persistent inward current
P	Postnatal day
sSTD	System short-term depression
sSTF	System short-term facilitation
mAHP	medium afterhyperpolarization
IK channel	Intermediate-conductance calcium-activated potassium channel

DA	Dopaminergic
SNc	Substantia nigra pars compacta
ADHD	Attention-deficit hyperactivity disorder
MITF	Microphthalmia-associated transcription factor
WT	Wild-type
WSU	Wright State University
IP	Intraperitoneal
mACSF	Modified artificial cerebrospinal fluid
nACSF	Normal artificial cerebrospinal fluid
DCC	Discontinuous current clamp
RMP	Resting membrane potential
R_{in}	Input resistance
G_{in}	Input conductance
Tau	Time constant
I_{SK}	SK channel current amplitude
ISI	Interspike interval
I_{on}	Current level at firing onset
I_{off}	Current level at firing cessation
deltaI	I_{off} - I_{on}
F-I	Frequency-current
$F-I_{Asc}$	The ascending slope of the F-I relationship
$F-I_{Desc}$	The descending slope of the F-I relationship
CoAP	Compound action potential
S	Sensory input
M	Descending motor input
S&M	Simultaneous stimulation of sensory and descending motor inputs
S+M	Linear summation of the individual sensory and descending motor inputs

ACKNOWLEDGEMENTS

First and foremost, I want to give praise and honor to God. Without his grace and favor, I would not have been able to continue this challenging but worthwhile Ph.D. journey.

I would also like to thank the present and past faculty and staff of the Biomedical Sciences (BMS) Ph.D. department. To the former director, Dr. Mill Miller, thank you for guiding me into and through the program. Without your help, I would not have been accepted into the BMS Ph.D. program. To the current director, Dr. David Ladle, thank you for continuing to support me throughout this last but most challenging year. To Karen Luchin, thank you for all the work that you do behind the scenes, most departments don't have a gem like you.

To my dissertation committee, thank you for your dedication, time, and mentorship throughout this process. You all have continued to encourage, teach, and show up for me at every opportunity. I would like to express additional gratitude to my BMS program representative, Dr. Mark Rich. I remember being in Medical Neuroscience during my 2nd year of medical school and I would have never imagined picking you to be on my committee, but in hindsight, it is one of the best decisions I made. Despite your busy schedule and full roster of students, you always came by during my long and extensive experiments to encourage and support me. For every grant submission, you were willing to serve and help out in any capacity and most importantly, throughout this

last year, you made sure I had everything I needed to graduate and complete my dissertation. From consistent check in phone calls and emails to sharing your wisdom and experience, you have done it all.

To all current and former members of the Neuro-Engineering, Rehabilitation, and Degeneration (NERD) lab including Teresa Garrett, Mohamed Mousa, Maura Curran, Dr. Amr Mahrous, Lori Goss, and Leyla Dereci, thank you for making lab life tolerable, my experiments and data analyses processes easier, and providing your time and input during scheduled and impromptu lab discussions.

Lastly and most importantly, I would like to thank my all friends and family for their love and support throughout my entire academic career, especially my parents, siblings, grandparents, aunt and uncles, Annette Carter, Sherri Mitchell, Amber Banks, Shanda Kennedy, Dr. Thaiesha Wright, JaLisa Elkins, Laura Carrington, and Cynara Saunders.

Chapter I: Purpose and Specific Aims

Purpose

Amyotrophic lateral sclerosis (ALS) is a progressive neurodegenerative disease that predominantly affects the middle-aged population. ALS is characterized by the loss of both upper and lower motorneurons (MNs), which leads to paralysis and ultimately death, within 3-5 years following diagnosis. To date, the pathogenesis underlying ALS is largely unknown, but abnormalities in MN excitability remain the most tightly linked to disease mechanisms. For decades, researchers have investigated the excitability state of MNs in ALS, but the results are widely inconsistent and vary depending on the study. In addition, most of these researchers investigated changes in individual MNs but very few examined the effects of ALS on the spinal MN network. This project addressed these gaps in the literature and investigated the long-term effects of a novel treatment for ALS, CyPPA[1].

In the first specific aim, we examined the excitability state of individual MNs and the spinal MN network at symptom onset in SOD1-G93A$^{\text{High-Copy}}$ (SOD) mice, which are the standard rodent model of ALS. Also, symptom onset is the critical time-point in diseases where despite maximum compensation, disease alterations prevail, and the first external evidence of a problem emerges (i.e., symptoms).

---

[1] Cyclohexyl-[2-(3,5-dimethyl-pyrazol-1-yl)-6-methyl-pyrimidin-4-yl]-amine

Next, we examined the long-term effects of a small-conductance calcium-activated potassium (SK) channel activator, CyPPA, in SOD mice. Under normal physiological conditions, SK channels regulate MN excitability, but previous investigations in our lab revealed SK channel deficits in SOD mice (Dukkipati, 2016). Early treatment with CyPPA improved these deficits and prolonged survival and motor function in these animals (Dancy, 2017; Murphy, 2020). However, the long-term effects of CyPPA on the excitability of SOD MNs at the individual and network levels was not investigated. Hence, this project furthers our understanding of the disease versus compensatory mechanisms associated with ALS, the inconsistencies concerning MN excitability in ALS within the literature, and the mechanisms underlying the therapeutic benefits of CyPPA in ALS.

Specific Aims

Specific Aim 1: Investigate ALS-induced excitability changes in individual MNs and the spinal MN network in SOD mice at symptom onset.

Hypothesis: Disease and compensatory mechanisms in ALS cause opposing changes in MN excitability. Thus, at symptom onset, individual SOD MNs exhibit both hypo- and hyperexcitable changes in intrinsic electrical properties. Additionally, because MN excitability is also influenced by synaptic inputs, alterations in sensory and descending motor inputs in the spinal MN network of SOD mice at symptom onset contribute to changes in MN excitability.

Aim 1A: Examine the effects of ALS on the excitability of individual MNs in SOD mice at symptom onset.

Aim 1B: Examine the effects of ALS on the excitability of the spinal MN network in SOD mice at symptom onset.

Rationale: Presently, the literature examining MN excitability in ALS is widely inconsistent, showing evidence of hyperexcitability, hypoexcitability, or no change in the excitability of MNs depending on the study. Many of these studies also focus on individual MNs rather than the spinal MN network, whose output[2] collectively drives muscle activity. Using intracellular and ventral root recordings, we studied the effects of ALS on the excitability of individual MNs and the spinal MN network in SOD mice at symptom onset. Altogether, these data explain the controversial state of ALS literature surrounding MN excitability and identify a novel mechanism contributing to the development of motor dysfunction in ALS.

---

[2] The sum of the spiking activities of MNs, interneurons, and their synapses

Specific Aim 2: Determine the long-term effects of early treatment of SOD mice with CyPPA on the excitability of individual MNs and the spinal MN network.

Hypothesis: Early treatment of SOD mice with CyPPA increases the conductance of SK channels (G_{SK} density) and the amplitude of the afterhyperpolarization (AHP) in individual SOD MNs at symptom onset. Additionally, because SK channels influence synaptic transmission and plasticity (Faber et al., 2005; Nanou et al., 2013), early treatment with CyPPA alters one or both of these synaptic properties in the spinal MN network of SOD mice at symptom onset.

Aim 2A: Examine the long-term effects of early treatment of SOD mice with CyPPA on the excitability of individual MNs.

Aim 2B: Investigate the long-term effects of early treatment of SOD mice with CyPPA on the excitability of the spinal MN network.

Rationale: In ALS, large, fast (F)-type MNs are more vulnerable to degeneration than small, slow (S)-type MNs (Hegedus et al., 2007; Hegedus et al., 2008; Pun et al., 2006; Saxena et al., 2013). Previous data has also shown that F-type MNs have an intrinsically lower expression of SK channels than S-type MNs (Deardorff et al., 2013). SK channels mediate the AHP (Meech, 1978; Ransom et al., 1975; Wikström & El Manira, 1998) and subsequently influence MN discharge or firing rates (Manuel et al., 2006; Viana et al., 1993). More recently, our lab found SK channel downregulation throughout disease progression in SOD mice using immunohistochemistry (Dukkipati, 2016) and established the therapeutic potential of an SK channel activator, CyPPA, in ALS. CyPPA restores the somatic clustering profile of SK channels, improves motor function, and prolongs the survival of SOD mice (Dancy, 2017; Murphy, 2020). However, SK channels are not only

found on the soma of MNs but exist on the dendrites to modulate synaptic inputs (Nanou et al., 2013) and influence the spinal MN network. Using intracellular and ventral root recordings from adult SOD mice treated with CyPPA during the neonatal period, we investigated the long-term effects of CyPPA on the excitability of individual MNs and the spinal MN network in SOD mice. Together, these data further elucidate the therapeutic potential of CyPPA in ALS.

Chapter II: Background

Amyotrophic lateral sclerosis (ALS)

ALS is the most common motorneuron (MN) disease with an estimated prevalence of 5.2 cases per 100,000 people in the United States (Mehta et al., 2018). ALS is hallmarked by the progressive degeneration of MNs in the brain, brainstem, and spinal cord, resulting in the dysfunction of somatic muscles in the body (Rowland & Shneider, 2001; Talbot, 2009; Taylor et al., 2016). The onset of symptoms is typically between the ages of 50 and 65 and males carry a higher risk for developing the disease (Ingre et al., 2015; Kurtzke, 1982; Logroscino et al., 2010; PARALS, 2001; Zarei et al., 2015)

Patients with ALS initially present with muscle atrophy and weakness that progresses to paralysis. Within a short period, the disease spreads to the respiratory muscles impairing breathing and eventually causing death. Currently, there are no valid diagnostic biomarkers for ALS, which requires physicians to identify ALS solely based on the signs, symptoms, and medical history of patients. However, many of the initial symptoms associated with ALS are nonspecific and may resemble features of other neuromuscular diseases causing a delay in diagnosis (Longinetti & Fang, 2019). This delay is further extended by the required evidence of the progressive spread of symptoms in ALS. Altogether, the mean time from the onset of symptoms to diagnosis is approximately 12 months (Mitchell et al., 2010; Paganoni et al., 2014) and median survival from symptom onset ranges from 2-5 years, depending on the clinical and

pathological syndrome (Chancellor et al., 1993; Logroscino et al., 2008; Norris et al., 1993).

While the majority of ALS cases are sporadic (sALS), about 10 percent of patients have a familial (fALS) form of the disease due to mutations most commonly associated with the following: Cu/Zn superoxide dismutase 1 (SOD1), TAR-DNA binding protein 43 (TDP-43), fused in sarcoma (FUS), and chromosome 9 open reading frame 72 (C9ORF72) (Boylan, 2015; Haverkamp et al., 1995). The SOD1 gene was the first to be associated with ALS and mutations in this gene account for approximately 15 percent of fALS cases but fewer than 2 percent of sALS cases (Zou et al., 2017). To date, over 185 disease-associated variations in SOD1 have been identified and phenotype, disease duration, and severity differ depending on the variants involved (Yamashita & Ando, 2015). For instance, patients with a glycine-to-arginine mutation at amino acid 85 (G85R) typically exhibit rapid disease progression and shorter survival times (Yamashita & Ando, 2015).

TDP-43 is a DNA/RNA binding protein encoded by the TARDBP gene that forms ubiquitinated protein aggregates in the brain and spinal cord of most ALS patients (Arai et al., 2006; Mejzini et al., 2019; Neumann et al., 2006; Schipper et al., 2016). Presently, at least 48 variants in TARDBP have been identified in ALS (Lattante et al., 2013). In 2009, variants in a gene encoding another RNA binding protein, FUS, were discovered in a subset of ALS patients (Kwiatkowski et al., 2009; Vance et al., 2009). These variants are often associated with early onset and juvenile ALS rather than the typical late adulthood disease (Gromicho et al., 2017; Hübers et al., 2015; Zou et al., 2013). A few years later, a hexanucleotide repeat expansion (GGGGCC) in the noncoding region of the

C9ORF72 gene was discovered as the most common genetic cause of ALS in the

European population (DeJesus-Hernandez et al., 2011; Renton et al., 2011). This genetic

variant accounts for approximately 34 percent of fALS cases and 5 percent of sALS cases

in the European population (Zou et al., 2017). To date, researchers have conducted

extensive research examining the genetic basis of ALS and have identified more than 20

genes associated with the familial inheritance of this disease (Boylan, 2015; Yamashita &

Ando, 2015). Yet, despite this compilation of knowledge, there are only a few current

treatments for ALS.

Current ALS treatments

Current treatment options for ALS patients include multidisciplinary symptom

management, which involves nutrition, communication, and respiratory support (Hogden

et al., 2017; Mejzini et al., 2019) and two Food and Drug Administration (FDA)

approved medications. In 1995, the FDA approved the first drug to treat ALS, Riluzole

(Jaiswal, 2019; Petrov et al., 2017). Riluzole is a known glutamate antagonist that was

originally used as an anticonvulsant, but its mechanism of action (MOA) in ALS is much

more complex (Bellingham, 2011). Previous research shows that Riluzole has limited

effects on glutamate receptors in ALS and that its pharmacological benefits are likely

related to the inactivation of voltage-dependent sodium channels and interference with

intracellular events that follow neurotransmitter binding at excitatory amino acid

receptors (Jaiswal, 2019). Riluzole is only slightly effective in some ALS patients,

prolonging their lifespan for up to 2-3 months but offering little to no improvement in

their quality of life (Bensimon et al., 1994; Lacomblez et al., 1996; Miller et al., 2012).

Since 1995, researchers have investigated over 60 other molecules as potential treatments

for ALS (DeLoach et al., 2015; Mitsumoto et al., 2014). Many of these molecules delay progression in preclinical animal models of ALS but fail to show efficacy in human clinical trials (Jaiswal, 2019; Petrov et al., 2017).

In 2017, the FDA approved Edaravone to treat ALS (Rothstein, 2017). Edaravone is an anti-oxidative compound that likely reduces oxidative injury to MNs and glial cells at risk for degeneration in ALS (Mejzini et al., 2019), but its exact MOA is still unknown (Jaiswal, 2019). Patients treated with Edaravone for 6 months show a 33 percent reduction in the rate of decline of physical function when compared to patients receiving a placebo (Bhandari et al., 2018; Jaiswal, 2019; Sawada, 2017). Collectively, the current literature on Riluzole and Edaravone treatment in ALS patients shows modest positive outcomes with no evidence of halting the disease or improving quality of life (Bhandari et al., 2018; Jaiswal, 2019; Miller et al., 2012). The limited and ineffectual treatment options available for ALS patients are a consequence of the disease's unclear etiology.

Glutamate excitotoxicity theory in ALS

Currently, there are many theories regarding the pathogenesis of ALS including oxidative stress, mitochondrial dysregulation, deficits in neurofilament and axonal transport, and glutamate excitotoxity (Hirano et al., 1984; Mejzini et al., 2019; Rouleau et al., 1996; Shibata et al., 2001). Glutamate excitotoxicity is one of the most longstanding and well-studied hypotheses associated with ALS. It was first introduced in the 1990s following the discovery of significantly elevated N-acetyl-aspartyl glutamate and its metabolite N-acetyl aspartate in the cerebrospinal fluid (CSF) of patients with ALS (Rothstein et al., 1990). These findings led to the development of the excitotoxicity theory which attributes the pathophysiology of ALS to abnormal chronic exposure of

neurons to excitotoxic substances, such as glutamate or glutamate analogs. This excess

glutamate activity causes an increase in intracellular calcium via glutamate receptors

during synaptic transmission and voltage-gated calcium channels following an action

potential (AP). Thereafter, the surplus calcium entry induces neuronal cell death by

activation of enzymes, such as lipases and phospholipases, initiation of mitochondrial

dysfunction resulting in the production of oxidative reactive species, and/or facilitation of

numerous other putative mechanisms related to ALS (i.e., non-cell autonomous astrocyte

involvement) (Geevasinga et al., 2016; Spalloni et al., 2013; Van Den Bosch et al., 2006).

Correspondingly, the only FDA approved drug used to treat ALS prior to 2017,

Riluzole, has anti-excitotoxic properties (Bensimon et al., 1994; Lacomblez et al., 1996).

In addition, MNs, the cells that undergo degeneration in ALS, are extremely sensitive to

excessive stimulation of glutamate receptors due to their normal intrinsic properties

related to calcium. MNs have a decreased capacity to buffer or stabilize excess

intracellular calcium due to their low expression of calcium buffering proteins (Van Den

Bosch et al., 2006). Previous studies also demonstrate differences within MN

subpopulations where the most vulnerable MNs to ALS in the spinal cord lack calcium

binding proteins, such as parvalbumin and calbindin D28K, compared to the less

vulnerable MNs in the oculomotor, trochlear, abducens, and Onuf nuclei (Alexianu et al.,

1994; Celio, 1990; Ince et al., 1993). MNs also possess a higher portion of calcium

permeable AMPA[3] receptors and stimulation of these receptors leads to selective MN

death (Carriedo et al., 1996; Van Den Bosch et al., 2000). Under normal conditions, these

---

[3] α-amino-3-hydroxy-5-methyl-4-isoxazolepropionic acid

features allow MNs to carry out their physiological function, but under pathological conditions they may aid disease mechanisms.

Altogether, these data provide evidence to support the glutamate excitotoxicity hypothesis in ALS. However, if this theory holds true, MNs in ALS would be hyperexcitable. However, much of the current literature examining MN excitability in ALS is inconsistent.

MN excitability in ALS

MN excitability is determined by interacting cellular properties or "sub-components" such as cell size, passive membrane properties, voltage-gated sodium and calcium persistent inward currents (NaPIC and CaPIC), and synaptic input. To date, researchers have extensively examined MN excitability in ALS using spinal cord tissue from SOD1-G93A$^{\text{High-Copy}}$ (SOD) mice. SOD mice overexpress the SOD1 gene with a glycine-to-alanine mutation at amino acid 93. These mice were the first true ALS model to emerge (Gurney et al., 1994) and are still the most widely used. SOD mice develop a progressive paralysis beginning in the hindlimbs at postnatal day (P) 90 and reach end stage at roughly P135.

MNs from SOD embryos exhibit hyperexcitability due to upregulation of the NaPIC (Kuo et al., 2005; Pieri et al., 2003) and reduced dendritic elongation (Martin et al., 2013). Neonatal SOD MNs also display a robust upregulation of NaPIC and CaPIC (Quinlan et al., 2011; van Zundert et al., 2008). However, a substantial increase in input conductance counteracts this increase in PIC and the overall excitability of neonatal SOD MNs remain unchanged (Quinlan et al., 2011). These results are further supported by a study that examined the excitability of MN subtypes in neonatal SOD mice.

11

MN subtypes are differentially vulnerable to ALS whereby the large MNs that innervate the fast-contracting fibers (F-type MNs) are more vulnerable to the disease and degenerate first compared to the small MNs that innervate the slow-contracting fibers (S-type MNs) (Hegedus et al., 2008; Pun et al., 2006). Remarkably, S-type neonatal SOD MNs exhibit hyperexcitability characterized by a lower rheobase[4] and hyperpolarized spiking threshold, while F-type neonatal SOD MNs do not (Leroy et al., 2014). Together, these findings suggest that early intrinsic hyperexcitability does not contribute to the degeneration of MNs in ALS.

Conversely, some SOD adult MNs lose their ability to fire repetitively, exhibiting hypoexcitability before symptom onset (Delestrée et al., 2014; Martínez-Silva et al., 2018). Studies of specific proteins inside these MNs confirmed the hypoexcitable cells were further along in the disease process and thus represent F-type or disease vulnerable MNs (Martínez-Silva et al., 2018) These data provide evidence of hypo- rather than hyperexcitability as the key player in ALS disease processes. However, some researchers have recently attributed this hypoexcitability to an injury response to microelectrode impalement (Jensen et al., 2020). In fact, they found MNs from adult pre-symptomatic (P69-P75) and symptomatic (P107-P116) SOD mice to be intrinsically more responsive. These cells exhibited a lower rheobase and higher input resistance and gain, but lacked deficits in repetitive firing when electrodes had proper time to seal (Jensen et al., 2020).

To address the inconsistencies discussed above and further understand how MN excitability changes in ALS, Huh and colleagues (2021) conducted a time course study using SOD mice. This study examined the electrical alterations in MNs from SOD mice

---

[4] The minimal amount of current needed to produce an action potential

in three different age groups, P30-P60 (young adult), P60-P90 (pre-symptomatic), and P90-P120 (symptomatic). In these analyses, young adult SOD MNs exhibited abnormally large PICs coupled with an increased input conductance, leaving their net excitability unchanged. Later, in pre-symptomatic SOD MNs, these properties returned to normal. Then finally, in symptomatic SOD MNs, input conductance and recruitment current were reduced. While this study provided the first evidence of fluctuations in MN excitability parameters throughout ALS disease progression, it failed to explain the current state of the literature (Huh et al., 2021). Similar conflicting results have also been found in ALS patient-derived induced pluripotent stem cells (iPSCs) (Devlin et al., 2015; Naujock et al., 2016).

In total, the previous literature examining MN excitability in ALS is widely inconsistent. This variability could be attributed to experimental design or error and/or disease and compensatory mechanisms having opposing effects on MN excitability. In order to address these gaps in knowledge and explain the current literature, additional research examining MN excitability in ALS is needed.

The spinal MN network in ALS

The firing rate of a MN is influenced by its intrinsic electrical properties and its synaptic properties. Therefore, excitotoxicity in ALS could emerge from changes in the intrinsic electrical properties of MNs and/or from an increase or decrease in the activity of neurons that synapse onto MNs. Previous literature has provided key evidence supporting the involvement of synaptic mechanisms in ALS. Both ALS patients and rodent models exhibit loss of glutamate transporters in astrocytes, which may enhance extracellular glutamate (Bendotti et al., 2001; Bruijn et al., 1997; Rothstein et al., 1992;

Rothstein et al., 1995), and inefficient RNA editing of GluR2 mRNA leading to increased calcium permeability of AMPA receptors (Kwak et al., 2010; Tortarolo et al., 2006). In addition, hypoglossal and cortical MNs show an increase in synaptic transmission in SOD mice (Saba et al., 2015; van Zundert et al., 2008). Some data also suggests the involvement of a disinhibitory synaptic mechanism due to a breakdown in glycinergic transmission (Chang & Martin, 2011; McGown et al., 2013) and synapses between MNs and Renshaw cells (interneurons which receive synaptic inputs from MNs and inhibit those same MNs upon activation) (Wootz et al., 2013).

Even still, only a few studies have examined these changes at the system or spinal MN network level, which encompasses the summation of the spiking activities of MNs, interneurons, and their synapses in the spinal cord and thus represents the functional motor output. In the spinal cord, three inputs regulate the firing pattern of MNs, descending motor commands from supraspinal structures, sensory inputs from the periphery, and local interneuronal inputs within the spinal cord (Carp & Wolpaw, 2010). Integration of these inputs allow an individual to generate stable and appropriate motor output in response to a given motor task (Kim et al., 2017; Mahrous et al., 2019; Nielsen, 2004; Rossignol et al., 2006). More specifically, sensory inputs influence the prevention, allowance, and selection of motor patterns and play a pivotal role in responding to perturbations or obstacles during locomotion, while descending motor inputs activate the spinal locomotor networks to initiate locomotion (Rossignol et al., 2006). These two synaptic pathways converge onto common spinal interneurons (Nielsen, 2004) and the spinal MN pool (Brown & Fyffe, 1981; Eccles, 1946; Liang et al., 2014; Riddle et al., 2009; Witham et al., 2016) to permit the performance of skilled motor tasks and shape

locomotor output. The integration of this synaptic information in MNs is influenced by several factors (Heckman et al., 2004; Heckman & Lee, 1999; Magee, 2000; Spruston, 2008) including the pattern of synaptic plasticity, which plays an important role in determining motor input-output function under normal and disease conditions (Wolpaw & Tennissen, 2001).

Synaptic plasticity refers to the activity-dependent modification of the strength or efficacy of synaptic transmission at preexisting synapses (Citri & Malenka, 2008). With repetitive activation, synaptic transmission can either be enhanced or depressed and these changes can last for milliseconds (i.e. short-term plasticity) or days (i.e. long-term plasticity) (Citri & Malenka, 2008). Short-term modifications are common to all neurons in the nervous system (Regehr, 2012; Zucker & Regehr, 2002). Thus, with successive or repetitive stimuli, some synaptic inputs to MNs become progressively smaller or undergo synaptic depression, while others become progressively larger or undergo synaptic facilitation (Jiang et al., 2015; Mahrous et al., 2019). Recent studies demonstrated that sensory and descending motor inputs in the spinal cord exhibit variable forms of system short-term plasticity (Jiang et al., 2015; Mahrous et al., 2019).

Sensory inputs largely include a prominent low threshold monosynaptic component via activation of muscle spindle Ia afferents and exhibit system short-term depression (sSTD) following successive stimulation. However, descending motor inputs are composed of both monosynaptic and polysynaptic connections to MNs and exhibit frequency dependent bimodal plasticity, sSTD at low-stimulation frequencies but system short-term facilitation (sSTF) at high-stimulation frequencies (Jiang et al., 2015). The primary cause for these differences in these two synaptic pathways is due to the

activation of excitatory inputs from monosynaptic sources in the sensory system compared to local interneuronal networks in the descending system (Jiang et al., 2015). These differences also correspond to the functional role of each of these pathways. For example, normal locomotion evokes a strong increase in proprioceptive sensory inputs from the periphery and other sensory inputs to relay information about the position of the limbs and body relative to the surroundings. A reduction in this inflow may be necessary in order to prevent interference with movements (Jacobs & Fornal, 1993; Stein & Capaday, 1988) and thus sSTD in sensory inputs may facilitate this level of control.

Previous ALS research examining sensory inputs in SOD mice show conflicting results. One study found a decrease in the amplitude of sensory inputs throughout disease progression (P50-P130) and concluded these inputs do not contribute to hyperexcitability (Jiang et al., 2009), while another study showed sensory inputs in pre-symptomatic (P50-P90) SOD mice exhibit less sSTD resulting in enhanced repetitive firing and hyperexcitability (Jiang et al., 2017). These contradictory results, along with no studies that examine descending motor inputs or their integration with sensory inputs, demonstrate the need for additional research to determine the effects of ALS on the spinal MN network.

Neurodegenerative Diseases: Disease versus Compensation

ALS, like other neurodegenerative diseases, has three phases (Talbot, 2014). During normal development and progression, different genetic variations and environmental factors influence an individual's later susceptibility to degeneration, but there is no evidence of dysfunction during this time. This is known as the initial or susceptibility phase. During the pre-clinical or pre-symptomatic phase, susceptible

individuals have abnormal neuronal function, but do not display clinical symptoms due to the system's intrinsic reserve capacity or other compensatory mechanisms in operation. When the reserve capacity or compensatory mechanisms are exceeded by disease mechanisms, individuals develop symptoms (i.e., the first external evidence of a problem) and the clinical phase begins.

Evidence of these phases are supported by the numerous genetic variants and environmental factors which increase the risk of ALS (Ingre et al., 2015). In addition, before symptom onset, ALS patients and rodent models exhibit neuronal cell loss but no alterations in motor function or behavior (Aggarwal & Nicholson, 2002; Hegedus et al., 2007). During this time, numerous compensatory mechanisms maintain the neural drive to the muscles and thwart clinical manifestation of the disease. Conversely, at symptom onset, despite maximum compensation, disease processes predominate impairing the neural drive which sparks rapid motor decline.

Throughout disease progression, dynamic interactions between disease and compensatory mechanisms cause unstable fluctuations or alterations in MN cellular properties (Huh et al., 2021; Mitchell & Lee, 2012). The conflicting results in studies investigating the excitability of individual MNs and the spinal MN network in ALS may be due to these oscillations or variations throughout disease progression. Thus, depending on the time of the study or the state of the regulatory mechanisms compared to the disease mechanisms, researchers may find different changes in the same cellular properties. In Chapter IV of the current study, we investigated the excitability state of individual MNs and the spinal MN network in SOD mice at symptom onset. Presently, none of the literature examining individual MN excitability in SOD mice focus on this

key time point. In addition, the few studies that examine the spinal MN network in SOD mice focus solely on the sensory inputs. Our data helps explain the inconsistencies within the literature surrounding individual MN excitability in ALS, provides additional information about disease versus compensatory mechanisms in ALS, and reveals novel information about the effects of ALS on the spinal MN network.

Small-Conductance Calcium-Activated Potassium (SK) Channels

More than 70 years ago, researchers discovered that the injection of bee venom or apamin is toxic and detrimental to the nervous system (Habermann, 1984) due to the blockage of voltage insensitive potassium channels (Hugues et al., 1982). These channels are gated directly by concentrations of intracellular calcium and were identified as SK channels (Blatz & Magleby, 1986). SK channels are expressed in a variety of neurons, such as neurosecretory neurons in the supraoptic area of the hypothalamus (Bourque & Brown, 1987), pyramidal neurons in the sensory cortex (Schwindt et al., 1988), striatal cholinergic interneurons (Goldberg & Wilson, 2005), and spinal MNs (Zhang & Krnjević, 1987).

In most neurons, APs are followed by a prolonged afterhyperpolarization (AHP) (Barrett & Barret, 1976), which influences their intrinsic excitability (Adelman et al., 2012). The AHP influences the voltage trajectory between APs and subsequently sets the frequency of cell firing or the discharge rate (Adelman et al., 2012). In addition, the summation of the AHP over a burst of APs can block AP firing, which is known as spike frequency adaptation (Madison & Nicoll, 1982). The AHP has three components based on differing kinetics, fast (f), medium (m), and slow (s) (Sah, 1996). The mAHP is activated rapidly and decays within several hundred milliseconds (Adelman et al., 2012).

It is blocked by apamin (Avanzini et al., 1989; Bourque & Brown, 1987; Sah & McLachlan, 1992; Schwindt et al., 1988; Zhang & Krnjević, 1987; Zhang & McBain, 1995), lowering the external calcium concentration (Viana et al., 1993), or replacing calcium with magnesium ions (Viana et al., 1993) and is thus a component regulated by SK channel activity.

SK channels in MNs

In spinal MNs, SK channels are located on the proximal dendrites and soma. Dendritic SK channels are activated by persistent L-type calcium channels and NMDA receptors and regulate synaptic inputs, transmission, and plasticity (Faber et al., 2005; Li & Bennett, 2007; Lin et al., 2008; Luján et al., 2009; Nanou et al., 2013). On the other hand, somatic SK channels are activated by transient N-type calcium channels and mediate the mAHP and MN firing (Deardorff et al., 2014; Li & Bennett, 2007; Ransom et al., 1975; Viana et al., 1993).

The duration of the AHP differs between MN subtypes and exhibits a correlation with the muscle fibers innervated by a particular MN (Bakels & Kernell, 1993; Burke, 1967; Gardiner, 1993). The F-type MNs, which innervate the fast twitch fibers, have the shortest AHP which allows them to fire at higher rates compared to S-type MNs that innervate the slow twitch fibers. Thus, the duration of the AHP in a MN is matched to the contractile speed of the muscle fiber it innervates. Different MN subtypes also exhibit different expression patterns of the various SK channel isoforms. There are four SK channel isoforms, but only three of them, SK1, SK2, and SK3, exhibit differential sensitivity to apamin (Gu et al., 2018; Ishii et al., 1997; Köhler et al., 1996; Shah & Haylett, 2000; Strøbaek et al., 2000). Presently, much of the literature examining spinal

MNs focuses on the SK2 and SK3 channel isoforms due to the lack of antibodies against SK1 (Deardorff et al., 2013). Previous literature found that all MNs express SK2 channels, but only small, presumably S-type MNs exhibit SK3 channel expression (Deardorff et al., 2013).

Possible role of SK channels in ALS

In ALS, F-type MNs die before S-type MNs (Hegedus et al., 2008; Pun et al., 2006). This degeneration differential suggests that S-type MNs exhibit some characteristics that decrease their vulnerability to disease mechanisms. MN subtypes exhibit a difference in their intrinsic expression of SK channels and SK channels regulate MN excitability; thus, SK channels may explain the vulnerability differential between F and S-type MNs in ALS.

To date, SK channels have not been directly implicated in ALS, but Riluzole, the primary ALS treatment, activates SK channels in recombinant expression systems and hippocampal neurons (Bellingham, 2011; Cao et al., 2002; Grunnet et al., 2001). In addition, N-type calcium channels, which activate SK channels, are overexpressed in SOD cortical neurons and spinal MNs (Chang & Martin, 2016; Pieri et al., 2013). These data, along with the limited therapeutic options and inconsistencies within the literature regarding MN excitability at both the cellular and system levels, led our lab to examine the role of SK channels in ALS using computer modeling, immunohistochemistry, and drug studies. From our initial investigations, we determined that SK channels are downregulated in neonatal SOD MNs and these changes persist throughout disease progression and likely contribute to ALS pathogenesis (Dukkipati, 2016). Thereafter, we

tested the therapeutic potential of an SK channel activator or positive modulator, CyPPA, in SOD mice.

CyPPA selectively stimulates SK2 and SK3 channel activity but exhibits no effects on SK1 or intermediate-conductance calcium-activated potassium (IK) channels (Hougaard et al., 2007). CyPPA administration in dopaminergic (DA) neurons of the substantia nigra pars compacta (SNc) results in decreased spontaneous firing and prolonged duration of the mAHP and may be a potential method of pharmacological modulation in psychiatric disorders, such as schizophrenia or attention-deficit hyperactivity disorder (ADHD) (Herrik et al., 2012). CyPPA administration has also been shown to suppress melanogenesis by downregulating microphthalmia-associated transcription factor (MITF) (Noh et al., 2019), which is the most important target in the treatment of hyperpigmentation disorders (Primot et al., 2010).

In our study, we administered CyPPA in SOD mice from P5-P20 in order to overlap drug administration with the following: normal ion channel maturation, the ages associated with our initial investigations, and the earliest documented morphological and N-type calcium changes in SOD mice. Early treatment with CyPPA sustained motor function and improved survival in SOD mice by 10 days (Dancy, 2017), which is fairly comparable to the therapeutic effects of Riluzole in these mice. To date, Riluzole treatment alone significantly prolongs the lifespan of SOD mice by 9-14 days (Bellingham, 2011; Del Signore et al., 2009; Gurney et al., 1996; Gurney et al., 1998).

Together, these studies established the therapeutic potential of SK channels in ALS, but the mechanism underlying the prolonged effects of this drug was still unknown. Therefore, we conducted additional immunohistochemistry studies to examine the

cellular mechanisms underlying the therapeutic benefits of CyPPA in SOD mice. These data revealed that CyPPA restored the somatic clustering profile (area, density, and intensity) of SK channels in SOD MNs and maintained these changes for up to 70 days following treatment (Murphy, 2020). Yet, the effects of CyPPA on the excitability of SOD MNs at the individual and network levels remained unknown. In Chapter V of the current study, we investigated this gap in knowledge.

Chapter III: General Methods

Animals

All electrophysiology data from individual MNs and the spinal MN network were recorded *in vitro* from sacrocaudal spinal cord tissue obtained from male SOD1-G93A$^{\text{High-Copy}}$ (SOD) mice at symptom onset (approximately postnatal day (P) 90) and their age-matched wild-type (WT) transgenic littermates. Originally, mice were obtained from Jackson Laboratory (Bar Harbor, ME) and then bred in our colony at Wright State University (WSU). Only male mice were used in order to eliminate the confounds of gender-related variability in disease onset, progression, and phenotype (Blasco et al., 2012; Cacabelos et al., 2016; Choi et al., 2008; Veldink et al., 2003). Males also have a higher prevalence of Amyotrophic lateral sclerosis (ALS) compared to females (Kurtzke, 1982; Logroscino et al., 2010). All surgical and experimental procedures were reviewed and approved by the WSU Animal Care and Use Committee.

***In Vitro* Sacrocaudal Spinal Cord Preparation**

In order to isolate the sacrocaudal spinal cord from all mice, we followed a combination of the procedures detailed in previous publications (Jiang et al., 2017; Mahrous et al., 2019) and outlined in Figure 1. Animals were deeply anesthetized with intraperitoneal (IP) injections of urethane (0.15g/100g for SOD mice and 0.18 g/100g for WT mice) and supplemental anesthetic was given as needed. Once each animal was no

longer responsive to toe pinching, it was placed in a dissection dish in ventral recumbency and supplied with carbogen (a mixture of carbon dioxide and oxygen gas in the following proportions: 95% O_2 and 5% CO_2) through a face mask. The skin on the back of each mouse was opened and the muscles attached to the vertebral column were carefully separated. The spinal cord was then exposed via dorsal laminectomy and longitudinal incision of the dura mater. During this time, the spinal cord was continuously perfused with modified artificial cerebrospinal fluid (mACSF) aerated with carbogen at a rate of approximately 6-7 ml/min.

Afterwards, each mouse was decapitated, and the spinal cord was transected at the L4 segment. The spinal cord was carefully raised up and the dorsal and ventral roots of the sacral and caudal regions were cut at their spinal outlets. The isolated spinal cord, with attached roots, was transferred to a Petri dish filled with mACSF aerated with carbogen. In the Petri dish, the dorsal and ventral spinal roots were separated and cleaned of any remaining dura mater. Lastly, the spinal cord was moved to a recording chamber and pinned ventral side upward. The recording chamber was continuously perfused with normal ACSF (nACSF) at a rate of 2.5-3 ml/min. Both ventral and dorsal roots were mounted on bipolar wire electrodes on the left and right sides of the recording chamber and immediately covered with petroleum jelly to prevent desiccation. Before any recordings were started, the spinal cord tissue was allowed to recover for approximately 1 hour in order to stabilize activity and wash out any residual anesthetic. This entire procedure was performed at room temperature (21°C).

Physiological Solutions

Normal artificial cerebrospinal fluid (nACSF)

The nACSF contained the following (in mM): 128 NaCl, 3 KCl, 1.5 $MgSO_4$, 1 NaH_2PO_4, 2.5 $CaCl_2$, 22 $NaHCO_3$, and 12 glucose. The osmolarity of the solution was approximately 295 mOsm and the pH was 7.35-7.4 when aerated with carbogen.

Modified artificial cerebrospinal fluid (mACSF)

Compared to the nACSF, the mACSF contained higher amounts of magnesium to block NMDA receptors and reduce cellular damage induced during spinal cord dissection and isolation. Specifically, the mACSF contained the following (in mM): 118 NaCl, 3 KCl, 1.3 $MgSO_4$, 5 $MgCl_2$, 1.4 NaH_2PO_4, 1.5 $CaCl_2$, 24 $NaHCO_3$, and 25 glucose. The osmolarity of the solution was approximately 310 mOsm and the pH was 7.35-7.4 when aerated with carbogen.

A

spinal column
muscle
fat
oxygen mask

B

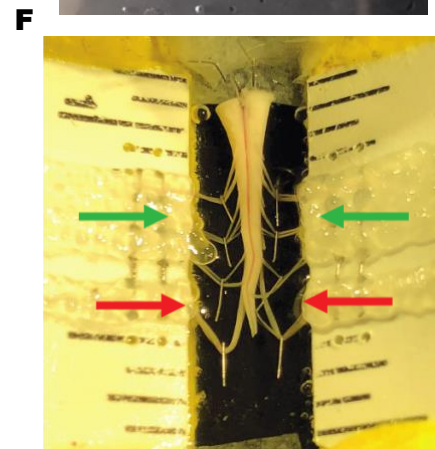meninges
spinal cord

D

C

5 mm

E

F
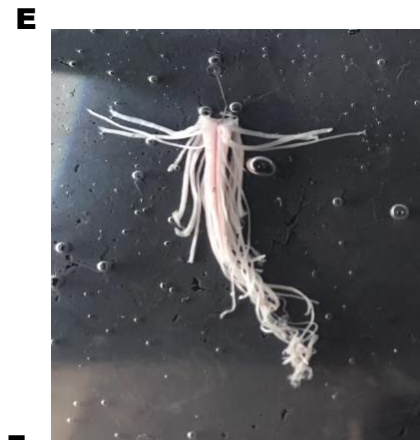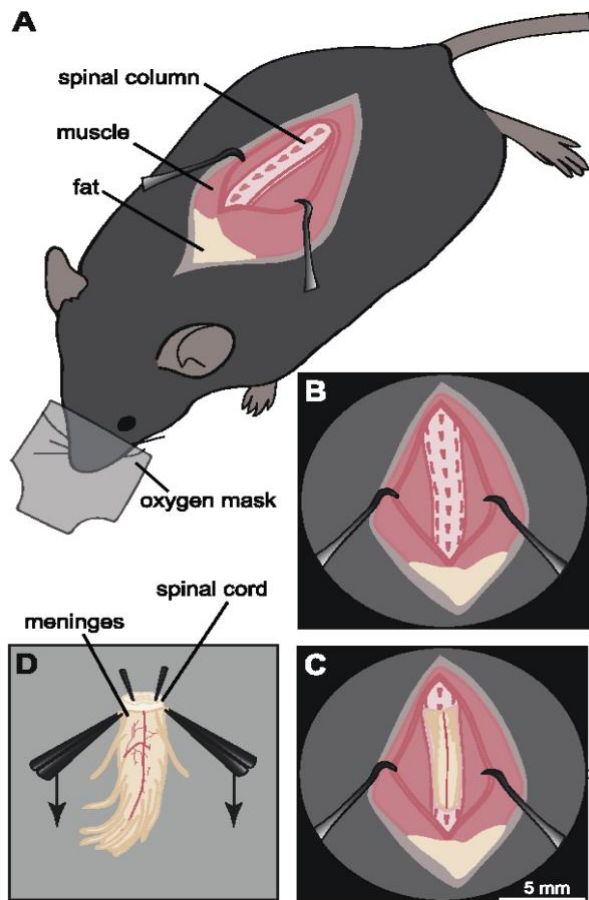
Figure 1: *In vitro* **sacrocaudal spinal cord preparation**

The skin on the back of each mouse is removed and the layers of muscle surrounding the vertebral column are detached **(A-B)**. *Modified from Husch, Cramer, and Harris-Warrick (2011)*. The spinal cord is then exposed via dorsal laminectomy and longitudinal incision of the dura mater **(C)**. The spinal cord, along with the ventral and dorsal roots at the sacral and caudal region, is carefully cut out **(D)** and placed into a Petri dish containing mACSF aerated with carbogen **(E)**. In the Petri dish, any remaining dura mater is removed, and the ventral and dorsal roots are separated. The spinal cord is transferred to a recording chamber perfused with nACSF aerated with carbogen **(F)**. The ventral and dorsal roots are mounted onto bipolar wire electrodes and covered with petroleum jelly, as indicated by the green and red arrows, respectively.

Electrophysiology Recordings

Intracellular recordings

Intracellular recordings were made from single motorneurons (MNs) while the whole sacrocaudal spinal cord was maintained intact (Figure 2). Sharp intracellular electrodes were pulled using a micropipette puller (P97, Sutter instruments, CA) and filled with 3M potassium acetate with 100 mM KCl. Each electrode, with a resistance of 25-40 MΩ, was advanced into the ventral horn of the spinal cord using a micro-positioner (2660, Kopf instruments, CA). Single cell recordings were sampled at 20 kHz and low-pass filtered at 3 kHz with an Axoclamp-2A or 2B amplifier (Molecular Devices, CA) running in bridge or discontinuous current clamp (DCC) modes. The outputs of the amplifiers were digitized using Power 1401-3 data acquisition interface (CED, UK) at 10-20 kHz. All data was acquired into a computer controlled by Spike2 software (version 8.06, CED) and stored offline for analysis.

MNs were identified by the presence of an antidromic action potential (AP) following ventral root stimulation. Cells with an unstable or depolarized resting membrane potential (RMP) were excluded. For each cell, we measured passive membrane properties, AP and afterhyperpolarization (AHP) properties, and repetitive firing behavior. The following passive membrane properties were recorded: RMP, input resistance (R_{in}) and its inverse input conductance (G_{in}), the time constant (tau), capacitance, and rheobase. RMP was documented after each cell was stabilized. R_{in} and G_{in} were measured as the slope of the linear portion of the current-voltage (I-V) relationship derived from a series of hyperpolarizing 500 ms current pulses from -1 to -0.25 nA. Tau was also determined from the 500 ms hyperpolarizing pulses during the

return to RMP using the graphical peeling method (Rall, 1969). The capacitance was calculated by dividing tau by R_{in}. Finally, rheobase, defined as the minimum amount of current necessary to evoke a single AP, was obtained from depolarizing 50 ms current pulses in increasing increments of 0.2 nA.

For the AP parameters, we measured the AP height, maximum rising slope, average rising slope, max falling slope, average falling slope, half-width, width, and time to rise or peak. For the AHP parameters, we measured the AHP amplitude, time to rise, half-decay, two-thirds decay, half-duration and conductance, which is denoted as G_{SK} because SK channels largely mediate the AHP. Since SK channels are not voltage dependent and instead activated via intracellular calcium, their activity cannot be measured experimentally but must be estimated from their ionic current amplitude (I_{SK}) using the following equation as described in Li and Bennett (2007):

$$I_{SK} = G_{SK} \ (V\text{-}E_K) \tag{1}$$

$$G_{SK} = G_{in} \ \frac{AHPslope}{(1-AHPslope)} \tag{2}$$

where the G_{SK} is the AHP conductance measured for each cell, V is the potential at the AHP peak, AHP_{slope} is the slope of the regression line fit through the AHP vs. holding potential relation, which is established by measuring the AHP amplitude from antidromic evoked spikes while varying the membrane potential systematically with bias currents (Li & Bennett, 2007), G_{in} is the input conductance of each cell, and E_K is the reversal potential for potassium, which is the holding potential at which the AHP amplitude is zero. After G_{SK} was calculated, we divided the G_{SK} by capacitance, which is directly correlated with cell size (Koch, 2004). Measurements of capacitance are often used to normalize for variability in cell size in neurons (Schulz et al., 2006; Swensen & Bean, 2005; Turrigiano et al., 1995) and changes in ionic conductance are expressed as

conductance densities to reflect this standardization (Iwasaki et al., 2008; Khorkova & Golowasch, 2007; Pineda et al., 2008; Zhang et al., 2019). In our study, this parameter is identified as G_{SK} density.

Lastly, we assessed firing behavior using intracellular injections of a series of long (2 s) depolarizing current pulses of increasing amplitude (1.5-2.5 times the cellular rheobase which is denoted as 1.5-2.5xR) and triangular current ramps with a constant speed of 0.25 nA/s. With long current pulses, we measured the following: slope of the regression line fitted to the membrane potential during the interspike interval (ISI) over time curve or the ISI slope, the membrane potential during the ISI or ISI voltage, firing frequency, maximum rising slope, maximum falling slope, and AP half-width. With triangular current ramps, we measured I_{on} (the current level at firing onset), I_{off} (the current level at firing cessation), deltaI (I_{off} - I_{on}), maximum firing frequency, and the frequency-current (F-I) gain, the ascending (F-I_{Asc}) and descending (F-I_{Desc}) slopes of the F-I relationship.

Intracellular sharp
microelectrodes

Ventral roots on
bipolar wire
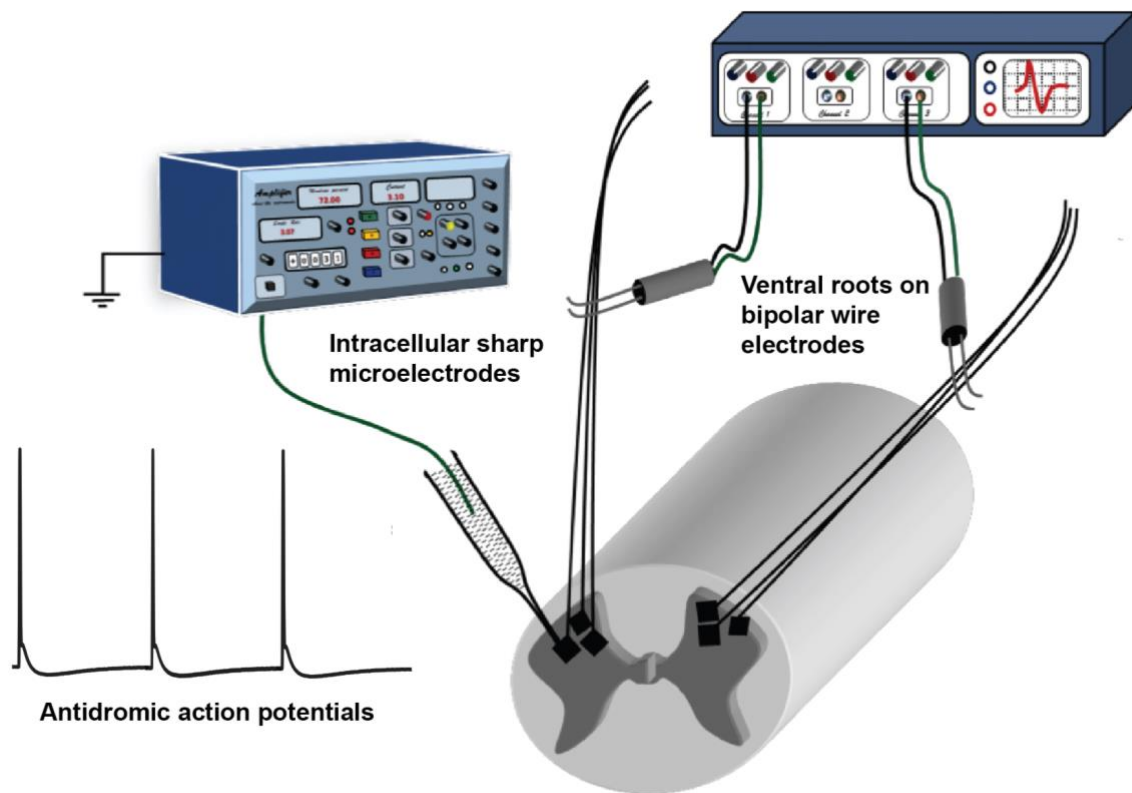electrodes

Antidromic action potentials

Figure 2: Experimental setup for intracellular recordings from MNs

The spinal cord is placed ventral side up in a recording chamber perfused with nACSF

aerated with carbogen. MNs are impaled by sharp electrodes and identified by the

presence of an antidromic AP. *Modified from Mahrous, Mousa, and Elbasiouny (2019)*.

Ventral root recordings

The protocol for ventral root recordings was previously outlined in Mahrous and Elbasiouny (2019). Both ventral and dorsal roots were mounted on bipolar wire electrodes (Figure 3) and connected to a custom-built six-channel amplifier (Kinetic Software, GA) in differential mode with 1000 times gain. All recordings were low pass filtered at 3 kHz and high pass filtered at 300 Hz and performed at the S3-CO2 segments where the responses or compound action potentials (coAPs) were most stable.

Sensory and descending motor inputs in the sacrocaudal spinal cord

Sensory input (S) was induced by electrical stimulation of the dorsal roots. Dorsal roots were connected through bipolar wire electrodes (Figure 3A) to a stimulator (Isoflex, AMPI) and stimulated with a train of five brief (0.1 ms) pulses at either 1.5 or 10-times threshold (1.5 or 10xT) with a frequency of 0.06 or 25 Hz. The threshold for sensory input was defined as the smallest amount of current needed to stimulate the dorsal roots in order to produce a minimal response or coAP in the ventral roots (Figure 3B). This value was on average 3.71 µA ± 2.42 SD in WT mice, 3.08 µA ± 1.23 SD in SOD mice, and 3.25 µA ± 1.19 SD in SOD mice treated with CyPPA, denoted as SOD-CyPPA mice.

Descending motor input (M) was induced by electrical stimulation of the remaining descending axons in the spinal cord (Figure 3C), which primarily originate from the lateral vestibular nucleus, oral pontine reticular nucleus, and gigantocellular reticular formation (Jiang et al., 2015; Liang et al., 2014; Liang et al., 2015, 2016). A custom-built concentric bipolar electrode (0.125 mm stainless steel contact diameter insulated by Teflon from a stainless-steel tube 0.2 ID/0.35 OD) was placed on the ventral surface of the spinal cord close to the midline at the S3 segment and a train of five 0.1 ms

electrical pulses were delivered through the electrode at 1.5 or 10xT with a frequency of

0.06 or 25 Hz. The threshold for descending motor input was defined as the smallest

amount of current needed to pass through the concentric electrode to produce a coAP in

the ventral roots. This value was on average 106.67 µA ± 63.01 SD in WT mice, 154.58

µA ± 109.24 SD in SOD mice, and 106.77 µA ± 73.59 SD in SOD-CyPPA mice. CoAPs

were evoked by stimulation of sensory and descending motor inputs separately and then

simultaneously (S&M) to study sensorimotor integration, as synaptic potentials generated

from these two inputs have similar delays[5] and thus reach the soma of MNs

synchronously (Mahrous et al., 2019). Descending motor inputs also exhibit a gradual

decay, which increases the overlap between these inputs when they are stimulated

concurrently (Mahrous et al., 2019).

Repetitive stimulation of sensory or descending motor inputs at frequencies lower

than 0.2 Hz results in weak or minimal synaptic plasticity (Jiang et al., 2015). Thus, the

five evoked coAPs following repetitive stimulation of sensory inputs, descending motor

inputs, or both inputs simultaneously at 0.06 Hz were almost identical in size and

therefore averaged together to measure coAP amplitude[6]. Repetitive stimulation of

sensory or descending motor inputs at frequencies between 25 and 100 Hz induces

system short-term plasticity (depression or facilitation) in coAPs (Jiang et al., 2015). As a

result, repetitive stimulation at 25 Hz was used to study these adaptation patterns in both

synaptic inputs and sensorimotor integration.

---

[5] Time from the stimulus trigger to the onset of the rising phase of the excitatory postsynaptic potential
(EPSP)
[6] Peak-to-peak value

Plasticity (system short-term depression (sSTD) or facilitation (sSTF)) in coAPs was quantified by converting the amplitudes of coAPs into percent changes from the amplitudes of their respective, first evoked coAP. In addition, the amount of sensorimotor integration was determined by subtracting the linear summation of the individual inputs (S+M) at each pulse from the evoked coAPs in response to both inputs stimulated simultaneously (S&M), as normal S&M stimulation follows a supralinear trend (Mahrous et al., 2019).

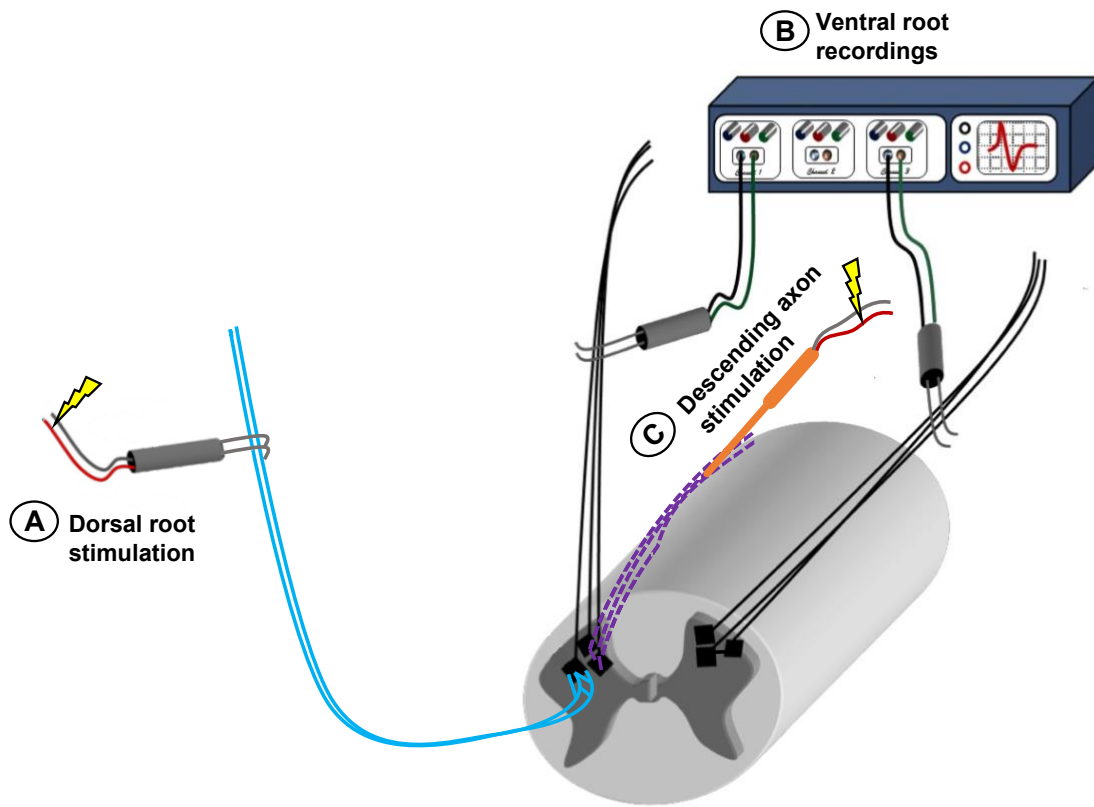**Figure 3: Experimental setup for ventral root recordings from the spinal MN network**

The dorsal roots **(A)** are connected to a stimulator while the ventral roots are connected to a multichannel extracellular amplifier **(B)** for recording. A concentric electrode **(C)** is placed on the ventral side of the spinal cord tissue to stimulate the remaining descending axons. *Modified from Mahrous, Mousa, and Elbasiouny (2019)*.

CyPPA Treatment in SOD Mice

CyPPA, a selective positive modulator of small-conductance calcium-activated potassium (SK) channel isoforms two and three or SK2 and SK3 (Hougaard et al., 2007), was administered to SOD mice for 16 days (P5-P20) within the same three-hour time frame each day. This drug was purchased from Sigma-Aldrich (CAT No. 5493 Lot #075U4604V) and given through IP injections at 14.6 mg/kg. Later, at approximately P90, these mice underwent the same surgery and electrophysiology protocols as previously described. These mice are denoted as SOD-CyPPA mice.

Statistical Analyses

All statistical analyses were performed using IBM SPSS Statistics (Armonk, New York, Version 26) and SAS (Cary, North Carolina). All graphs were constructed using Origin Pro (Wellesley Hills, Massachusetts, Version 2021). In order to study the effects of genotype (SOD vs. WT) and treatment with CyPPA (SOD-CyPPA) on passive membrane properties, AP and AHP properties, and repetitive firing behavior measured using triangular current ramps, a one-way ANOVA with a Tukey's or Games-Howell post-hoc test or a Kruskal Wallis test was performed depending on normality. When possible, non-normal data was transformed using the natural logarithm.

In order to study the effects of genotype and treatment with CyPPA on repetitive firing behavior measured with long current pulses of increasing amplitudes, a two-way mixed ANOVA was conducted in SAS. This was due to the fact that some cells had a higher repetitive firing threshold, and thus did not fire at all three time points or pulses, resulting in some missing values. Unlike SPSS, SAS is not influenced by missing values when conducting a mixed analysis.

To study the effects of genotype and treatment with CyPPA and intensity (1.5 or 10xT) on the amplitude of coAPs generated following stimulation of each synaptic input and both synaptic inputs simultaneously at 0.06 Hz, a two-way ANOVA was used. Lastly, to study the effects of genotype and treatment with CyPPA at each intensity on sSTD, sSTF, and sensorimotor integration, a two-way mixed ANOVA was performed.

In all two-way ANOVAs, the design was unbalanced and thus a Bonferroni multiple comparisons test was used to interpret main effects rather than Tukey's post-hoc test. This test was also used for the mixed ANOVA models. A p value < 0.05 was considered statistically significant for all analyses. All statistical tests were conducted once, but the results are presented in increments focusing on the post-hoc results or pairwise comparisons between SOD and WT data (Chapter IV) and then SOD-CyPPA data relative to SOD and WT data (Chapter V). Thus, the SOD and WT data discussed in Chapter V is the same SOD and WT data from Chapter IV.

Chapter IV: Specific Aim 1

Amyotrophic Lateral Sclerosis (ALS)-induced excitability changes in individual motorneurons (MNs) and the spinal MN network in SOD1-G93A[High-Copy] (SOD) mice at symptom onset

The overall objective of Specific Aim 1 was to examine the excitability state of individual MNs and the spinal MN network in SOD mice at symptom onset.

Introduction

ALS is the most common MN disorder and it was first described by French neurologist Jean-Martin Charcot in 1869 (Katz et al., 2015). ALS is characterized by the progressive degeneration of both upper and lower MNs at the spinal or bulbar levels (Rowland & Shneider, 2001). Most ALS cases are sporadic and only 5-10 percent of ALS cases have a familial link (R. Bonafede & R. Mariotti, 2017). The etiology of ALS is still poorly understood, but years of research has demonstrated the involvement of several altered signaling pathways with the most longstanding being glutamate excitotoxicity (Morgan & Orrell, 2016; Rothstein et al., 1990). ALS's association with glutamate excitotoxicity dates back to the 1990s when Rothstein and his colleagues discovered an abnormal amount of glutamate analogs in the cerebrospinal fluid (CSF) of ALS patients. The current excitotoxicity theory predicts that MN death in ALS results from excessive MN activation via glutamate (Shaw & Ince, 1997). This hyperexcitability of MNs leads

to high levels of calcium entering these cells, which triggers apoptosis. This hypothesis is supported by the discovery that MNs are extremely sensitive to increased glutamate activity (Carriedo et al., 1996; Rothstein et al., 1993; Van Den Bosch et al., 2000). The first approved treatment for ALS, Riluzole, also has anti-excitotoxic properties (Bensimon et al., 1994; Lacomblez et al., 1996). Yet, the research examining the excitability state of MNs in ALS is inconsistent. These studies provide evidence of hyperexcitability, hypoexcitability, and no change in the excitability of MNs in ALS (Delestrée et al., 2014; Jensen et al., 2020; Martínez-Silva et al., 2018; Quinlan et al., 2011). These conflicting results could be attributed to experimental design and/or disease and compensatory processes having opposing effects on MN excitability.

To date, most ALS research on alterations in MN excitability focus primarily on individual MNs, but excitotoxicity in ALS could emerge from an increase or decrease in the activity of neurons that synapse onto MNs. Additionally, it is the output of the spinal MN network which drives muscle activity, a major deficit in ALS patients. In the spinal cord, three inputs regulate the firing pattern of MNs, sensory inputs from the periphery, descending motor inputs from supraspinal structures, and local interneuronal inputs within the spinal cord (Carp & Wolpaw, 2010).

The integration of these inputs allows for the generation of stable motor outputs for any given motor task (Kim et al., 2017; Nielsen, 2004; Rossignol et al., 2006); and this complex process is influenced by synaptic plasticity (depression or facilitation). Following successive stimulation, sensory inputs exhibit system short-term depression (sSTD), while descending motor inputs exhibit frequency-dependent bimodal plasticity, favoring system-short term facilitation (sSTF) at high-stimulation frequencies (Jiang et

41

al., 2015). The few research studies examining MN excitability in ALS at the system or spinal MN network level only focus on sensory inputs and present conflicting results.

Currently, the state of the literature regarding MN excitability in ALS at the individual and network levels is inconclusive. As a result, this study investigated ALS-induced excitability changes in individual MNs and the spinal MN network in the standard mouse model of ALS, SOD mice, at symptom onset. In individual MNs, we assessed passive membrane properties, action potential (AP) and afterhyperpolarization (AHP) properties, and repetitive firing behavior, all factors that contribute to MN excitability. At the level of the spinal MN network, both sensory and descending motor inputs were examined separately, along with their integration.

Results

Specific Aim 1A: ALS-induced excitability changes in individual MNs in SOD mice at symptom onset

SOD MNs exhibit hypoexcitable changes in passive membrane properties at symptom onset

MN excitability is influenced by numerous interacting cellular properties or "sub-components", some passive and others active or a result of ion channel conductance. To determine the effects of ALS on passive membrane properties at symptom onset, we measured resting membrane potential (RMP), input resistance (R_{in}), input conductance (G_{in}), the time constant (tau), capacitance, and rheobase in MNs from 29 SOD (92.08 days $\pm$ 4.20 SD, actual range: 85-103) and 22 WT (93.61 days $\pm$ 2.80 SD, actual range: 87-101) mice. SOD and WT MNs both displayed an average RMP of -72 mV (Figure 4A). However, SOD MNs exhibited a significant decrease in R_{in} (Figure 4B, WT 12.87

MΩ ± 2.70 SD vs. SOD 10.75 MΩ ± 3.82 SD, p = 0.036) and a significant increase in G_{in} (Figure 4C, WT 0.08 µS ± 0.02 SD vs. SOD 0.11 µS ± 0.04 SD, p = 0.004). While there were no significant differences in tau (Figure 4D), SOD MNs exhibited a significant increase in capacitance (Figure 4E, WT 0.13 nF ± 0.04 SD vs. SOD 0.19 nF ± 0.08 SD, p = 0.004) which further confirms previous research that ALS causes an increase in the size of MNs (Amendola & Durand, 2008; Dukkipati et al., 2018; Shoenfeld et al., 2014). Despite these changes, rheobase values were comparable between SOD and WT MNs (Figure 4F). Collectively, the changes in passive membrane properties in SOD MNs at symptom onset suggest hypoexcitability. All measured passive membrane properties are summarized in Table 1.
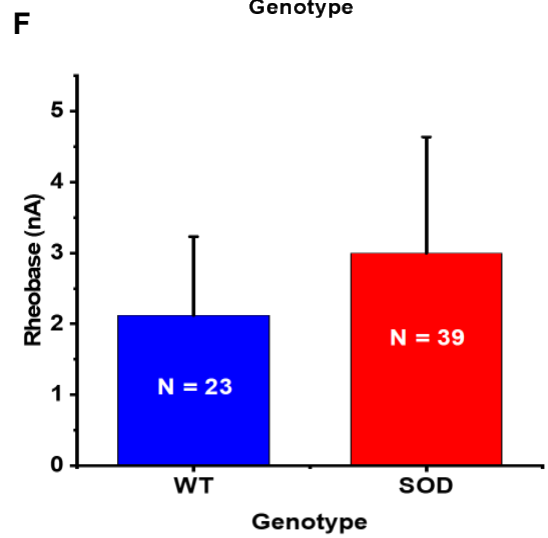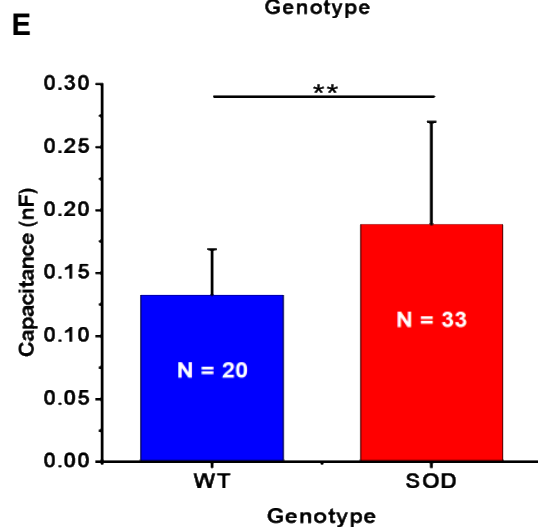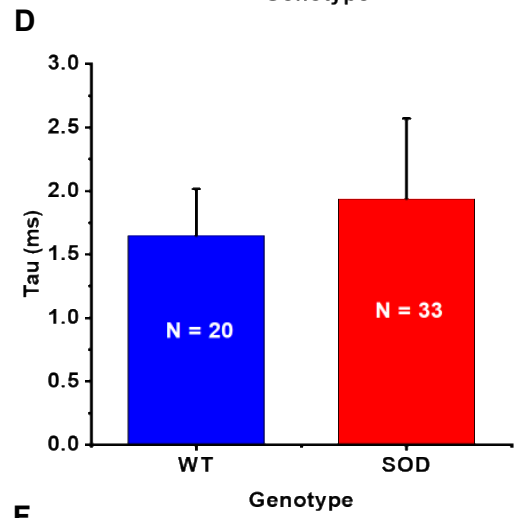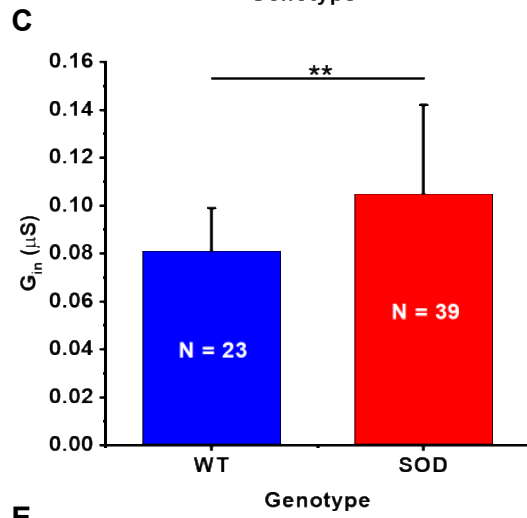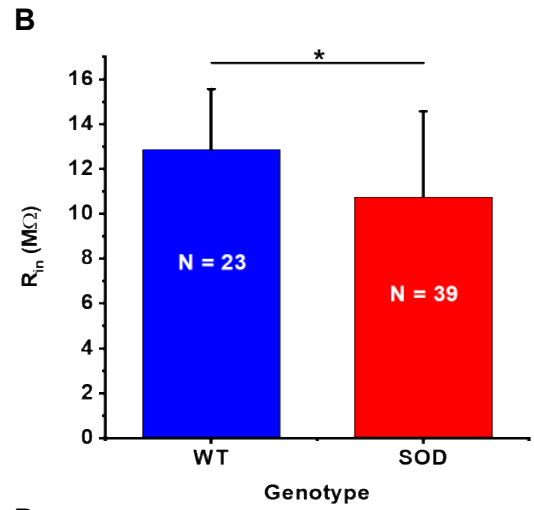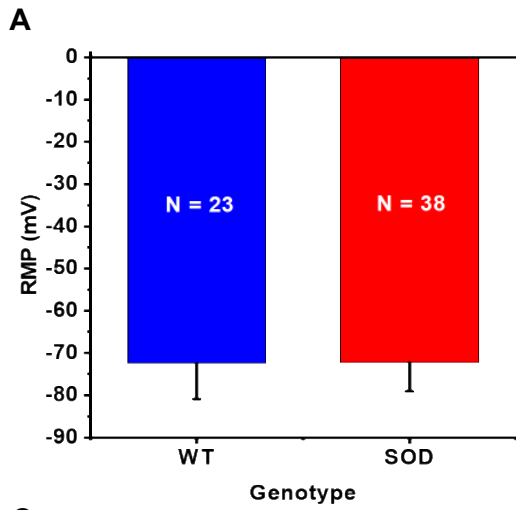
Figure 4: SOD MNs exhibit hypoexcitable changes in passive membrane properties at symptom onset

Passive membrane properties were measured in MNs from SOD and WT mice at or around postnatal day (P) 90, which is symptom onset in the SOD rodent model of ALS. **(A)** On average, both SOD and WT MNs had a RMP of -72 mV. SOD MNs exhibited a significant decrease in R_{in} **(B)** and a significant increase in G_{in} **(C)**. While SOD and WT MNs had similar tau measurements **(D)**, SOD MNs were significantly larger according to capacitance measurements **(E)**. However, rheobase values were comparable between SOD and WT MNs **(F)**. The bars represent the mean ± SD. Significant differences are shown (*****, $p < 0.05$ and ******, $p < 0.01$; Games-Howell post-hoc tests).

	WT	SOD
RMP, mV	-72.42 ± 8.48	-72.28 ± 6.81
R_{in}, MΩ	12.87 ± 2.70	10.75 ± 3.82*
G_{in}, µS	0.08 ± 0.02	0.11 ± 0.04**
Tau, ms	1.65 ± 0.37	1.94 ± 0.63
Capacitance, nF	0.13 ± 0.04	0.19 ± 0.08**
Rheobase, nA	2.12 ± 1.11	3.00 ± 1.64

Table 1. Passive membrane properties   ***mean $\pm$ SD, *p < 0.05, **p < 0.01***

SOD MNs exhibit no changes in AP properties, but hyperexcitable changes in AHP

properties at symptom onset

Another important contributor to MN excitability is AP and AHP properties, also known as active properties, because they are determined by various ion channels. To study the effects of ALS on AP and AHP properties, we measured a total of 13 properties (AP height, maximum and average rising slopes, maximum and average falling slopes, half-width, width, time to rise and AHP amplitude, time to rise, half-decay, two-thirds decay, and half-duration) and estimated SK channel conductance (G_{SK} density) using the calculation outlined in the methods section. There were no significant differences in any AP properties between SOD and WT MNs (Figure 5, Table 2). These same trends were found in some AHP properties including AHP time to rise, half decay, two-thirds decay, and half-duration (Table 3).

Nonetheless, SOD MNs exhibited a significant 24 percent reduction in AHP amplitude (Figure 6, WT 2.30 mV $\pm$ 0.86 SD vs. SOD 1.74 mV $\pm$ 0.75 SD, p = 0.038). The AHP is mediated via SK channels and thus AHP amplitude is determined by G_{SK} density. Expectedly, SOD MNs also exhibited a significant decrease in G_{SK} density (Figure 7A, WT 0.15 μS/nF $\pm$ 0.06 SD vs. SOD 0.11 μS/nF $\pm$ 0.13 SD). G_{SK} density data was non-normal and thus transformed using the natural logarithm (Figure 7B, p = 0.016), but for clarity, original mean values are reported. Together, these results support hyperexcitability in SOD MNs at symptom onset. Additionally, our data supports recent immunohistochemistry studies which determined that SK channels are significantly reduced in SOD mice throughout ALS disease progression (Dukkipati, 2016; Murphy, 2020).
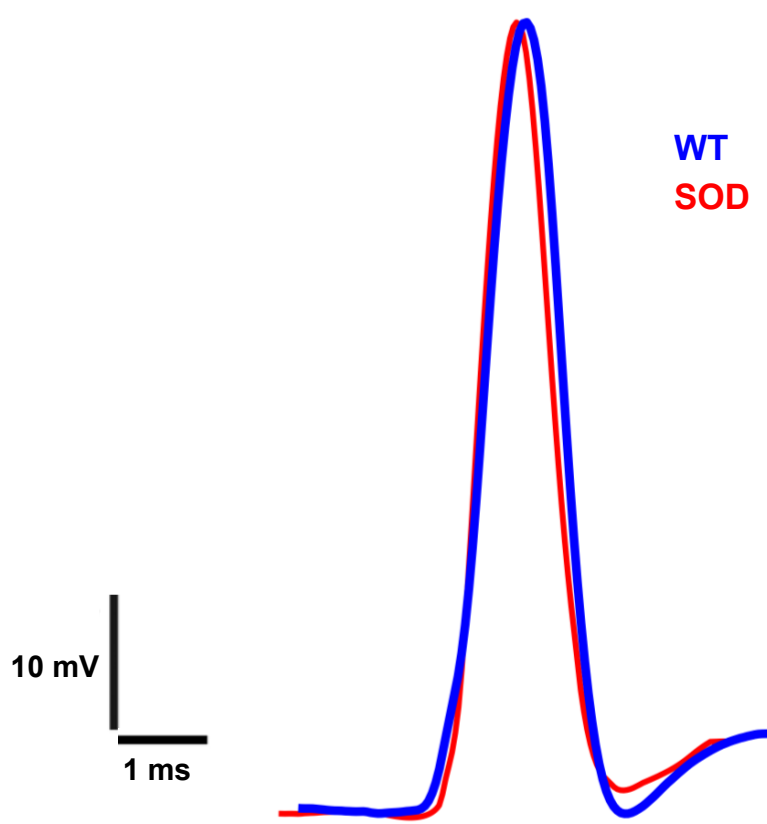
Figure 5. SOD MNs do not show any alterations in AP properties at symptom onset

Superimposition of representative sample APs recorded near rheobase for a WT (blue) and SOD (red) MN.

	WT	SOD
AP height, mV	63.03 ± 10.81	62.63 ± 9.70
Maximum rising slope, V/s	87.27 ± 33.08	85.98 ± 34.76
Average rising slope, V/s	44.60 ± 14.63	44.61 ± 16.04
Maximum falling slope, V/s	-71.91 ± 14.27	-70.00 ± 16.51
Average falling slope, V/s	-33.97 ± 8.03	-34.03 ± 9.97
AP half-width, ms	1.24 ± 0.19	1.23 ± 0.17
AP width, ms	3.22 ± 0.58	3.15 ± 0.61
AP time to rise, ms	1.42 ± 0.30	1.45 ± 0.39

Table 2. AP properties   *mean ± SD*

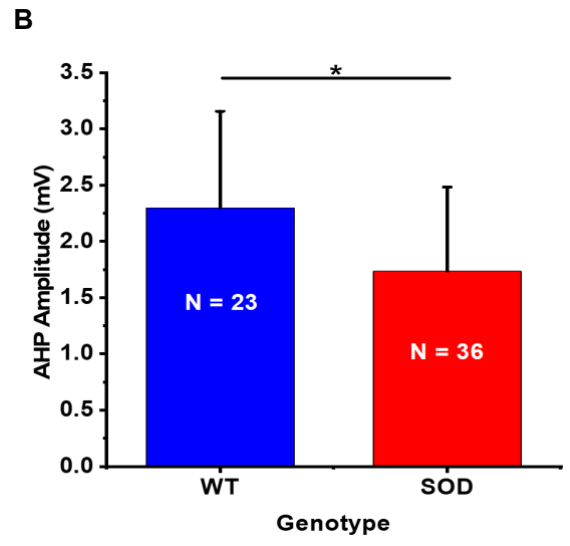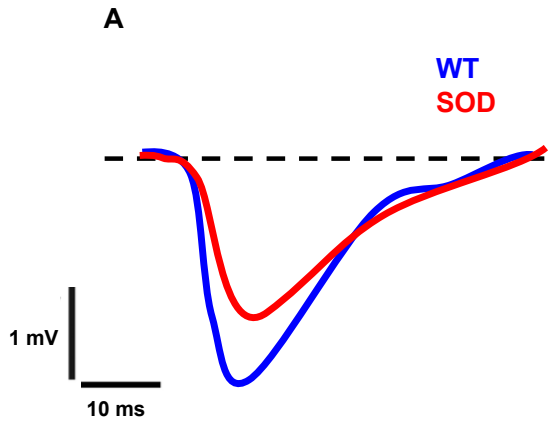**Figure 6. SOD MNs exhibit a significant reduction in AHP amplitude at symptom onset**

(A) Superimposition of representative sample AHPs recorded on isolated APs from a WT (blue) and SOD (red) MN. **(B)** At symptom onset, SOD MNs exhibited a significant reduction in AHP amplitude compared to their WT littermates. Bars represent the mean ± SD. Statistical difference indicated (*****, $p < 0.05$; Tukey's post-hoc test).
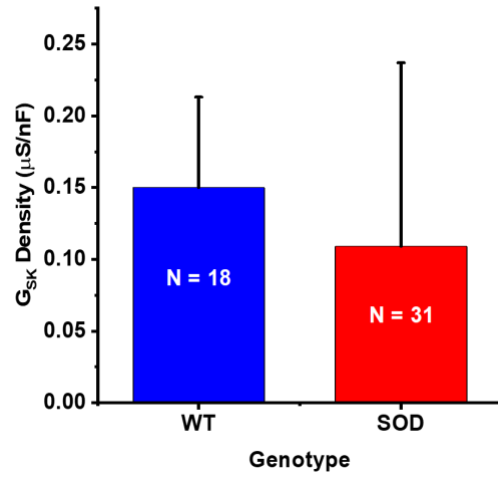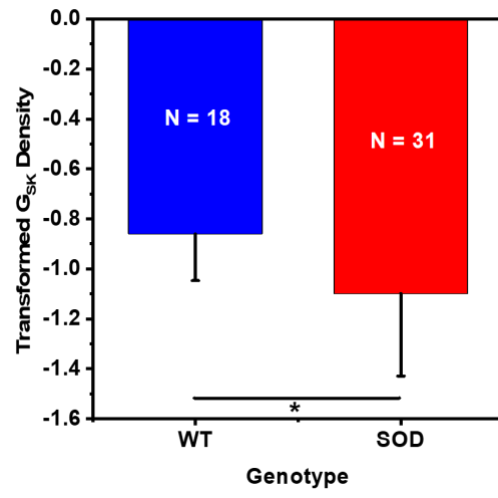
Figure 7. SOD MNs exhibit a significant reduction in G$_{SK}$ density at symptom onset

SOD MNs exhibited a significant reduction in G$_{SK}$ density compared to WT MNs. Both

original **(A)** and transformed **(B)** mean values are reported, as G$_{SK}$ density had a non-

normal distribution. The original values were transformed using the natural logarithm.

The bars represent the mean ± SD. Statistical difference indicated (*****, $p < 0.05$; Tukey's

post-hoc test).

	WT	SOD
AHP amplitude, mV	2.30 ± 0.86	1.74 ± 0.75*
AHP time to rise, ms	12.73 ± 4.72	11.89 ± 4.23
AHP half-decay, ms	19.99 ± 8.10	19.35 ± 9.01
AHP two-thirds decay, ms	53.87 ± 18.01	59.50 ± 21.35
AHP half-duration, ms	29.92 ± 10.93	27.87 ± 10.62
G_{SK} density, $\mu S/nF$	0.15 ± 0.06	0.11 ± 0.13
G_{SK} density transformed	-0.86 ± 0.19	-1.10 ± 0.33*

Table 3. AHP properties   *mean $\pm$ SD, *p < 0.05*

During repetitive firing, SOD MNs exhibit a consistent rate of decrease or

hyperpolarization in the membrane potential during the interspike interval (ISI)

To study repetitive firing behavior, we first used long (2 s) current pulses of increasing amplitudes (1.5-2.5 times the cellular rheobase or 1.5-2.5xR) (Figure 8). During each current pulse, we measured ISI slope (rate of change in the membrane potential during the ISI), ISI voltage (the membrane potential during the ISI), firing frequency, maximum rising and falling slopes, and AP half-width.

Since the amount of current injected into each cell depended on rheobase, an intrinsic cellular property, we controlled for these values during the statistical analysis. For all measured parameters, there were no significant interactions between rheobase and genotype. However, there were no main effects of genotype (Table 4), but there was a statistically significant interaction between genotype and current pulse for ISI slope (p = 0.033). Specifically, WT MNs exhibited a significant increase in ISI slope with increasing current pulse intensity (Figure 9, Table 4). At 1.5xR current pulses, the ISI voltage in WT MNs decreased or hyperpolarized at a rate of 0.39 mV per second. However, at 2- and 2.5xR current pulses, the ISI voltage in WT MNs increased or depolarized at a rate of 1.23 or 0.99 mV per second, respectively. Similar changes were not observed in SOD MNs which maintained a steady negative ISI slope with increasing current pulse amplitude. Together, these data show that at symptom onset, SOD MNs exhibit a consistent rate of decrease or hyperpolarization in the ISI voltage during repetitive firing.
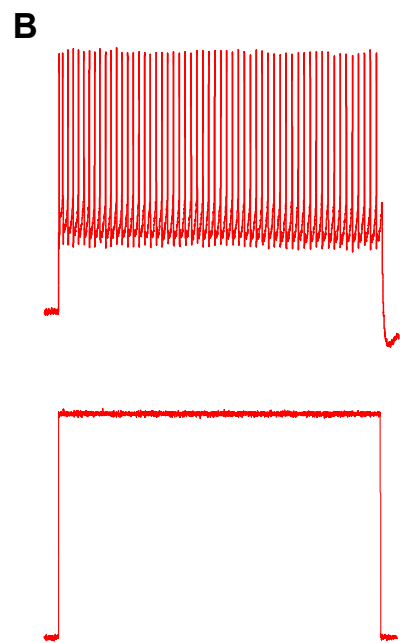
A

B

20 mv

0.5 s

1 nA

0.5 s
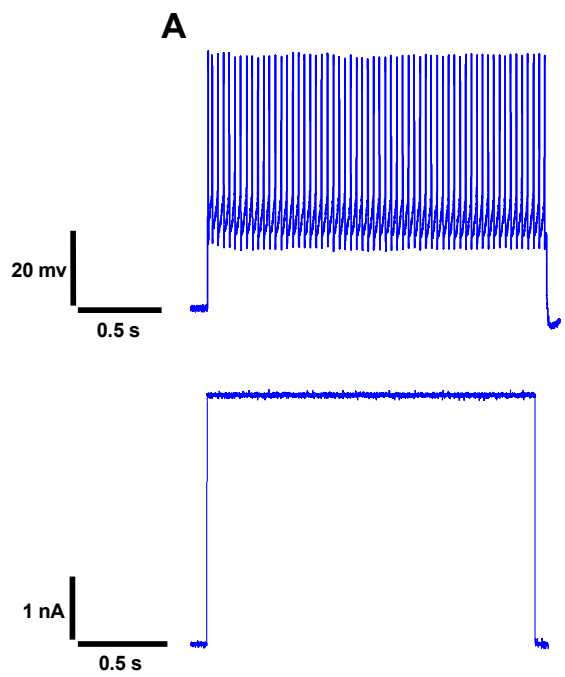
Figure 8. Repetitive firing induced by long (2 s) current pulses

Long depolarizing current pulses of amplitudes ranging from 1.5-2.5xR were injected into MNs to study repetitive firing behavior. Shown are examples from a WT **(A)** and SOD **(B)** MN.

	1.5xR		2xR		2.5xR	
	WT	**SOD**	**WT**	**SOD**	**WT**	**SOD**
ISI slope, mV/s	-0.39 ± 0.49	-0.77 ± 0.27	1.23 ± 0.85**	-0.82 ± 0.34	0.99 ± 1.05*	-1.00 ± 0.38
ISI voltage, mV	-47.78 ± 2.64	-48.12 ± 2.37	-43.94 ± 3.01	-46.85 ± 2.02	-39.46 ± 4.29	-41.39 ± 3.87
Firing frequency, Hz	24.18 ± 1.26	27.23 ± 1.20	34.17 ± 1.70	35.62 ± 1.76	41.39 ± 2.10	41.24 ± 2.46
Maximum rising slope, V/s	59.75 ± 1.33	57.52 ± 1.64	57.79 ± 1.54	54.64 ± 1.58	54.61 ± 1.99	52.57 ± 1.68
Maximum falling slope, V/s	-72.10 ± 2.42	-68.78 ± 1.81	-68.94 ± 2.56	-65.11 ± 2.22	-64.35 ± 3.00	-62.32 ± 2.33
AP half-width, ms	1.34 ± 0.03	1.30 ± 0.01	1.38 ± 0.03	1.34 ± 0.02	1.42 ± 0.05	1.37 ± 0.02

Table 4. Repetitive firing properties measured during long (2 s) current pulses
mean ±SE, * p < 0.05, ** p < 0.01
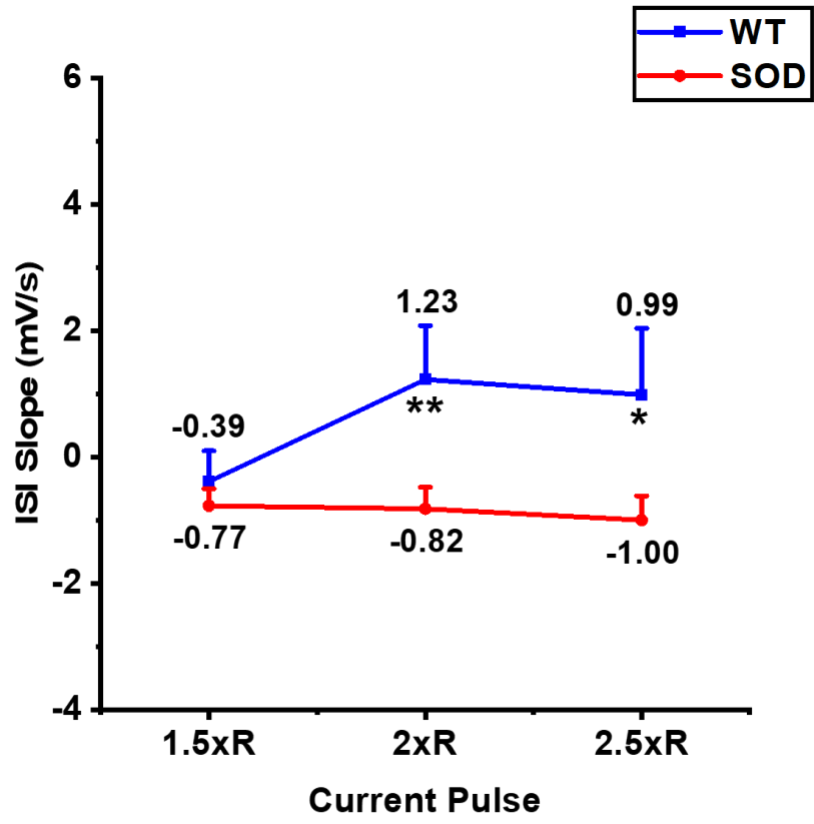
Figure 9. At symptom onset, SOD MNs exhibit a steady negative ISI slope during repetitive firing

Compared to WT MNs, SOD MNs exhibited a steady negative ISI slope with increasing current pulse amplitude. Thus, SOD MNs showed a consistent rate of decrease or hyperpolarization in ISI voltage at each current pulse. WT MNs exhibited a significant increase in ISI slope with increasing current pulse amplitude. At 1.5xR current pulses, the ISI voltage in WT MNs decreased or hyperpolarized at a rate of 0.39 mV per second. These rates significantly shifted at 2- and 2.5xR current pulses. At these current pulses, the ISI voltage in WT MNs increased or depolarized at a rate of 1.23 or 0.99 mV per second, respectively. Each data point represents the mean and error bars denote the SE. Significant differences are shown (*****, $p < 0.05$ and ******, $p < 0.01$; Bonferroni multiple comparisons test) and each asterisk indicates the difference from the first WT data point at the 1.5xR current pulse.

Frequency-current (F-I) gain is significantly reduced in SOD MNs at symptom onset

The repetitive firing behavior of MNs can be further characterized using increasing and decreasing (triangular) current ramps. These ramps are typically used to uncover the input-output relationship of MNs and the properties of persistent inward currents (PICs) (Hounsgaard et al., 1988; Lee & Heckman, 1998). PICs are primarily mediated via voltage-sensitive sodium and potassium channels located in the dendrites of MNs (Carlin et al., 2000; Hounsgaard & Kiehn, 1993; Lee & Heckman, 1999; Li et al., 2004). These channels increase the excitability of a MN and generate a greater output for a given input (Heckman et al., 2009).

In order to study the effects of ALS on the input-output relationship and PICs in MNs at symptom onset, we measured I_{on} (the current level at firing onset), I_{off} (the current level at firing cessation), deltaI (I_{off} - I_{on}), maximum firing frequency, and the F-I gain, the ascending (F-I_{Asc}) and descending (F-I_{Desc}) slopes of the F-I relationship, in SOD and WT MNs using triangular current ramps with a constant speed of 0.25 nA/s (Figure 10).

There were no significant differences in I_{on}, I_{off}, maximum firing frequency, and deltaI between SOD and WT MNs (Table 5). DeltaI values are typically used to estimate total PICs and more negative values indicate the presence of a PIC. Thus, SOD MNs at symptom onset do not demonstrate an alteration in PICs, but deltaI is an indirect and less sensitive measurement of PICs (Quinlan et al., 2011). At symptom onset, SOD MNs exhibited a significant decrease in F-I_{Asc} (Figure 11, WT 7.96 Hz/nA ± 3.12 SD vs. SOD 5.21 Hz/nA ± 2.61 SD, p = 0.003). F-I_{Desc} was also reduced in SOD MNs, but these values were not significantly different from WT MNs.

Many intrinsic MN properties impact the gain of the F-I function including PICs, the AHP, and input conductance (Hounsgaard et al., 1988; Powers & Binder, 2001; Rekling et al., 2000). As a result, F-I gain is typically referred to as the 'net' excitability of a MN (Kuo et al., 2004; Kuo et al., 2005; Quinlan et al., 2011). Thus, despite both hypoexcitable (reduced R_{in} and increased G_{in} and capacitance) and hyperexcitable (reduced AHP amplitude and G_{SK} density) changes in SOD MNs at symptom onset, the net excitability of these cells is reduced and thus hypoexcitability predominates.
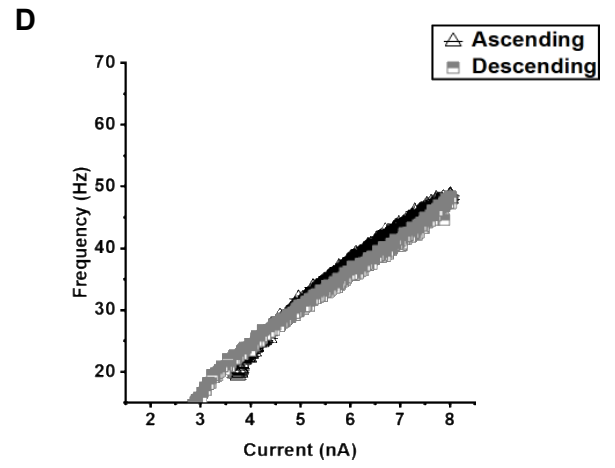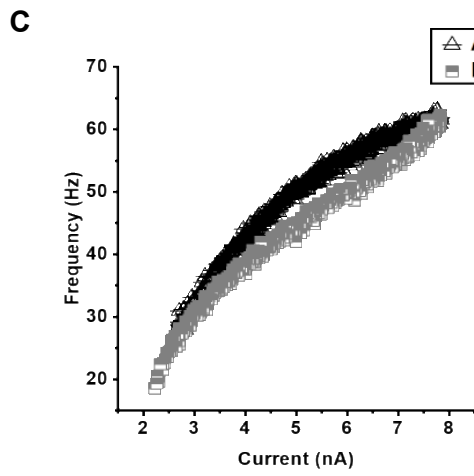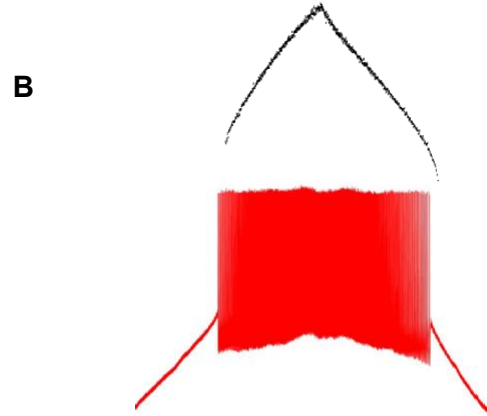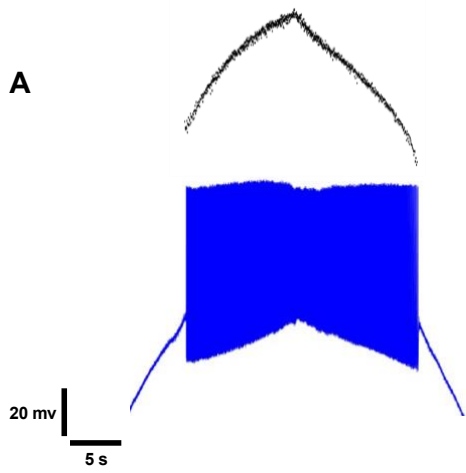
Figure 10. Repetitive firing induced by triangular current ramps and frequency-current (F-I) relationships

Depolarizing ramps of current were injected into MNs to study the F-I relationship and PICs. Shown are examples from a WT **(A)** and SOD **(B)** MN. The relationship between firing frequency and current is plotted below each MN, labeled **(C)** and **(D)**, respectively.

	WT	SOD
I_{on}, nA	2.97 ± 1.71	4.06 ± 2.66
I_{off}, nA	2.83 ± 1.76	3.79 ± 3.25
deltaI (I_{off} - I_{on})	0.14 ± 0.89	0.27 ± 1.15
Maximum firing frequency, Hz	47.42 ± 17.44	41.77 ± 12.21
F-I_{Asc}, Hz/nA	7.96 ± 3.12	5.21 ± 2.61**
F-I_{Desc}, Hz/nA	7.33 ± 3.56	6.27 ± 2.58

Table 5. Repetitive firing properties measured during triangular current ramps mean $\pm$ SD, **p < 0.01
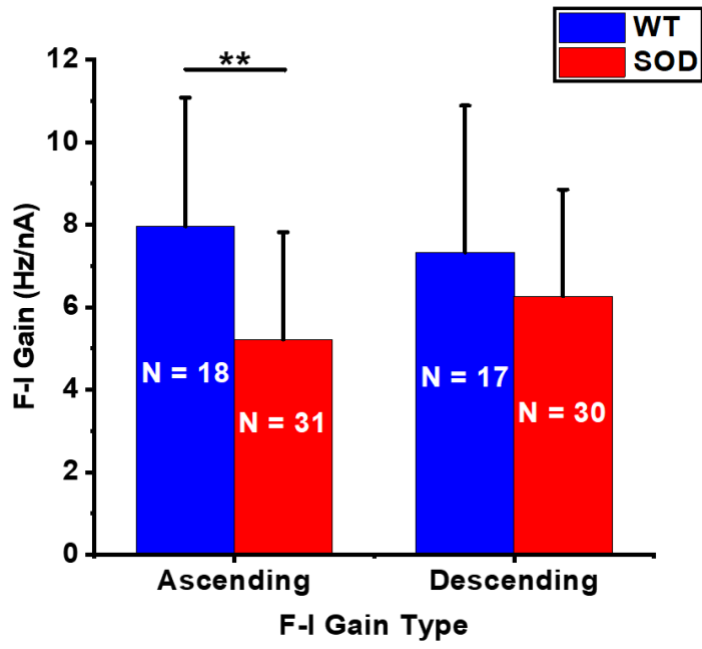
Figure 11. SOD MNs exhibit a significant reduction in net excitability or F-I gain at symptom onset

SOD MNs exhibited a significant reduction in F-I$_{Asc}$ at symptom onset compared to WT MNs. Similar changes were observed in F-I$_{Desc}$, but these values were not significantly different from WT MNs. The bars represent the mean $\pm$ SD. Statistical difference indicated (**, $p < 0.01$; Tukey's post-hoc test).

Specific Aim 1B: ALS-induced excitability changes in the spinal MN network of SOD mice at symptom onset

Sensory and descending motor inputs in the spinal MN network of SOD mice at symptom onset do not contribute to MN excitability alterations

To investigate the excitability state of the spinal MN network in SOD mice at symptom onset, we examined sensory and descending motor inputs in 12 SOD (93.20 days ± 2.88 SD, actual age range: 87-99) and 14 WT (95.50 days ± 5.33 SD, actual age range: 86-110) mice. Specifically, we measured compound action potentials (coAPs) evoked by repetitive stimulation (5-pulse train) of sensory (via dorsal roots) or descending motor (via remaining descending axons in the spinal cord tissue) inputs at frequencies of 0.06 or 25 Hz and intensities of 1.5 or 10-times threshold (1.5 or 10xT). Threshold denotes the smallest amount of current needed to evoke a coAP. From these measurements, we evaluated the amplitudes of evoked coAPs, which is proportional to the number of cells activated by each synaptic input and the degree of system short-term plasticity (depression or facilitation) produced in these responses, which represents a form of excitability (Jiang et al., 2015).

All five coAPs that were evoked following sensory or descending motor input stimulation at 0.06 Hz were averaged to examine differences in coAP amplitudes. Surprisingly, evoked coAPs were comparable in SOD and WT mice for both synaptic inputs irrespective of stimulation intensity (Figure 12 and 13). However, stimulation of descending motor inputs at 10xT resulted in significantly larger coAPs for both genotypes compared to 1.5xT stimulation (Figure 13B, $p < 0.001$). All coAP amplitude

data was non-normal and thus transformed using the natural logarithm, but for clarity original mean values are also reported.

Previous research has determined that sensory and descending motor inputs produce different patterns of system short-term plasticity in motor outputs. High frequency repetitive stimulation (25-100 Hz) of sensory inputs causes system short-term depression (sSTD), while identical stimulation of descending motor inputs yields system short-term facilitation (sSTF) (Jiang et al., 2015; Mahrous et al., 2019). Identical adaptation patterns were present in both genotypes following stimulation of sensory (sSTD) or descending motor (sSTF) inputs at 25 Hz (Figure 14 and 15). The degree of sSTD and sSTF was quantified as outlined in the methods section. Sensory and descending motor inputs in SOD and WT mice produced comparable amounts of sSTD or sSTF, respectively (Figure 14 and 15). However, sSTD increased over the five pulses of sensory input stimulation at 1.5 and 10xT in both SOD and WT mice (Figure 14, $p < 0.001$).

A

B
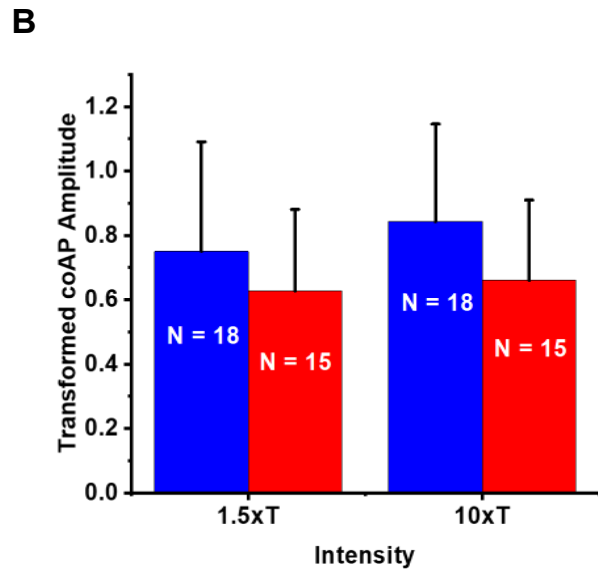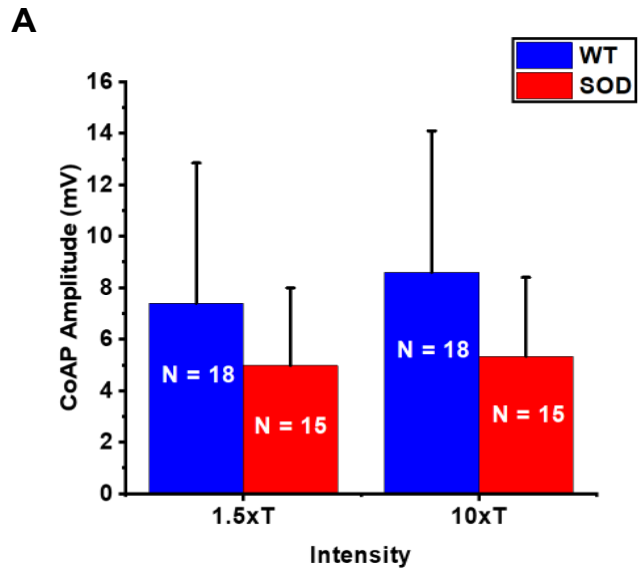
Figure 12. Evoked coAPs following stimulation of sensory inputs in SOD mice at symptom onset

Repetitive stimulation (0.06 Hz at 1.5 or 10xT) of sensory inputs evoked comparable coAPs in WT and SOD mice. Both original **(A)** and transformed **(B)** mean values are reported, as coAP amplitude data for sensory input stimulation had a non-normal distribution. The original values were transformed using the natural logarithm. The bars represent the mean ± SD.
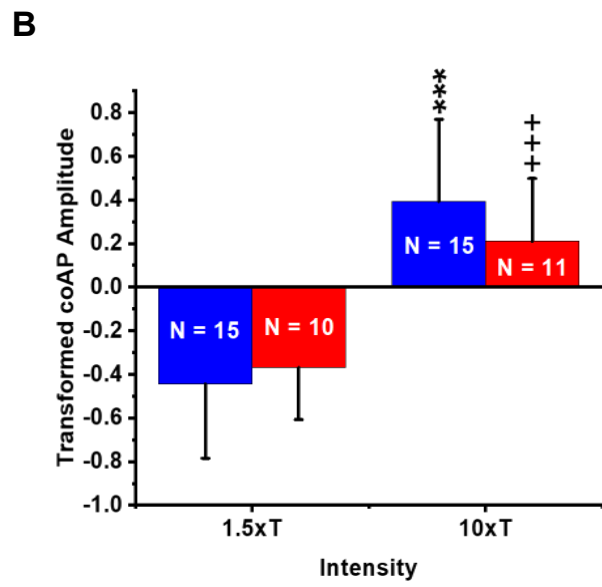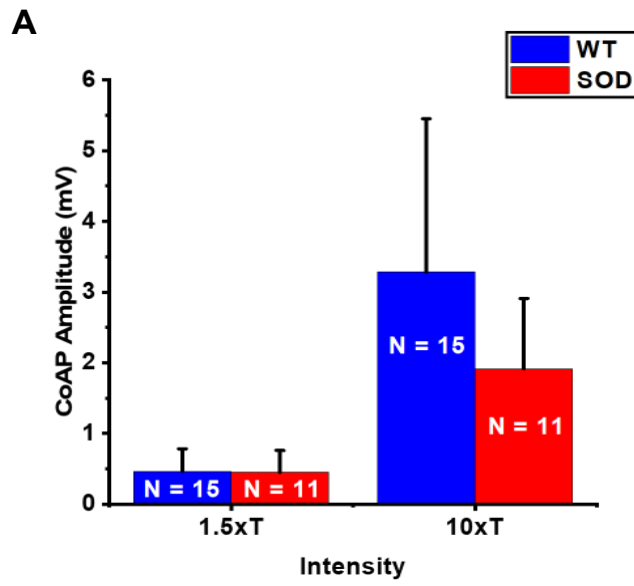
Figure 13. Evoked coAPs following stimulation of descending motor inputs in SOD mice at symptom onset

Repetitive stimulation (0.06 Hz at 1.5 or 10xT) of descending motor inputs evoked comparable coAPs in WT and SOD mice. In addition, both WT and SOD mice exhibited significantly larger coAPs in response to descending motor input stimulation at 10xT compared to 1.5xT. Both original **(A)** and transformed **(B)** mean values are reported, as coAP amplitude data for descending motor input stimulation had a non-normal distribution. The original values were transformed using the natural logarithm. The bars represent the mean ± SD. Statistical differences are shown (*******: WT 10xT vs. 1.5xT and +++: SOD 10xT vs. 1.5xT, $p < 0.001$; Bonferroni multiple comparisons test).

WT

SOD

A

B

1 mV

40 ms

C   *1.5xT*

sSTD (%)

WT (N=18)
SOD (N=15)

D   *10xT*

sSTD (%)

WT (N=18)
SOD (N=15)
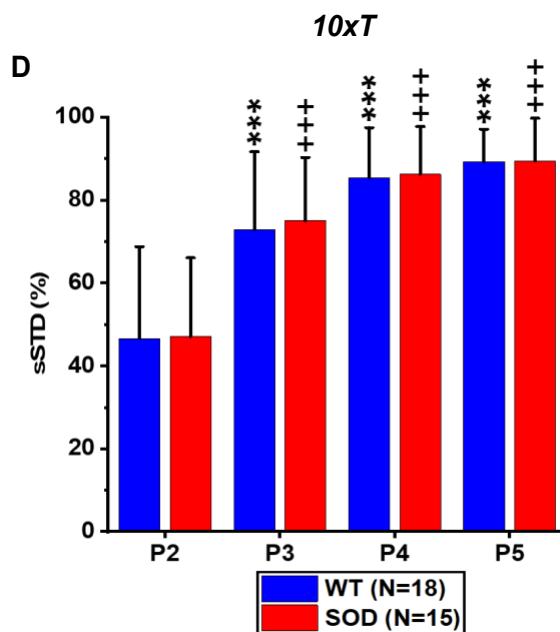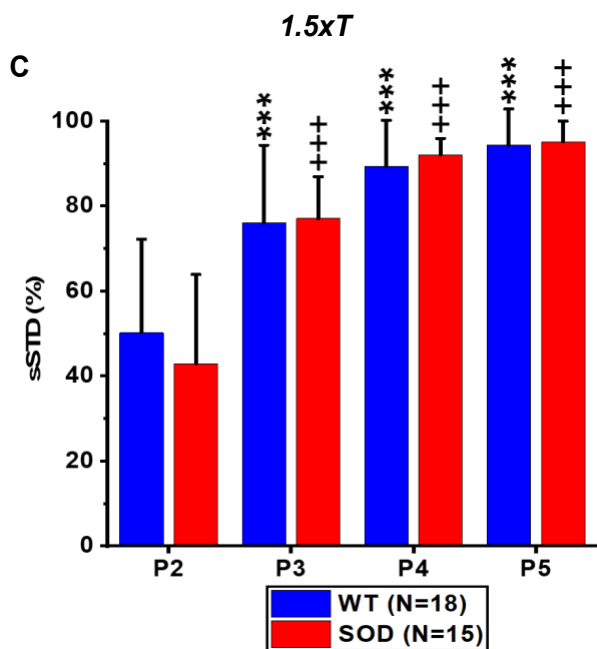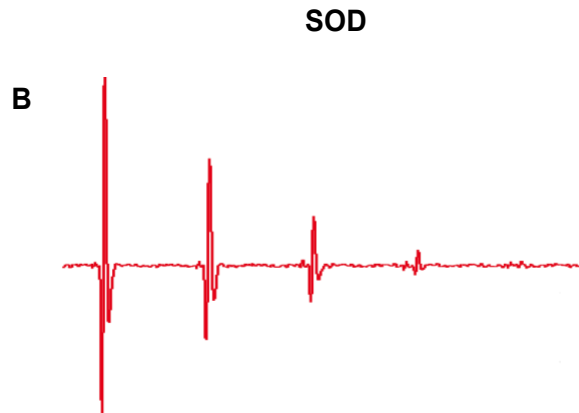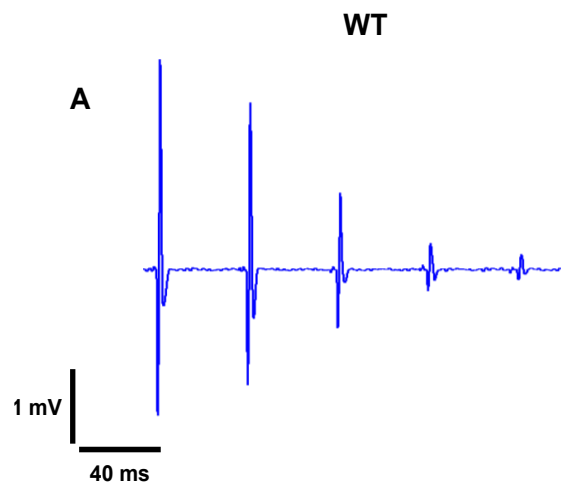
Figure 14. Sensory inputs exhibit normal sSTD in SOD mice at symptom onset

Sensory inputs in both WT **(A)** and SOD **(B)** mice showed sSTD following 25 Hz

repetitive stimulation at 1.5xT. These same adaptation patterns were also found at 10xT

(not pictured). At both stimulation intensities **(C and D)**, sensory inputs exhibited

comparable amounts of sSTD in WT and SOD mice. However, the degree of sSTD

significantly increased over the five pulses of stimulation at both 1.5 and 10xT in WT and

SOD mice. Bars represent mean ± SD. Statistical differences are shown (*******: different

from WT P2 at 1.5 or 10xT and +++: different from SOD P2 at 1.5 or 10xT, $p < 0.001$;

Bonferroni multiple comparisons test).

A WT

B SOD

1 mV

40 ms

C *1.5xT*

sSTF (%)

WT (N=14)
SOD (N=10)

D *10xT*

sSTF (%)

WT (N=15)
SOD (N=11)
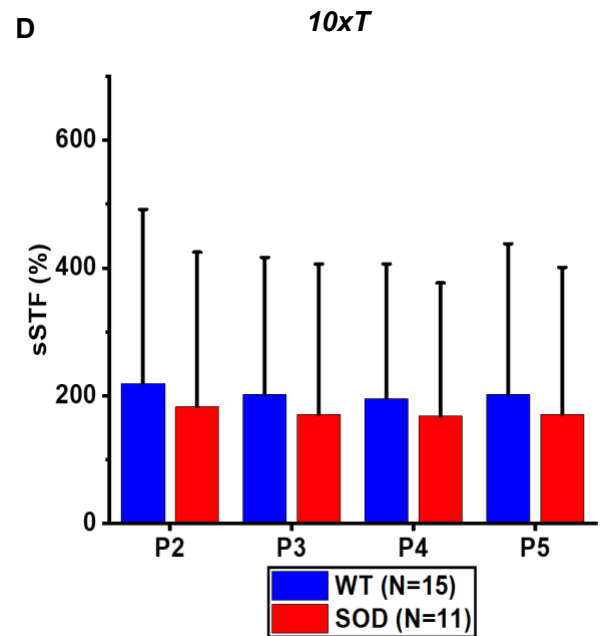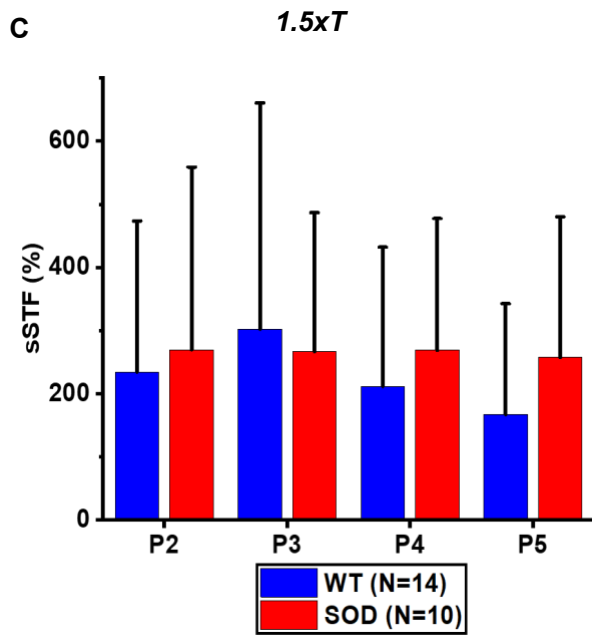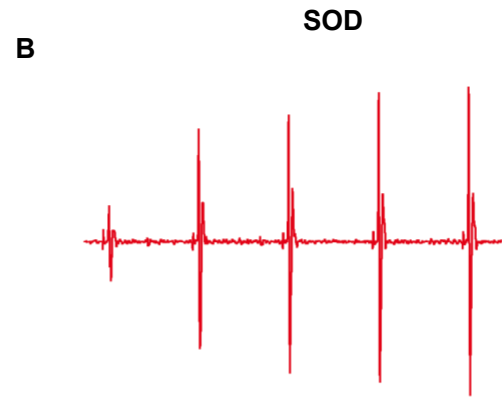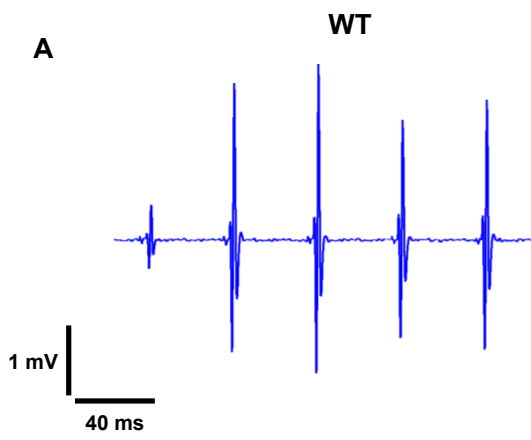
Figure 15. Descending motor inputs exhibit normal sSTF in SOD mice at symptom onset

Descending motor inputs in both WT **(A)** and SOD **(B)** mice exhibited sSTF following 25 Hz repetitive stimulation at 1.5xT. These same adaptation patterns were also found at 10xT (not pictured). At both stimulation intensities **(C and D)**, descending motor inputs exhibited comparable amounts of sSTF in WT and SOD mice. Data is represented as mean ± SD.

Sensorimotor integration is significantly impaired in SOD mice at symptom onset

Individually, sensory and descending motor inputs generate different patterns of system short-term plasticity in motor output. Yet, the motor output of the spinal cord is stable during most tasks and simultaneous stimulation of both sensory and descending motor inputs produces similar responses or coAPs (Mahrous et al., 2019). Thus, sensorimotor integration, the combination of both sensory inputs from the periphery and descending motor commands from supraspinal structures, is necessary to produce suitable motor output for any given motor task (Kim et al., 2017; Mahrous et al., 2019; Rossignol et al., 2006). In ALS, motor function is significantly impaired, and the onset of these deficits is primarily attributed to the progressive loss of MNs over the course of the disease. However, the integration of sensory and descending motor inputs may also be compromised and consequently contribute to the development of motor deficits in ALS.

To investigate the effects of ALS on sensorimotor integration at symptom onset, we measured evoked coAPs or motor output following repetitive stimulation (5-pulse train) of sensory (S) and descending motor (M) inputs simultaneously (S&M) at frequencies of 0.06 or 25 Hz and intensities of 1.5 or 10xT in the same sample discussed in the previous section. All five coAPs that were evoked following S&M stimulation at 0.06 Hz were averaged to examine differences in coAP amplitudes. SOD mice exhibited smaller coAPs following S&M stimulation at 1.5xT, but these values were not significantly different from WT mice. However, these differences reached statistical significance at 10xT (Figure 16A, WT 14.28 mV $\pm$ 4.88 SD vs. SOD 8.09 mV $\pm$ 4.75 SD). S&M coAP amplitude data was non-normal and thus transformed using the natural logarithm (Figure 16B, p = 0.008), but for clarity original mean values are reported.

S&M stimulation at 25 Hz using 5-pulse trains produced stable motor output or coAPs in both SOD and WT mice (Figure 17). In order to quantify sensorimotor integration, we used the calculation outlined in the methods section. SOD mice exhibited a significant deficit in sensorimotor integration at 1.5 and 10xT (Figure 17). In addition, sensorimotor integration in WT mice was significantly amplified over the five pulses of stimulation at both 1.5 and 10xT ($p < 0.001$). Sensorimotor integration data at 1.5xT (Figure 17C) was non-normal and thus transformed using the natural logarithm.

Taken together, these data demonstrate that sensory and descending motor inputs in SOD mice at symptom onset evoke normal motor output. Additionally, these inputs do not contribute to MN excitability alterations at this time point, as stimulation of these synaptic inputs separately results in comparable system short-term plasticity in the motor output of SOD and WT mice. Despite apparently normal sensory and descending motor inputs, SOD mice demonstrate a significant impairment in the integration of these inputs at symptom onset.

In conclusion, the data in Specific Aim 1 of this dissertation showed for the first time the state of individual MN excitability at symptom onset in SOD mice. Despite both hypoexcitable and hyperexcitable changes in intrinsic properties, net excitability of SOD MNs was reduced. In addition, the excitability state of the spinal MN network in SOD mice at symptom onset was characterized. These studies revealed that sensory and descending motor inputs to spinal MNs do not contribute to differences in SOD MN excitability at symptom onset. These studies also discovered a new mechanism contributing to the development of motor deficits in SOD mice at symptom onset, impairments in sensorimotor integration.

A

B
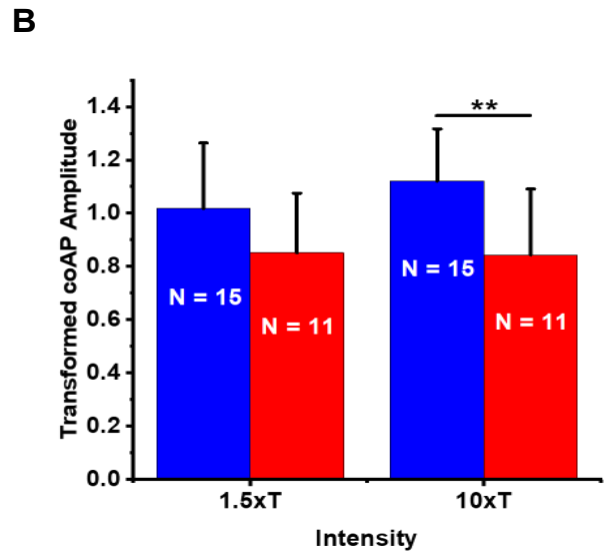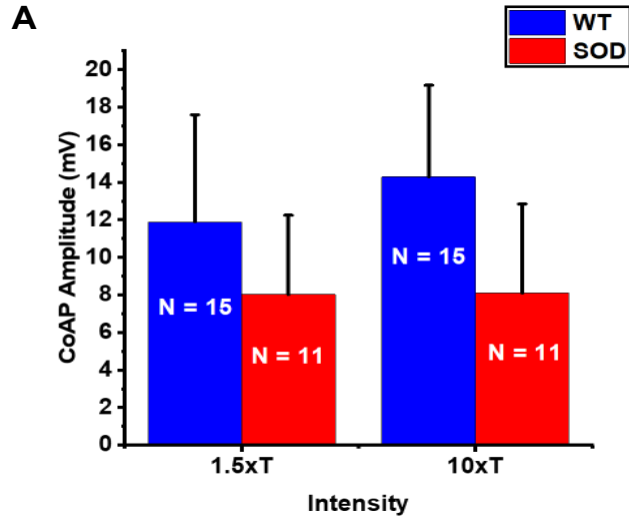
Figure 16. S&M stimulation evokes smaller coAPs in SOD mice at symptom onset

Simultaneous stimulation (0.06 Hz at 1.5 or 10xT) of sensory and descending motor inputs evoked smaller coAPs in SOD mice at symptom onset at both 1.5 and 10xT, but these differences were only statistically significant at 10xT. Both original **(A)** and transformed **(B)** mean values are reported, as coAP amplitude data for simultaneous stimulation of sensory and descending motor inputs had a non-normal distribution. The original values were transformed using the natural logarithm. The bars represent the mean ± SD. Statistical difference indicated (******, $p < 0.01$; Bonferroni multiple comparisons test).

WT

SOD

A

B

1 mV

40 ms

1.5xT

10xT

C

D

WT (N=15)
SOD (N=11)

WT (N=15)
SOD (N=11)

83
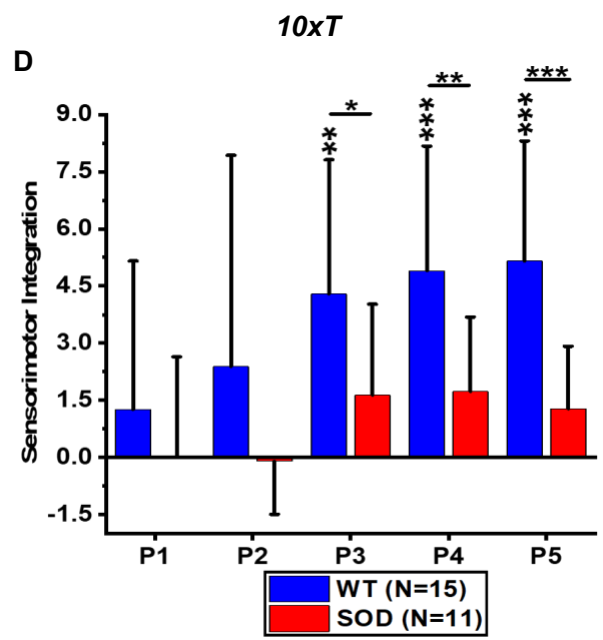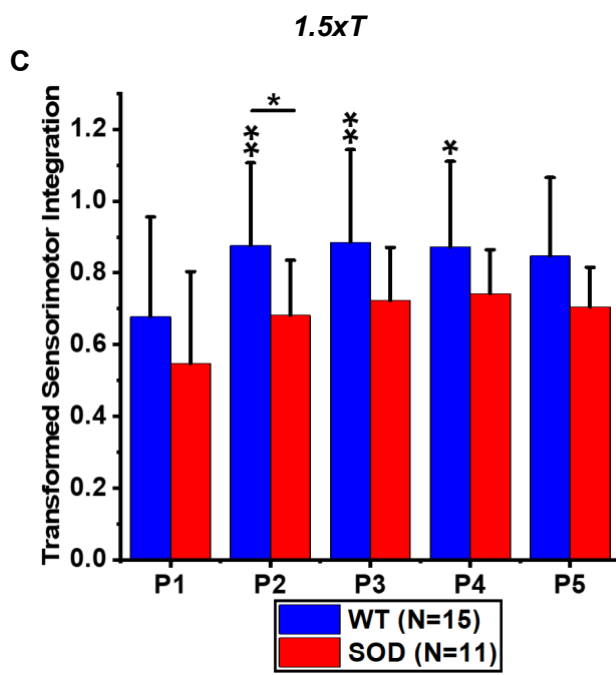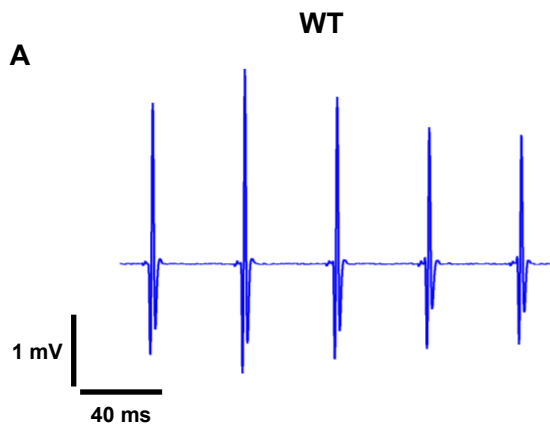
Figure 17. Integration of sensory and descending motor inputs is significantly impaired in SOD mice at symptom onset

Simultaneous stimulation (25 Hz at 1.5xT) of sensory and descending motor inputs evoked stable motor outputs in both WT **(A)** and SOD **(B)** mice. Similar patterns were also observed at 10xT (not pictured). However, SOD mice exhibited a significant deficit in sensorimotor integration at both 1.5 **(C)** and 10xT **(D)**. Additionally, at both 1.5 and 10xT, sensorimotor integration was amplified in WT mice over the five pulses of stimulation. Sensorimotor integration data at 1.5xT was non-normal and thus transformed using the natural logarithm. The bars represent the mean $\pm$ SD. Statistical differences are indicated (*, $p < 0.05$, **, $p < 0.01$, and ***, $p < 0.001$; Bonferroni multiple comparisons test). Asterisks over the WT bars are comparing WT P1 vs. WT P2-P5 and asterisks above a single black bar are comparing differences between SOD and WT mice).

Chapter V: Specific Aim 2

The long-term effects of early treatment of SOD1-G93A$^{\text{High-Copy}}$ (SOD) mice with CyPPA on the excitability of individual motorneurons (MNs) and the spinal MN network

The overall objective of Specific Aim 2 was to determine the long-term effects of early treatment of SOD mice with CyPPA, an SK channel activator, on the excitability of MNs at the individual and network levels.

Introduction

Currently, there are only two drugs approved to treat ALS in the United States, Riluzole and Edaravone, but neither cures the disease nor improves quality of life in patients (Jaiswal, 2019). Still, over 60 other molecules have been investigated as potential treatments for ALS. However, many of these molecules delayed progression in preclinical animal models of ALS but failed to show efficacy in human clinical trials (Petrov et al., 2017). This disconnect between animal research and human clinical trials is attributed to the complex and unknown etiology of ALS. Consequently, our lab began investigating a new molecule likely involved in ALS, the small-conductance calcium-activated potassium (SK) channel. SK channels are unevenly expressed in MN subtypes and regulate MN excitability via the afterhyperpolarization (AHP). Specifically,

large or F-type MNs only express SK2 channels, while small or S-type MNs express both SK2 and SK3 channel isoforms (Deardorff et al., 2013; Dukkipati et al., 2018). SK3 channels in S-type MNs primarily facilitate their longer duration/larger amplitude AHPs (Elbasiouny laboratory, unpublished). Interestingly, S-type MNs are also less susceptible to degeneration in ALS. Thus, differences in SK channels may underlie the vulnerability differential of MN subtypes in ALS.

In order to study the role of SK channels in ALS, we initially used a high-fidelity computational model of neonatal SOD MNs. These simulations found SK channel current to be downregulated in SOD MNs (Elbasiouny laboratory, unpublished). Next, we confirmed our simulations with immunohistochemistry studies which demonstrated SK channel downregulation throughout disease progression in SOD MNs (Dukkipati, 2016). These deficits were improved by early treatment (postnatal day (P) 5- P20) with CyPPA. Treatment with CyPPA restored the somatic clustering profile of SK channels in SOD MNs up to 70 days following treatment cessation (i.e., P90 or symptom onset) (Murphy, 2020). In addition, CyPPA treatment delayed motor function decline and prolonged survival by 10 days in SOD mice (Dancy, 2017).

These data established the therapeutic potential of CyPPA in SOD mice but did not elucidate the functional effects of CyPPA on the excitability of individual MNs and the spinal MN network. Therefore, this study examined the long-term effects of early treatment of SOD mice with CyPPA on the excitability of individual MNs and the spinal MN network.

Results

Specific Aim 2A: The long-term effects of early treatment of SOD mice with CyPPA on the excitability of individual MNs

Early treatment with CyPPA does not restore passive membrane properties in SOD MNs at symptom onset

In order to determine the long-term effects of early treatment of SOD mice with CyPPA on the excitability of individual MNs, we first administered CyPPA to 9 SOD mice for the same 16-day period (P5-P20) used in our initial studies. These mice or MNs from these mice are denoted as 'SOD-CyPPA'. Next, we aged SOD-CyPPA mice until approximately symptom onset (95.19 days $\pm$ 5.05 SD, actual range: 89-104) and examined the same intrinsic properties measured in Chapter IV. In that chapter, we characterized the excitability of individual MNs and the spinal MN network in untreated SOD mice at symptom onset relative to their age-matched wild-type (WT) transgenic littermates. These SOD mice served as our official control for the current study and thus the SOD and WT data discussed in this chapter is the same data from Chapter IV.

At symptom onset, SOD MNs exhibit both hypo- and hyperexcitable changes in intrinsic properties relative to WT MNs. Thus, if early treatment of SOD mice with CyPPA has long term effects on the excitability of individual SOD MNs, one or more of these intrinsic properties would be restored in SOD-CyPPA MNs. Initially, we examined passive membrane properties. At symptom onset, SOD MNs exhibit hypoexcitable changes in passive membrane properties with a significant decrease in input resistance (R_{in}) and a significant increase in input conductance (G_{in}) and capacitance compared to WT MNs (Figure 4 and Figure 18). Following treatment with CyPPA, these deficits

persisted. Accordingly, SOD-CyPPA MNs exhibited a significant decrease in R_{in} relative

to WT MNs (Figure 18A, WT 12.87 MΩ ± 2.70 SD vs. SOD-CyPPA 8.68 MΩ ± 1.91

SD, p = 0.00001). These values were also significantly lower than our measurements

from SOD MNs at baseline (10.75 MΩ ± 3.82 SD, p = 0.026). The significant increase in

G_{in} (Figure 18B, WT 0.08 μS ± 0.02 SD vs. SOD-CyPPA 0.12 μS ± 0.02 SD, p =

0.00001) and capacitance (Figure 18C, WT 0.13 nF ± 0.04 SD vs. SOD-CyPPA 0.19 nF

± 0.06 SD, p = 0.027) also continued in SOD-CyPPA MNs relative to WT MNs, but

these differences were absent between SOD-CyPPA and SOD MNs.

Similar to SOD MNs, SOD-CyPPA MNs exhibited no differences in RMP, time

constant (tau), and rheobase relative to WT MNs (Figure 18). These properties were also

similar between SOD-CyPPA and SOD MNs. Altogether, these data indicate that early

treatment of SOD mice with CyPPA does not restore passive membrane properties in

SOD MNs at symptom onset.
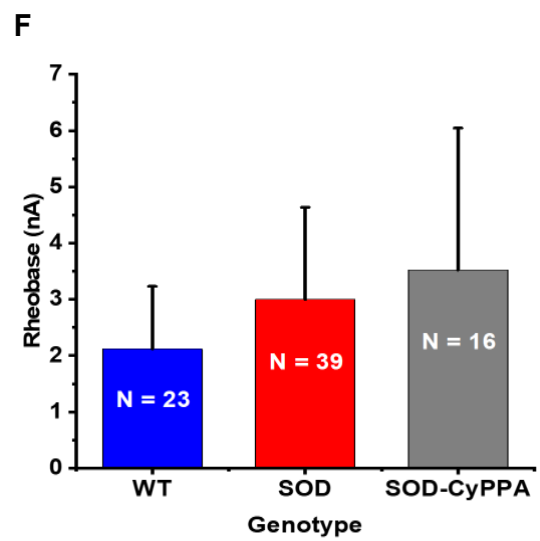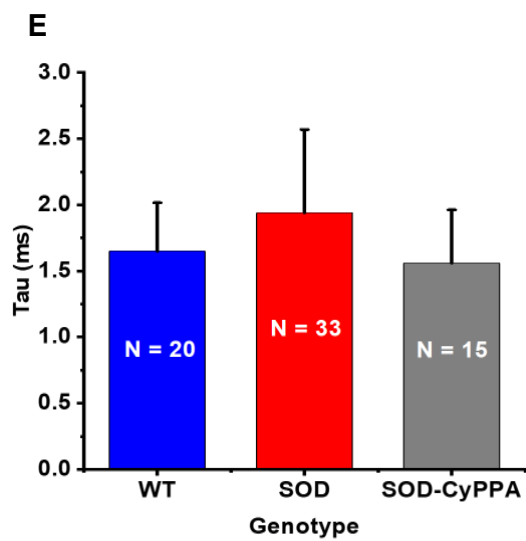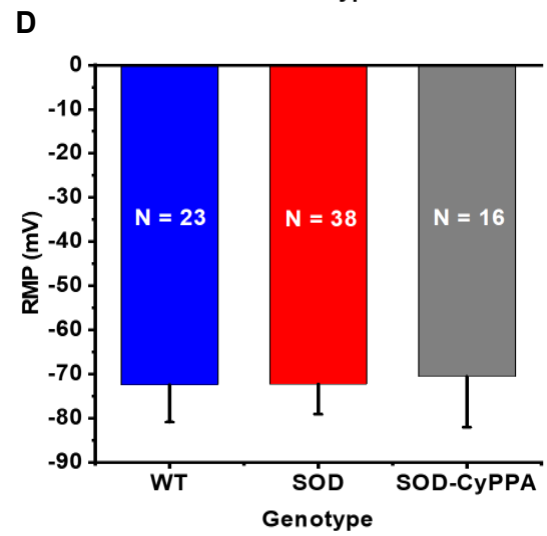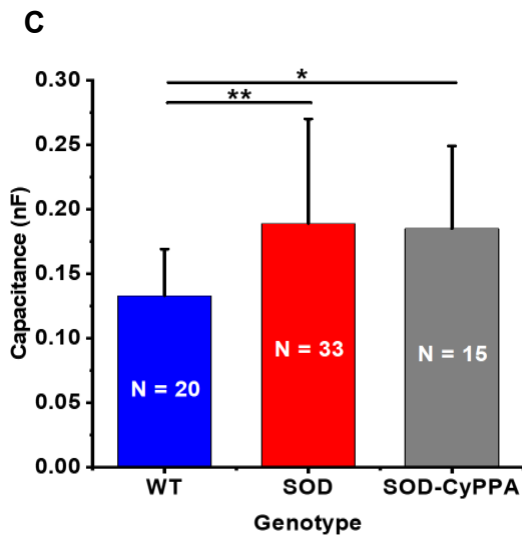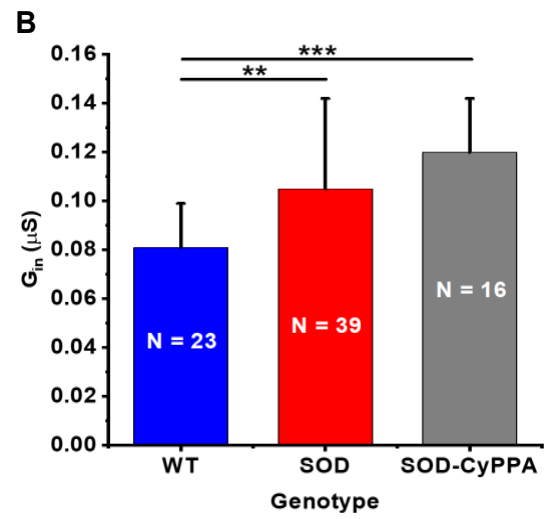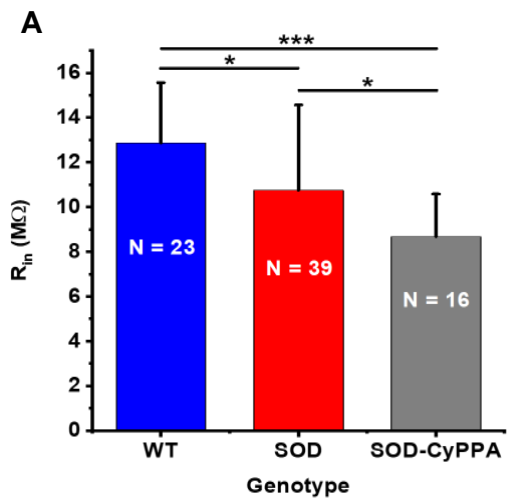
Figure 18. Early treatment of SOD mice with CyPPA does not restore passive membrane properties in SOD MNs at symptom onset

Passive membrane properties were measured in MNs from SOD mice treated with CyPPA. Similar to SOD MNs, SOD-CyPPA MNs exhibited a significant decrease in R_{in} **(A)** and a significant increase in G_{in} **(B)** and capacitance **(C)**, but no differences in RMP **(D)**, tau **(E)**, or rheobase **(F)** relative to WT MNs. R_{in} in SOD-CyPPA MNs was also significantly lower compared to SOD MNs, but all other properties were similar between these two groups. The bars represent the mean $\pm$ SD. Significant differences are shown (*, $p < 0.05$; **, $p < 0.01$, and ***, $p < 0.001$; Games-Howell post-hoc tests).

Early treatment of SOD mice with CyPPA does not alter AP properties nor restore AHP amplitude or SK channel conductance (G$_{SK}$ density) in SOD MNs at symptom onset

At symptom onset, SOD MNs exhibit no alterations in AP properties (Table 2) but show a significant reduction in AHP amplitude (Figure 6) and G$_{SK}$ density (Figure 7) compared to WT MNs. Similar to SOD MNs, SOD-CyPPA MNs exhibited no changes in AP properties relative to WT MNs (Table 6). AP properties in SOD-CyPPA MNs were also comparable to SOD MNs. In addition, early treatment with CyPPA did not restore AHP amplitude or G$_{SK}$ density in SOD MNs at symptom onset. While AHP amplitude and G$_{SK}$ density in SOD-CyPPA MNs were not statistically different from WT MNs, these properties were also similar between SOD-CyPPA and SOD MNs (Figure 19 and Figure 20). Additionally, SOD-CyPPA MNs exhibited no differences in AHP time to rise, half-decay, two-thirds decay, and half-duration relative to WT MNs (Table 7). These properties were also similar between SOD-CyPPA and SOD MNs.

Early treatment of SOD mice with CyPPA does not alter repetitive firing properties measured by long (2 s) current pulses or restore net excitability in SOD MNs at symptom onset

At symptom onset, all repetitive firing properties measured by long current pulses are comparable between SOD and WT MNs with the exception of the interspike interval slope (ISI) (Table 4). Specifically, WT MNs exhibit a significant increase in ISI slope as current pulse amplitude increases, whereas SOD MNs maintain a steady negative ISI slope (Figure 9). A similar relationship between ISI slope and current pulse was also found in SOD-CyPPA MNs (Figure 21). Thus, compared to WT MNs, ISI voltage in

SOD and SOD-CyPPA MNs hyperpolarizes over time with increasing current pulse amplitude.

Lastly, we examined repetitive firing behavior measured by triangular current ramps. At symptom onset, despite both hypo- and hyperexcitable changes in intrinsic MN properties, the net excitability or F-I gain[7] of SOD MNs is reduced compared to WT MNs (Figure 11). Following early treatment of SOD mice with CyPPA, these deficits were still present (Figure 22). In addition, SOD-CyPPA MNs exhibited no differences in I_{on}, I_{off}, deltaI, or maximum firing frequency relative to WT MNs, which is identical to our findings in SOD MNs at baseline (Table 8). Also, F-I gain, I_{on}, I_{off}, deltaI, and maximum firing frequency were comparable between SOD-CyPPA and SOD MNs.

Since ALS-induced deficits in intrinsic MN properties were not restored in SOD-CyPPA MNs, the data from Specific Aim 2A suggests that early treatment of SOD mice with CyPPA does not alter individual MN excitability.

---

[7] The ascending (F-I_{Asc}) and descending (F-I_{Desc}) slopes of the F-I relationship

	WT	SOD	SOD-CyPPA
AP height, mV	63.03 ± 10.81	62.63 ± 9.70	60.88 ± 10.37
Maximum rising slope, V/s	87.27 ± 33.08	85.98 ± 34.76	81.60 ± 35.87
Average rising slope, V/s	44.60 ± 14.63	44.61 ± 16.04	39.65 ± 14.76
Maximum falling slope, V/s	-71.91 ± 14.27	-70.00 ± 16.51	-69.43 ± 15.42
Average falling slope, V/s	-33.97 ± 8.03	-34.03 ± 9.97	-32.66 ± 8.23
AP half-width, ms	1.24 ± 0.19	1.23 ± 0.17	1.26 ± 0.17
AP width, ms	3.22 ± 0.58	3.15 ± 0.61	3.26 ± 0.62
AP time to rise, ms	1.42 ± 0.30	1.45 ± 0.39	1.59 ± 0.40

Table 6. AP properties in SOD-CyPPA MNs relative to WT and SOD MNs mean ±SD
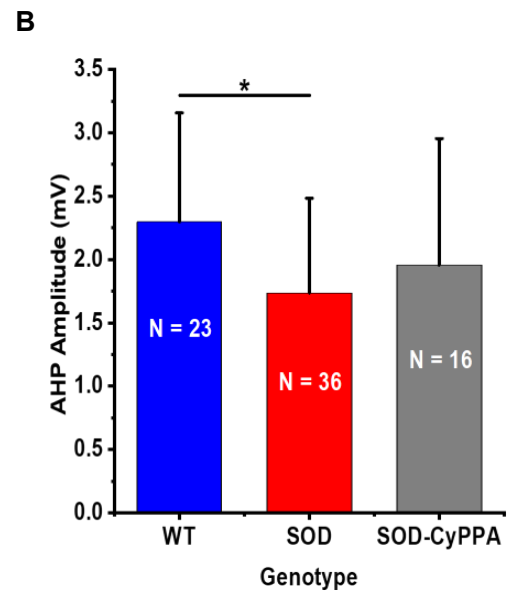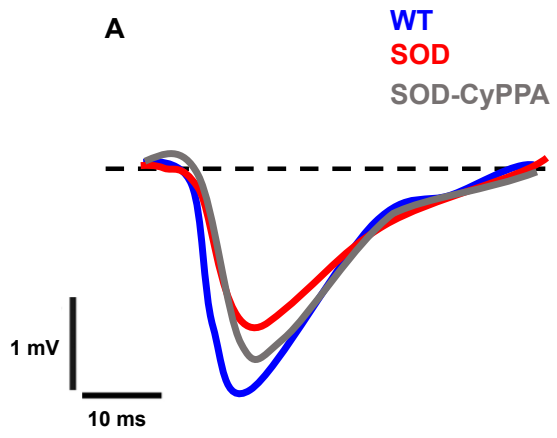
Figure 19. Early treatment of SOD mice with CyPPA does not restore AHP amplitude in SOD MNs at symptom onset

(A) Superimposition of representative sample AHPs recorded on isolated APs from a WT (blue), SOD (red), and SOD-CyPPA (gray) MN. At symptom onset, SOD MNs exhibit a significant decrease in AHP amplitude relative to WT MNs **(B)**, but this statistical difference was absent following early treatment of SOD mice with CyPPA. However, AHP amplitude was comparable between SOD-CyPPA and SOD MNs. Bars represent the mean $\pm$ SD. Statistical difference indicated (*****, $p < 0.05$; Tukey's post-hoc test).

A

B
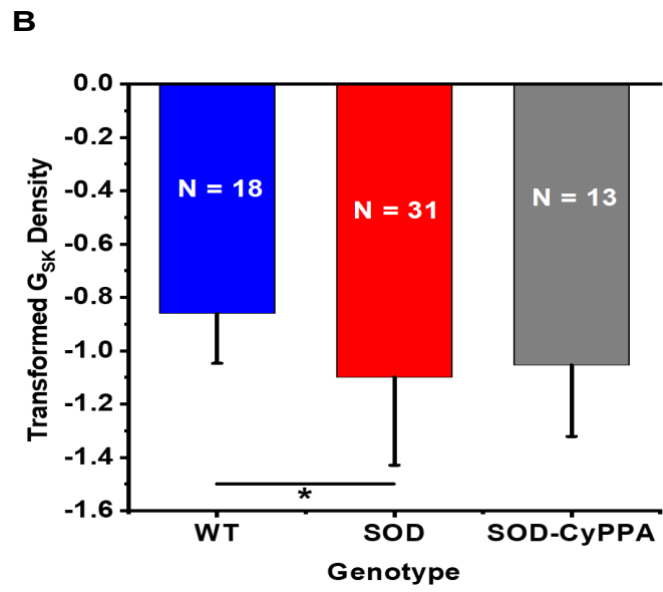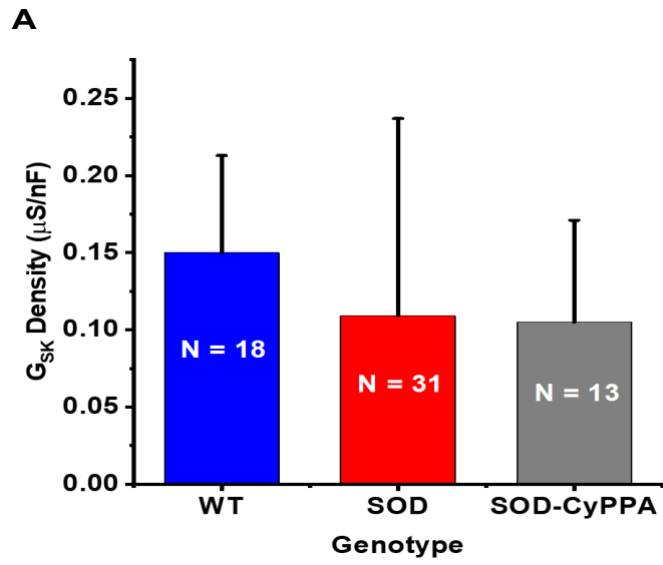
Figure 20. Early treatment of SOD mice with CyPPA does not restore G_{SK} density in SOD MNs at symptom onset

At symptom onset, SOD MNs exhibit a significant reduction in G_{SK} density compared to WT MNs, but this statistical difference was absent after early treatment of SOD mice with CyPPA. However, G_{SK} density was comparable between SOD-CyPPA and SOD MNs. Both original (**A**) and transformed (**B**) mean values are reported, as G_{SK} density had a non-normal distribution. The original values were transformed using the natural logarithm. The bars represent the mean $\pm$ SD. Statistical difference indicated (*****, $p < 0.05$; Tukey's post-hoc test).

	WT	SOD	SOD-CyPPA
AHP amplitude, mV	2.30 ± 0.86	1.74 ± 0.75*	1.96 ± 1.00
AHP time to rise, ms	12.73 ± 4.72	11.89 ± 4.23	11.83 ± 3.58
AHP half-decay, ms	19.99 ± 8.10	19.35 ± 9.01	19.43 ± 6.44
AHP two-thirds decay, ms	53.87 ± 18.01	59.50 ± 21.35	60.84 ± 28.20
AHP half-duration, ms	29.92 ± 10.93	27.87 ± 10.62	27.83 ± 6.44
G_{SK} density, µS/nF	0.15 ± 0.06	0.11 ± 0.13	0.11 ± 0.07
G_{SK} density transformed	-0.86 ± 0.19	-1.10 ± 0.33*	-1.05 ± 0.27

Table 7. AHP properties in SOD-CyPPA MNs relative to WT and SOD MNs
mean $\pm$ SD, *p < 0.05, **p < 0.01
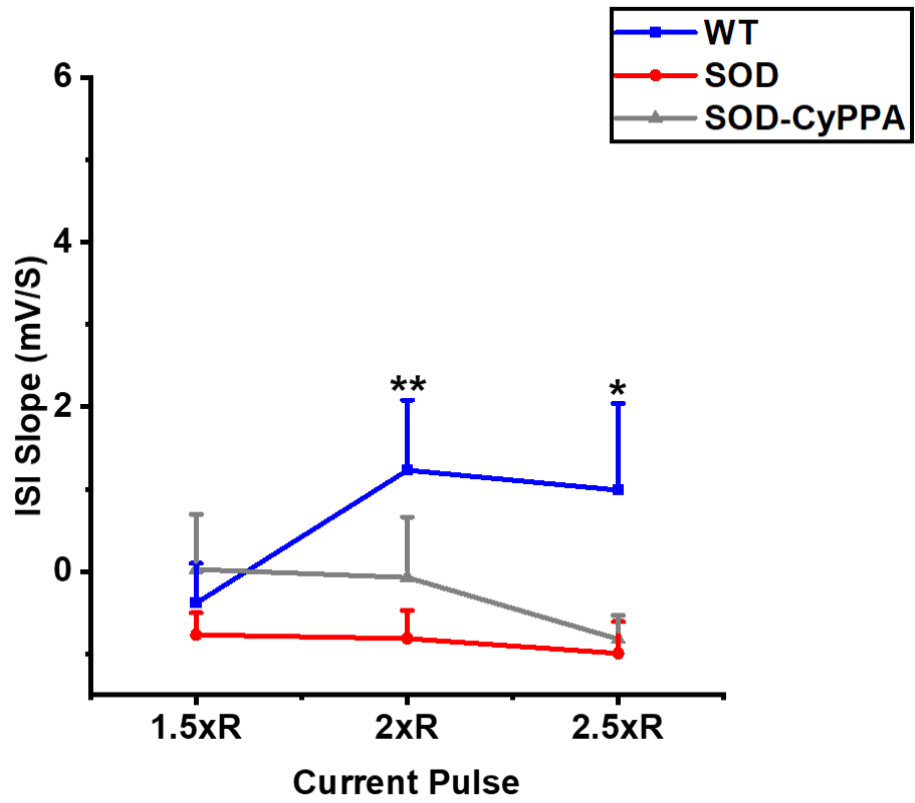
Figure 21. Early treatment of SOD mice with CyPPA does not alter the ISI slope

At symptom onset, SOD MNs exhibit a steady negative ISI slope with increasing current amplitude and a similar relationship between ISI slope and current pulse was found in SOD-CyPPA MNs. Hence, compared to WT MNs, ISI voltage in SOD and SOD-CyPPA MNs hyperpolarizes over time with increasing current pulse amplitude. Each data point represents the mean and error bars denote the SE. Significant differences are shown (*****, $p < 0.05$ and ******, $p < 0.01$; Bonferroni multiple comparisons test) and each asterisk indicates the difference from the first WT data point at the 1.5xR current pulse.
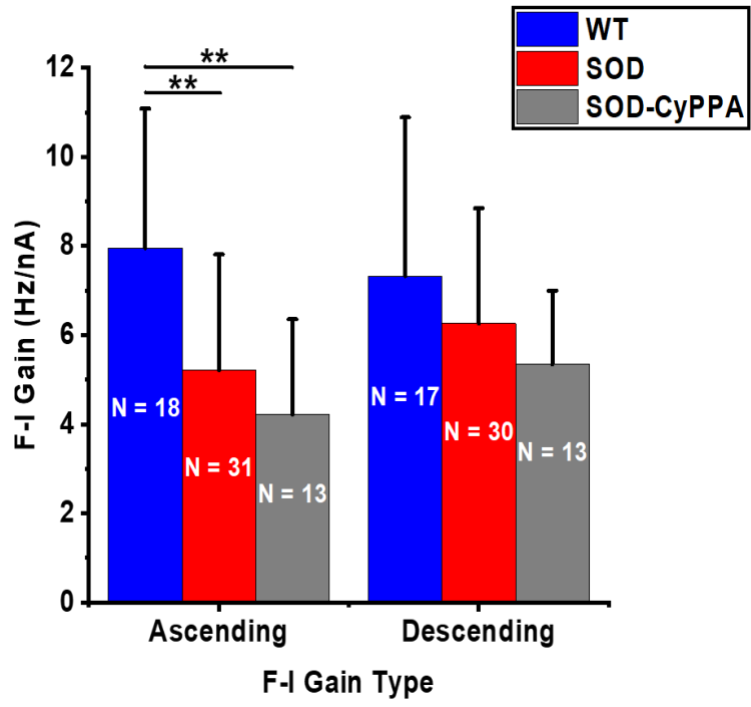
Figure 22. Early treatment of SOD mice with CyPPA does not restore net excitability in SOD MNs at symptom onset

At symptom onset, SOD MNs exhibit a significant reduction in F-I_{Asc} compared to WT MNs and this deficit was still present in SOD-CyPPA MNs. Similar to SOD MNs, F-I_{Desc} was also reduced in SOD-CyPPA MNs relative to WT MNs, but these differences were not statistically significant. There were no differences between F-I_{Asc} or F-I_{Desc} between SOD-CyPPA and SOD MNs. The bars represent the mean $\pm$ SD. Statistical differences indicated (**, $p < 0.01$; Tukey's post-hoc test).

	WT	SOD	SOD-CyPPA
I_{on}, nA	2.97 ± 1.71	4.06 ± 2.66	5.39 ± 2.97
I_{off}, nA	2.83 ± 1.76	3.79 ± 3.25	4.89 ± 2.79
deltaI (I_{off} - I_{on})	0.14 ± 0.89	0.27 ± 1.15	0.50 ± 0.93
Maximum firing frequency, Hz	47.42 ± 17.44	41.77 ± 12.21	40.31 ± 13.79
F-I_{Asc}, Hz/nA	7.96 ± 3.12	5.21 ± 2.61**	4.22 ± 2.14**
F-I_{Desc}, Hz/nA	7.33 ± 3.56	6.27 ± 2.58	5.35 ± 1.65

Table 8. Repetitive firing properties measured during triangular current ramps in SOD-CyPPA MNs relative to WT and SOD MNs   *mean $\pm$ SD, **p < 0.01*

Specific Aim 2B: The long-term effects of early treatment of SOD mice with CyPPA on the excitability of the spinal MN network

Early treatment with CyPPA does not alter sensory or descending motor inputs in the spinal MN network of SOD mice at symptom onset

While SK channels are well-known for their regulation of the AHP, these channels also regulate synaptic inputs, transmission, and plasticity (Faber et al., 2008; Faber et al., 2005; Nanou et al., 2013; Ngo-Anh et al., 2005). Thus, early treatment of SOD mice with CyPPA may alter the excitability of the spinal MN network. In Chapter IV, we examined sensory and descending motor inputs and their integration in the spinal MN network of SOD mice at symptom onset. To do so, we measured compound action potentials (coAPs) produced by repetitive stimulation (5-pulse train) of sensory (via dorsal roots) or descending motor (via remaining descending axons in the spinal cord tissue) inputs at frequencies of 0.06 or 25 Hz and intensities of 1.5 or 10-times threshold (1.5 or 10xT). Threshold denotes the smallest amount of current needed to evoke a coAP and from these measurements we evaluated the amplitudes of evoked coAPs and the degree of system short-term depression (sSTD) and facilitation (sSTF). Together, these measurements depict the excitability of the spinal MN network. In order to determine the long-term effects of early treatment of SOD mice with CyPPA on the excitability of the spinal MN network, we examined these same measurements in 19 SOD-CyPPA mice near symptom onset (99.00 days ± 5.20 SD, actual range: 89-109).

Similar to SOD mice, sensory and descending motor inputs in SOD-CyPPA mice evoked comparable coAPs (Figure 23 and 24) and produced similar amounts of system short-term plasticity (Figure 25 and 26) relative to WT mice. CoAP amplitude and

system-short term plasticity measurements were also comparable between SOD-CyPPA and SOD mice for both inputs. However, stimulation of descending motor inputs in SOD-CyPPA mice at 10-times threshold (10xT) evoked larger coAPs than at 1.5xT (Figure 24B, p < 0.001) and sSTD increased over the five pulses of sensory input stimulation at 1.5 and 10xT in these mice (Figure 25, p < 0.001). These findings were also present in both SOD and WT mice. These data suggest that early treatment of SOD mice with CyPPA does not influence the excitability of the spinal MN network.

Early treatment with CyPPA does not restore deficits in sensorimotor integration in SOD mice at symptom onset

Individually, sensory and descending motor inputs trigger different patterns of system short-term plasticity in motor output, but the integration of these two inputs allows the production of stable and appropriate motor output for any given motor task. In Chapter IV, we found deficits in sensorimotor integration in SOD mice at symptom onset. Despite comparable coAPs and system-short term plasticity in SOD and WT mice following stimulation of sensory (S) and descending motor (M) inputs separately, SOD mice exhibited smaller coAPs in response to simultaneous stimulation (S&M) of these inputs at 0.06 Hz irrespective of intensity, but these differences were only significant at 10xT (Figure 16). SOD mice also demonstrated significant deficits in sensorimotor integration following 25 Hz S&M stimulation (Figure 17). These data revealed a new mechanism contributing to the development of motor deficits in SOD mice at symptom onset. Furthermore, early treatment of SOD mice with CyPPA may restore these deficits, as CyPPA has been shown to sustain motor function in these mice (Dancy, 2017). Consequently, we examined the integration of sensory and descending motor inputs in

SOD-CyPPA mice. Similar to SOD mice, SOD-CyPPA mice exhibited smaller evoked coAPs following S&M stimulation relative to WT mice (Figure 27). The degree of sensorimotor integration was also significantly reduced in SOD-CyPPA mice compared to WT mice (Figure 28). However, there were no differences in coAP amplitude and sensorimotor integration following S&M stimulation between SOD-CyPPA and SOD mice.

In conclusion, the data in Specific Aim 2 of this dissertation showed for the first time the long-term effects of early treatment of SOD mice with CyPPA on the excitability of individual MNs and the spinal MN network. In previous studies, we showed that early treatment of SOD mice with CyPPA prolongs survival, sustains motor function, and restores the somatic clustering profile of SK channels in SOD mice. During these studies, treatment with CyPPA was administered for just 16 days during the neonatal period (P5-P20), but the effects of this drug continued throughout disease progression. As a result, we hypothesized that CyPPA's impact was due to changes in the excitability of individual MNs and/or the spinal MN network.

Nevertheless, the current study shows that early treatment of SOD mice with CyPPA does not alter the excitability of individual MNs or the spinal MN network, as CyPPA failed to restore ALS-induced excitability changes in individual MNs and did not alter sensory or descending motor inputs in the spinal MN network. CyPPA also failed to restore sensorimotor deficits in the spinal MN network of SOD mice. Therefore, it is unlikely that the long-term therapeutic benefits of CyPPA in SOD mice are a result of excitability changes in individual MNs or the spinal MN network.
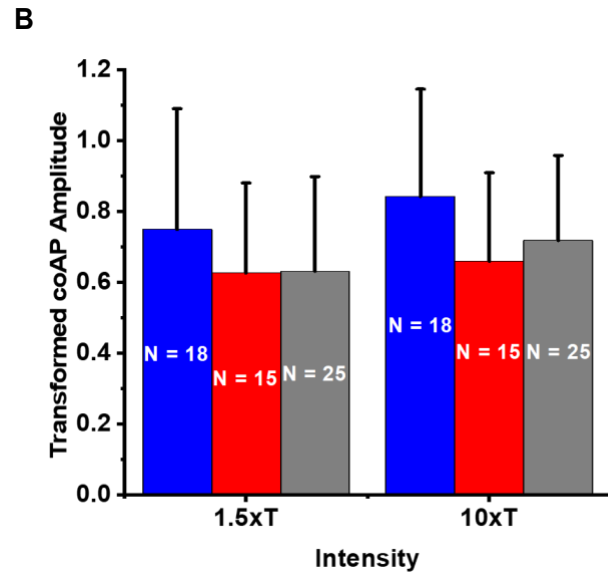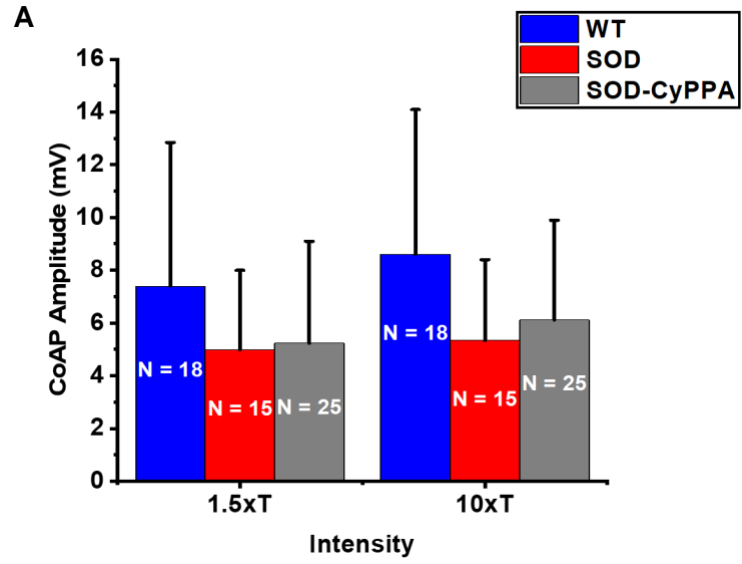
Figure 23. Early treatment of SOD mice with CyPPA does not alter evoked coAPs following stimulation of sensory inputs

Repetitive stimulation (0.06 Hz at 1.5 or 10xT) of sensory inputs in SOD-CyPPA mice evoked comparable coAPs to both SOD and WT mice. Both original **(A)** and transformed **(B)** mean values are reported, as coAP amplitude data for sensory input stimulation had a non-normal distribution. The original values were transformed using the natural logarithm. The bars represent the mean ± SD.

A

B
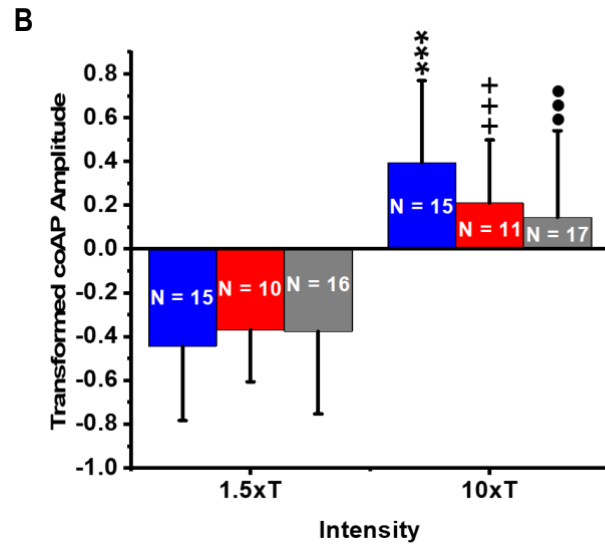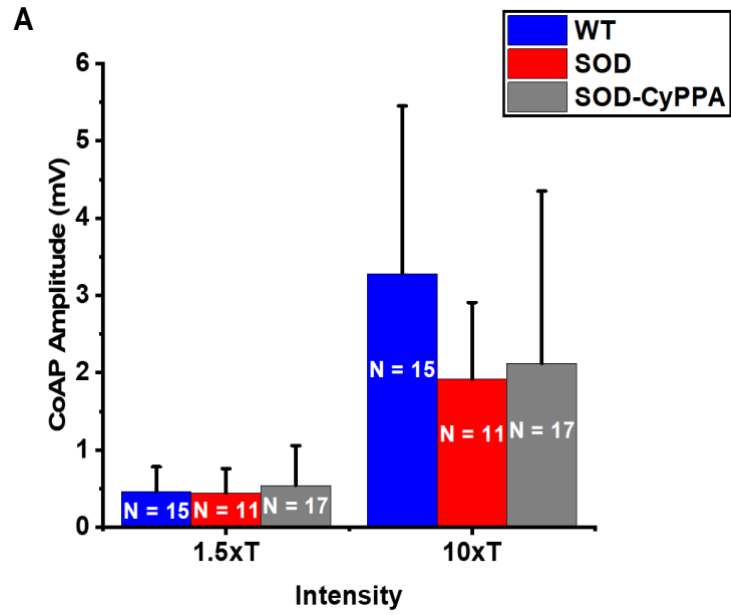
Figure 24. Early treatment of SOD mice with CyPPA does not alter evoked coAPs following stimulation of descending motor inputs

Repetitive stimulation (0.06 Hz at 1.5 or 10xT) of descending motor inputs in SOD-CyPPA mice evoked comparable coAPs to both SOD and WT mice. Additionally, much like SOD and WT mice, stimulation of descending motor inputs in SOD-CyPPA mice at 10xT evoked significantly larger coAPs compared to 1.5xT stimulation. Both original **(A)** and transformed **(B)** mean values are reported, as coAP amplitude data for descending motor input stimulation had a non-normal distribution. The original values were transformed using the natural logarithm. The bars represent the mean ± SD. Statistical differences shown (*******: WT 10xT vs. 1.5xT, +++: SOD 10xT vs. 1.5xT, and ●●●: SOD-CyPPA 10xT vs. 1.5xT, $p < 0.001$; Bonferroni multiple comparisons test).

111
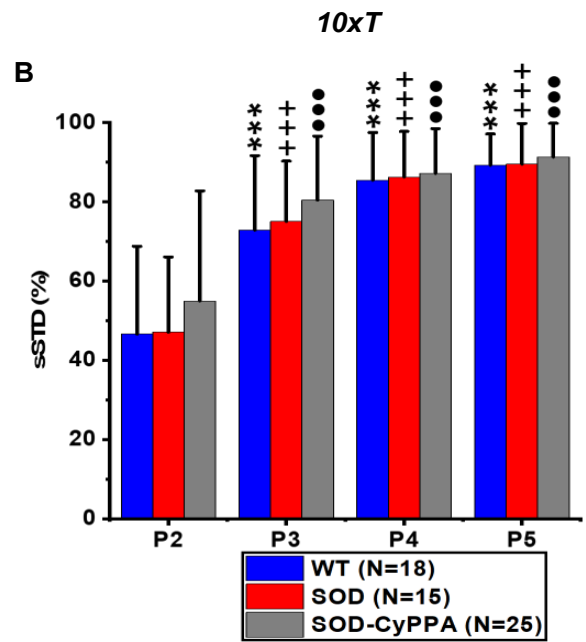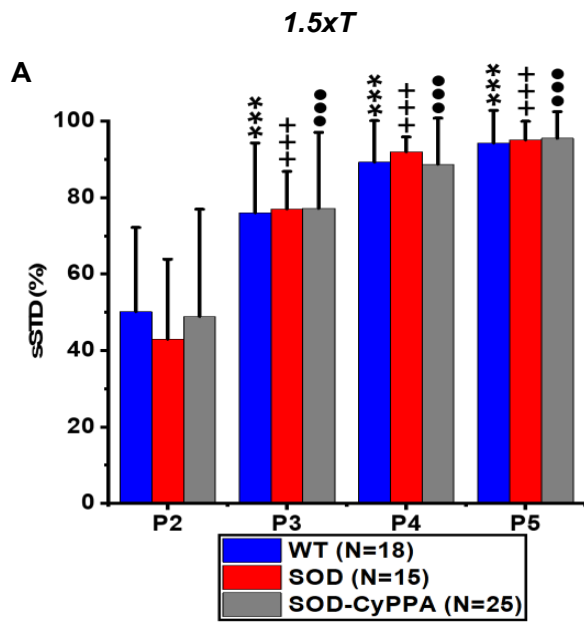
Figure 25. **Early treatment of SOD mice with CyPPA does not alter sSTD in sensory inputs**

At both stimulation intensities, sensory inputs in SOD-CyPPA mice exhibited comparable amounts of sSTD to both SOD and WT mice **(A and B)**. Additionally, similar to SOD and WT mice, the degree of sSTD significantly increased over the five pulses of stimulation at both 1.5 and 10xT in SOD-CyPPA mice. Bars represent mean ± SD. Statistical differences shown (*******: different from WT P2 at 1.5 or 10xT, +++: different from SOD P2 at 1.5 or 10xT, and •••: different from SOD-CyPPA P2 at 1.5 or 10xT, $p < 0.001$; Bonferroni multiple comparisons test).

1.5xT

A

10xT

B

WT (N=14)
SOD (N=10)
SOD-CyPPA (N = 14)

WT (N=15)
SOD (N=11)
SOD-CyPPA (N=16)

113
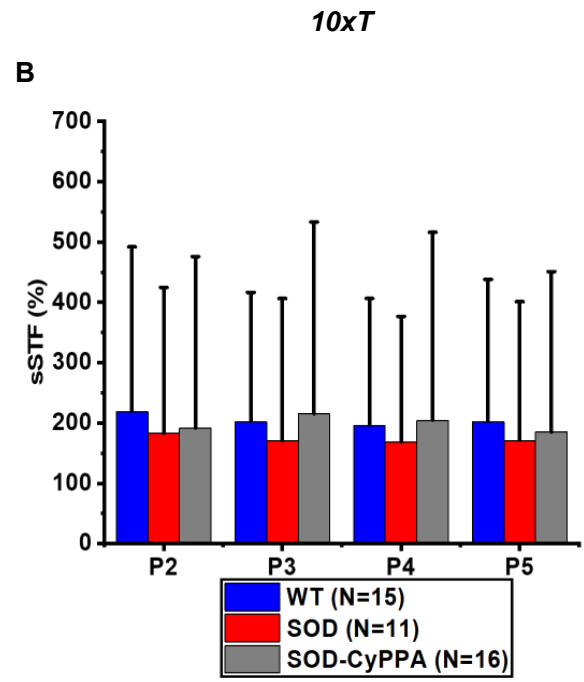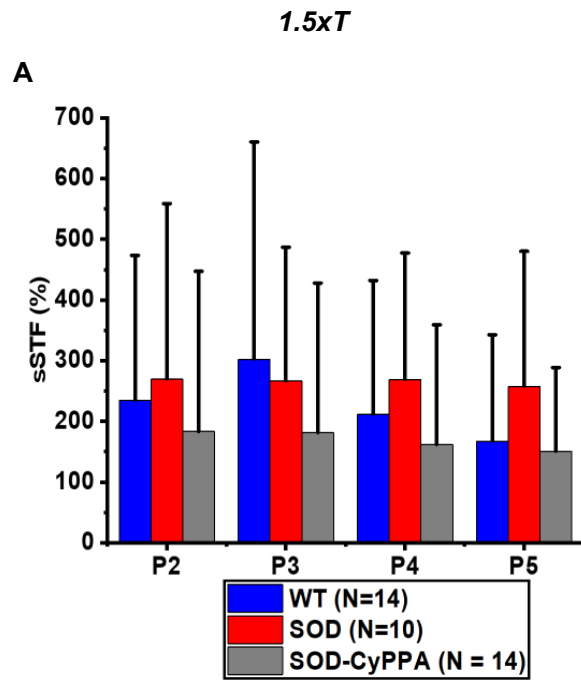
Figure 26. Early treatment of SOD mice with CyPPA does not alter sSTF in descending motor inputs

At both stimulation intensities, descending motor inputs in SOD-CyPPA mice exhibited comparable amounts of sSTF to both SOD and WT mice (**A and B**). Data is represented as mean ± SD.

A

B
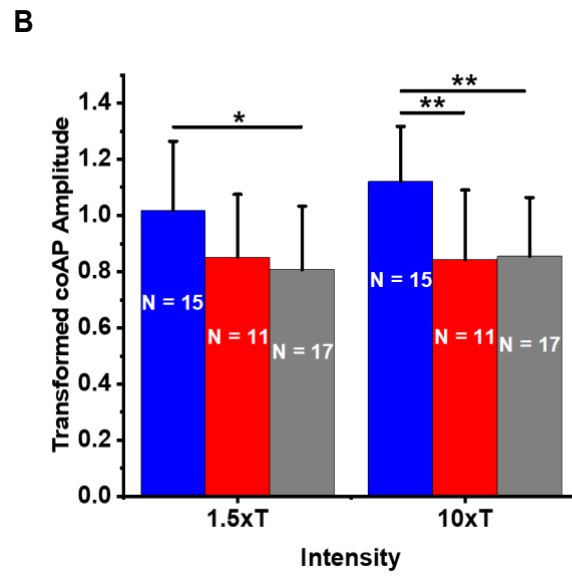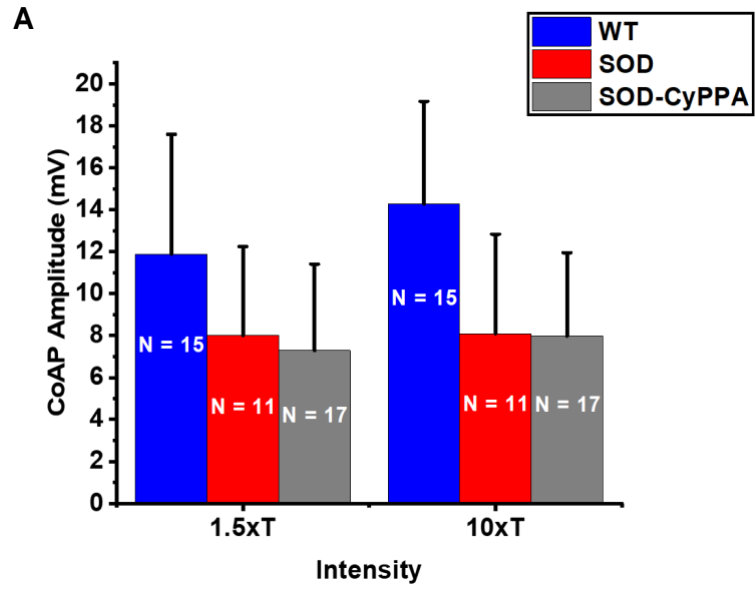
Figure 27. Early treatment of SOD mice with CyPPA does not restore deficits in evoked coAPs following S&M stimulation in SOD mice at symptom onset

Simultaneous stimulation (0.06 Hz at 1.5 or 10xT) of sensory and descending motor inputs in SOD-CyPPA mice evoked significantly smaller coAPs at both 1.5 and 10xT relative to WT mice, but there were no differences between SOD-CyPPA and SOD mice. Both original **(A)** and transformed **(B)** mean values are reported, as coAP amplitude data for simultaneous stimulation of sensory and descending motor inputs had a non-normal distribution. The original values were transformed using the natural logarithm. The bars represent the mean ± SD. Statistical differences are shown (*****, $p < 0.05$ and ******, $p < 0.01$; Bonferroni multiple comparisons test).

1.5xT

A

10xT

B
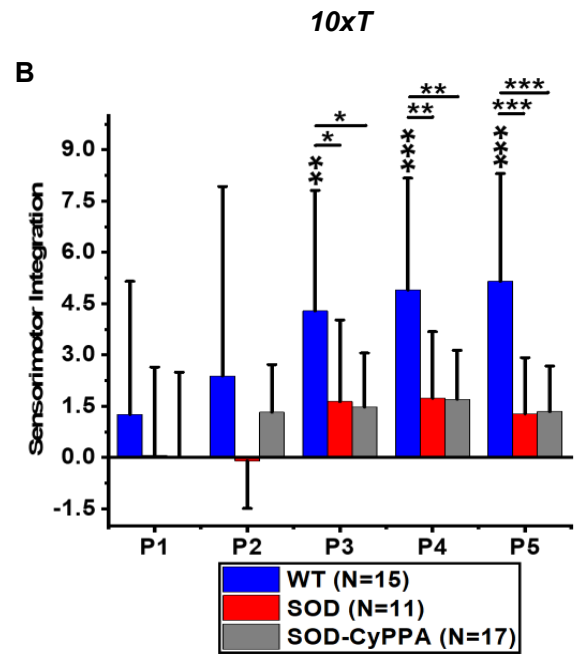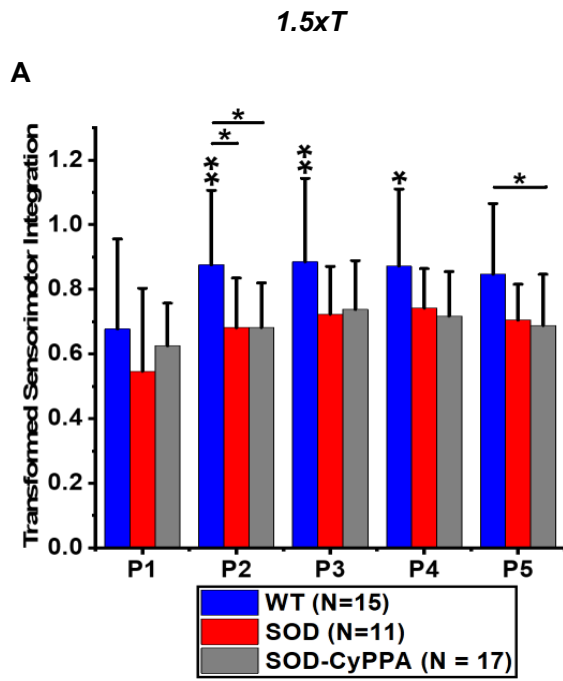
Figure 28. Early treatment of SOD mice with CyPPA does not restore impairments in the integration of sensory and descending motor inputs in SOD mice at symptom onset

SOD-CyPPA mice exhibited a significant deficit in sensorimotor integration at both 1.5 **(C)** and 10xT **(D)** relative to WT mice. There were no differences in sensorimotor integration between SOD-CyPPA and SOD mice. Statistical differences are indicated (*****, $p < 0.05$, ******, $p < 0.01$, and *******, $p < 0.001$, Bonferroni multiple comparisons test). Asterisks over the WT bars are comparing WT P1 vs. WT P2-P5 and asterisks above a single black bar are comparing between groups).

Chapter VI: Discussion

For the first time, the present study investigated ALS-induced excitability changes in individual MNs at symptom onset using the standard rodent model of Amyotrophic lateral sclerosis (ALS), SOD1-G93A$^{High\text{-}Copy}$ (SOD) mice. This study also characterized the excitability and activity of the spinal MN network in SOD mice at symptom onset by examining sensory and descending motor inputs and their integration. This is the first study to examine descending motor inputs and their integration with sensory inputs in SOD mice. In these initial studies, we sought to further understand disease versus compensatory mechanisms in ALS, as symptom onset is the key time point in a disease, where despite maximum compensation, disease mechanisms prevail, and signs of an illness emerge.

The second portion of this dissertation examined the long-term effects of early treatment of SOD mice with CyPPA on the excitability of individual MNs and the spinal MN network. CyPPA is a small-conductance calcium-activated potassium (SK) channel activator and in previous studies conducted in our lab, early treatment of SOD mice with CyPPA improved their survival, prolonged their motor function, and increased the somatic clustering profile of SK channels in their MNs. However, these studies did not examine the effects of early treatment of SOD mice with CyPPA on the excitability of individual MNs and the spinal MN network.

MN Excitability in SOD Mice at Symptom Onset

Individual MN excitability

Previous studies have extensively examined individual MN excitability in SOD mice, but these investigations are widely inconsistent and together, unclear. Throughout the current literature, SOD MNs show hyperexcitability, hypoexcitability, or no change in excitability depending on the study. These inconsistent findings could be the result of 1) experimental design, such as the use of both males and females or wide age ranges, 2) experimental error, such as the use of suboptimal discontinuous current clamp (DCC) switching rates, which results in overestimation of MN excitability (Manuel, 2021), and/or 3) disease and compensatory processes in ALS causing opposing changes in MN excitability.

In the current study, we demonstrate favorable evidence of the latter in which disease mechanisms alter MN excitability in one direction and compensatory mechanisms pull MN excitability in the opposite direction. For the first time, we investigated changes in MN excitability in SOD MNs at symptom onset and these MNs exhibit hypoexcitable changes in passive membrane properties, but hyperexcitable changes in afterhyperpolarization (AHP) properties. Also, during repetitive firing, SOD MNs demonstrate a consistent rate of hyperpolarization in the ISI voltage. These changes could increase sodium channel availability in SOD MNs to sustain repetitive firing. Yet, despite evidence of both hypo- and hyperexcitable changes in different intrinsic MN properties, the net excitability of SOD MNs at symptom onset is reduced.

The spinal MN network

Because the firing rate of a MN is influenced by its intrinsic electrical properties and its synaptic properties, alterations in MN excitability in ALS may develop from changes in the synaptic inputs received by MNs. A reduction in inhibitory inputs or increase in excitatory inputs would lead to an increase in MN firing rates, while the exact opposite would reduce MN firing rates. In the spinal cord, three inputs regulate the firing pattern of MNs, sensory inputs from the periphery, descending motor commands from supraspinal structures, and local interneuronal inputs.

In the current study, we characterized sensory and descending motor inputs in the spinal MN network of SOD mice at symptom onset. Our data demonstrates that neither sensory nor descending motor inputs contribute to alterations in MN excitability in SOD mice at symptom onset. Sensory and descending motor inputs from SOD and WT mice evoked similar compound action potentials (coAPs), which suggests that these synaptic inputs activated the same number of MNs in both SOD and WT mice. However, SOD mice have reduced MNs prior to symptom onset (Aggarwal & Nicholson, 2002; Hegedus et al., 2007). In addition, a previous study demonstrated a significant reduction in coAP amplitude in sensory inputs of SOD mice starting at symptom onset (Jiang et al., 2009). One possible explanation for the dissimilarity between the current and previous study may be the age of mice used. While the previous study reports the age range (postnatal day (P) 90 - P100) of mice used, the average age of these mice is unknown, which may be misrepresentative.

In the present study, we used SOD mice ranging from P87-P99, but the average age was P93, which is fairly close to symptom onset. Conversely, the average age of

SOD mice from the previous study could be closer to P100 rather P90, which would put these mice at a different clinical time point compared to the mice used in our study, as disease processes cause rapid deterioration of SOD mice following symptom onset. Accordingly, maximum compensatory processes at or near symptom onset may mask the loss of MNs in SOD mice causing normal motor output or evoked coAPs and this assumption is supported by previous studies which demonstrate that some MNs offset the loss of neighboring MNs through sprouting (Frey et al., 2000; Mancuso et al., 2016).

At symptom onset, sensory inputs and descending motor inputs in SOD mice also exhibit similar system short-term plasticity (depression or facilitation) relative to WT mice. However, previous research found less system short-term depression (sSTD) in sensory inputs of SOD mice (postnatal day (P) 50 – P90) (Jiang et al., 2017). Dissimilarity in age range could also explain this difference relative to our results and thus maximum compensatory processes at symptom onset may also hide these deficits.

Sensorimotor Integration in SOD Mice

Independently, sensory and descending motor inputs trigger different adaptation patterns in motor output (Jiang et al., 2015; Mahrous et al., 2019), but together, they produce stable and appropriate motor output for any given motor task (Kim et al., 2017; Mahrous et al., 2019; Rossignol et al., 2006). This process is known as sensorimotor integration and it is commonly impaired in movement disorders (Abbruzzese & Berardelli, 2003) including Parkinson's disease (Fellows et al., 1998; Lewis & Byblow, 2002; Rickards & Cody, 1997), Huntington's disease (Quinn et al., 2001; Schwarz et al., 2001), and dystonia (Ikeda et al., 1996; Serrien et al., 2000).

122

Deficits in motor function are also found in ALS patients and the progressive loss and wasting of MNs were long thought to underlie these impairments. However, recent research suggests sensorimotor integration may contribute to the development of motor deficits in ALS (Swash, 2018). Specifically, late somatosensory evoked potentials (SEPs), which are involved in higher-order sensorimotor and cognitive functions, are depressed in ALS patients (Sangari et al., 2018). Our current study also supports this new hypothesis.

Despite normal sensory and descending motor inputs, SOD mice exhibited significant deficits in the integration of these inputs at symptom onset. One potential explanation for these results is spinal interneurons. There are numerous types of spinal interneurons, each of which has different functions. Commissural interneurons, which are well-known for their role in right-left coordination during locomotion (Butt et al., 2002; Butt & Kiehn, 2003; Lanuza et al., 2004) also receive inputs from descending motor tracts and relay somatosensory information to spinal neurons (Côté et al., 2018). As such, commissural interneurons likely play a role in sensorimotor integration and could be impaired in SOD mice at symptom onset.

Nonetheless, the role of spinal interneurons in locomotion is not fully understood since this process involves many complex pathways and circuits. Thus, further research must first be done to completely delineate the neural mechanisms underlying locomotor behavior and control. Still, our study is one of several to implicate interneurons in the pathogenesis of ALS (Do-Ha et al., 2018; Jiang et al., 2009; Martin & Chang, 2012).

The Excitotoxicity Hypothesis in ALS

The excitotoxicity hypothesis implicates the glutaminergic system as the trigger for MN death in ALS (King et al., 2016; Van Den Bosch et al., 2006). Put simply, this hypothesis states that MNs in ALS are exposed to excess glutamate which causes an increase in intracellular calcium and triggers apoptosis. Presently, this theory is widely accepted, but it rests on several indirect findings and support from data obtained years ago. One of the most favorable arguments in support of this theory is the fact that Riluzole, the first and only drug shown to have a beneficial effect in ALS patients until 2017, has anti-excitotoxic properties (Bensimon et al., 1994; Lacomblez et al., 1996). This theory has also received a lot of support from studies conducted in the 1990s which found elevated levels of glutamate and its analogs in the cerebrospinal fluid (CSF) of ALS patients (Rothstein et al., 1990) and deficits in glutamate transport in the spinal cord and brain of ALS patients (Rothstein et al., 1992; Rothstein et al., 1995). Still, if the excitotoxicity hypothesis holds true, MNs in ALS would be hyperexcitable.

To date, numerous studies have investigated MN excitability in ALS using SOD mice. Many of these studies found hyperexcitability (Jensen et al., 2020; Kuo et al., 2004; Kuo et al., 2005; Martin et al., 2013) in SOD MNs which supports the excitotoxicity hypothesis, but others contradicted this hypothesis with evidence of hypoexcitability or no change in excitability in SOD MNs (Delestrée et al., 2014; Leroy et al., 2014; Martínez-Silva et al., 2018). The results of the current study help to explain this disagreement within current ALS literature. At symptom onset, SOD MNs exhibit both hypo- and hyperexcitability changes in intrinsic MN properties. This data supports

evidence of both hypo- and hyperexcitability in MNs in ALS, in which one is a disease mechanism and the other is a compensatory mechanism.

Nevertheless, despite both hypo- and hyperexcitable changes in SOD MNs at symptom onset, the net excitability of these cells is reduced. Because symptom onset is the unique time point of a disease where despite maximum compensation, disease mechanisms predominate, these results suggest hypoexcitability as the disease mechanism in ALS. Accordingly, our results do not support the excitotoxicity theory, but previous research demonstrates that reducing MN excitability in SOD mice accelerates disease, while enhancing MN excitability promotes neuroprotection (Saxena et al., 2013). MN hypoexcitability also predominates in sporadic ALS patients and increases with disease progression (Marchand-Pauvert et al., 2019). Still, additional research must be conducted in order to confirm hypoexcitability reflects disease processes in ALS. Additionally, some limitations from our study should also be noted. Compared to a recent study conducted by Jensen and colleagues (2020), which found MNs from presymptomatic (P69-P75) and symptomatic (P107-P116) SOD mice to be more responsive or hyperexcitable, the sample size in our study was small. Nevertheless, our post-hoc power values are within appropriate limits (see the Appendix) and unlike the study conducted in 2020, our results are supported by immunohistochemistry and computer modeling studies and we used appropriate discontinuous current clamp (DCC) sampling rates. Also, the MNs we recorded from in the current study were mostly (83%) fast or F-type MNs according to AHP half decay measurements (Table 7). Consequently, our results reflect the excitability state of the most vulnerable MNs in ALS at symptom

onset, but do not represent the excitability state of slow or S-type MNs, the disease resistant MNs in ALS.

CyPPA Treatment in SOD mice

The effects of early treatment of SOD mice with CyPPA

Due to the limited therapeutic options for ALS, our lab began investigating a new molecule potentially involved in ALS disease pathogenesis, the SK channel. Collectively, our past studies demonstrate a significant reduction in SK channels in SOD mice throughout disease progression (Dukkipati, 2016). Following treatment with CyPPA, an SK channel activator, for a single, 16-day period (P5-P20), these deficits are restored immediately (P21) and last long-term (symptom onset or P90) (Murphy, 2020). CyPPA also sustains motor function and prolongs survival in SOD mice by 10 days (Dancy, 2017).

The longstanding effects of early treatment of SOD mice with CyPPA suggest that CyPPA has functional effects on MNs and likely alters their excitability at the individual and/or network levels. Since CyPPA is an SK channel activator, we hypothesized that CyPPA alters AHP properties and/or synaptic properties in SOD MNs. In the current study, we tested this hypothesis and surprisingly, early treatment with CyPPA failed to restore deficits in AHP properties and all other intrinsic MN properties, including passive membrane properties and net excitability, in SOD MNs at symptom onset.

In addition, CyPPA did not alter sensory or descending motor inputs nor restore deficits in the integration of these inputs in SOD mice at symptom onset. Altogether, these data suggest CyPPA's long-term therapeutic effects in SOD mice are not related to

alterations in MN excitability at the individual or network levels. However, these results contradict the previous immunohistochemistry studies conducted in our lab which found CyPPA to restore the somatic clustering profile of SK channels in SOD mice at symptom onset. This could be due to the small and unbalanced sample sizes used in the current study or because changes in ion channel cluster size do not equate to changes in ion channel conductance.

Possible mechanisms underlying the therapeutic benefit of CyPPA in SOD mice

Despite the extensive focus on the glutamate excitotoxicity hypothesis in ALS, several other hypotheses have been proposed as mechanisms contributing to MN degeneration in this disease (R. Bonafede & R. Mariotti, 2017). Two examples of these mechanisms are mitochondrial dysfunction and neuroinflammation, both of which are modified by SK channel activation (Dolga et al., 2012; Gold, 2013; Honrath et al., 2018; Richter et al., 2015). More recently SK channels have been shown to be expressed and functional at the level of the mitochondrial membrane (Dolga et al., 2013; Stowe et al., 2013) and activation of these channels via CyPPA reduces mitochondrial respiration, oxygen consumption, and ROS production (Richter et al., 2015). Therefore, early treatment of SOD mice with CyPPA could target mitochondrial dysfunction and oxidative stress-related mechanisms in ALS.

SK channels are also linked to microglia activation processes (Khanna et al., 2001; Schlichter et al., 2010) and these cells are the first line of defense for the CNS against infection or injury, and accordingly, these cells initiate neuroinflammation (Roberta Bonafede & Raffaella Mariotti, 2017; Carroll & Chesebro, 2019; Rodríguez-Gómez et al., 2020). Activation of SK channels by CyPPA reduces lipopolysaccharide-

induced microglia activation via attenuation of calcium influx and decreases cytokine production, a characteristic feature of microglia activation (Dolga et al., 2012). Thus, CyPPA could also target microglia activity in SOD mice. Remarkably, studies in these transgenic mice have shown that replacement of mutant microglia with normal cells significantly reduces MN degeneration and extends the lifespan of these animals (Beers et al., 2006; Boillée et al., 2006). SK channel activation via CyPPA also protects against cell death induced by ER-stress, another pathogenic mechanism proposed in ALS (Richter et al., 2016). Taken together, CyPPA could impact various disease processes involved in ALS. Consequently, additional research must be conducted in order to delineate the exact mechanism underlying the long-term therapeutic benefits of CyPPA in SOD mice.

Chapter VII: Appendix

Analysis	Test	Test value	P-value	Power
R_{in}		15.982	0.00001	0.954
G_{in}	One-way ANOVA	18.081	0.000002	0.962
Capacitance		7.971	0.001	0.770
AHP amplitude		3.151	0.049	0.587
G_{SK} density		4.173	0.020	0.714
ISI slope	Two-way Mixed ANOVA	2.880	0.0332	0.734
F-I$_{Asc}$	One-way ANOVA	8.854	0.0004	0.965
Descending Motor Input coAP amplitude	Two-way ANOVA (Intensity)	68.616	< 0.001	1.000
sSTD 1.5xT	Two-way Mixed ANOVA (Pulse)	209.588	< 0.001	1.000
sSTD 10xT	Two-way Mixed ANOVA (Pulse)	186.727	< 0.001	1.000
S&M coAP amplitude	Two-way ANOVA	10.465	< 0.001	0.986
Sensorimotor Integration 1.5xT	Two-way Mixed ANOVA (Genotype)	3.918	0.028	0.673
Sensorimotor Integration 1.5xT	Two-way Mixed ANOVA (Pulse)	15.478	< 0.001	0.997
Sensorimotor Integration 10xT	Two-way Mixed ANOVA (Genotype)	5.476	0.008	0.822
Sensorimotor Integration 10xT	Two-way Mixed ANOVA (Pulse)	17.504	< 0.001	1.000

Chapter VIII: References

Abbruzzese, G., & Berardelli, A. (2003, Mar). Sensorimotor integration in movement disorders. *Mov Disord, 18*(3), 231-240. https://doi.org/10.1002/mds.10327

Adelman, J. P., Maylie, J., & Sah, P. (2012). Small-Conductance Ca2+-Activated K+ Channels: Form and Function. *Annual Review of Physiology, 74*(1), 245-269. https://doi.org/10.1146/annurev-physiol-020911-153336

Aggarwal, A., & Nicholson, G. (2002, Aug). Detection of preclinical motor neurone loss in SOD1 mutation carriers using motor unit number estimation. *J Neurol Neurosurg Psychiatry, 73*(2), 199-201. https://doi.org/10.1136/jnnp.73.2.199

Alexianu, M. E., Ho, B. K., Mohamed, A. H., La Bella, V., Smith, R. G., & Appel, S. H. (1994, Dec). The role of calcium-binding proteins in selective motoneuron vulnerability in amyotrophic lateral sclerosis. *Ann Neurol, 36*(6), 846-858. https://doi.org/10.1002/ana.410360608

Amendola, J., & Durand, J. (2008, Nov 20). Morphological differences between wild-type and transgenic superoxide dismutase 1 lumbar motoneurons in postnatal mice. *J Comp Neurol, 511*(3), 329-341. https://doi.org/10.1002/cne.21818

Arai, T., Hasegawa, M., Akiyama, H., Ikeda, K., Nonaka, T., Mori, H., Mann, D., Tsuchiya, K., Yoshida, M., Hashizume, Y., & Oda, T. (2006, Dec 22). TDP-43 is a component of ubiquitin-positive tau-negative inclusions in frontotemporal lobar degeneration and amyotrophic lateral sclerosis. *Biochem Biophys Res Commun, 351*(3), 602-611. https://doi.org/10.1016/j.bbrc.2006.10.093

Avanzini, G., de Curtis, M., Panzica, F., & Spreafico, R. (1989, Sep). Intrinsic properties of nucleus reticularis thalami neurones of the rat studied in vitro. *J Physiol, 416*, 111-122. https://doi.org/10.1113/jphysiol.1989.sp017752

Bakels, R., & Kernell, D. (1993, Apr). Matching between motoneurone and muscle unit properties in rat medial gastrocnemius. *J Physiol, 463*, 307-324. https://doi.org/10.1113/jphysiol.1993.sp019596

Barrett, E. F., & Barret, J. N. (1976, Mar). Separation of two voltage-sensitive potassium currents, and demonstration of a tetrodotoxin-resistant calcium current in frog motoneurones. *J Physiol, 255*(3), 737-774. https://doi.org/10.1113/jphysiol.1976.sp011306

Beers, D. R., Henkel, J. S., Xiao, Q., Zhao, W., Wang, J., Yen, A. A., Siklos, L., McKercher, S. R., & Appel, S. H. (2006, Oct 24). Wild-type microglia extend survival in PU.1 knockout mice with familial amyotrophic lateral sclerosis. *Proc Natl Acad Sci U S A, 103*(43), 16021-16026. https://doi.org/10.1073/pnas.0607423103

Bellingham, M. C. (2011, Feb). A review of the neural mechanisms of action and clinical efficiency of riluzole in treating amyotrophic lateral sclerosis: what have we learned in the last decade? *CNS Neurosci Ther, 17*(1), 4-31. https://doi.org/10.1111/j.1755-5949.2009.00116.x

Bendotti, C., Tortarolo, M., Suchak, S. K., Calvaresi, N., Carvelli, L., Bastone, A., Rizzi, M., Rattray, M., & Mennini, T. (2001, Nov). Transgenic SOD1 G93A mice develop reduced GLT-1 in spinal cord without alterations in cerebrospinal fluid glutamate levels. *J Neurochem, 79*(4), 737-746. https://doi.org/10.1046/j.1471-4159.2001.00572.x

Bensimon, G., Lacomblez, L., & Meininger, V. (1994, Mar 3). A controlled trial of riluzole in amyotrophic lateral sclerosis. ALS/Riluzole Study Group. *N Engl J Med, 330*(9), 585-591. https://doi.org/10.1056/nejm199403033300901

Bhandari, R., Kuhad, A., & Kuhad, A. (2018, Jun). Edaravone: a new hope for deadly amyotrophic lateral sclerosis. *Drugs Today (Barc), 54*(6), 349-360. https://doi.org/10.1358/dot.2018.54.6.2828189

Blasco, H., Guennoc, A. M., Veyrat-Durebex, C., Gordon, P. H., Andres, C. R., Camu, W., & Corcia, P. (2012, Oct). Amyotrophic lateral sclerosis: a hormonal condition? *Amyotroph Lateral Scler, 13*(6), 585-588. https://doi.org/10.3109/17482968.2012.706303

Blatz, A. L., & Magleby, K. L. (1986, Oct 23-29). Single apamin-blocked Ca-activated K+ channels of small conductance in cultured rat skeletal muscle. *Nature, 323*(6090), 718-720. https://doi.org/10.1038/323718a0

Boillée, S., Yamanaka, K., Lobsiger, C. S., Copeland, N. G., Jenkins, N. A., Kassiotis, G., Kollias, G., & Cleveland, D. W. (2006, Jun 2). Onset and progression in inherited ALS determined by motor neurons and microglia. *Science, 312*(5778), 1389-1392. https://doi.org/10.1126/science.1123511

Bonafede, R., & Mariotti, R. (2017, 2017-March-21). ALS Pathogenesis and Therapeutic Approaches: The Role of Mesenchymal Stem Cells and Extracellular Vesicles [Review]. *Frontiers in Cellular Neuroscience, 11*(80). https://doi.org/10.3389/fncel.2017.00080

Bonafede, R., & Mariotti, R. (2017). ALS Pathogenesis and Therapeutic Approaches: The Role of Mesenchymal Stem Cells and Extracellular Vesicles. *Front Cell Neurosci, 11*, 80. https://doi.org/10.3389/fncel.2017.00080

Bourque, C. W., & Brown, D. A. (1987, Nov 23). Apamin and d-tubocurarine block the afterhyperpolarization of rat supraoptic neurosecretory neurons. *Neurosci Lett, 82*(2), 185-190. https://doi.org/10.1016/0304-3940(87)90127-3

Boylan, K. (2015, Nov). Familial Amyotrophic Lateral Sclerosis. *Neurol Clin, 33*(4), 807-830. https://doi.org/10.1016/j.ncl.2015.07.001

Brown, A. G., & Fyffe, R. E. (1981). Direct observations on the contacts made between Ia afferent fibres and alpha-motoneurones in the cat's lumbosacral spinal cord. *J Physiol, 313*, 121-140. https://doi.org/10.1113/jphysiol.1981.sp013654

Bruijn, L. I., Becher, M. W., Lee, M. K., Anderson, K. L., Jenkins, N. A., Copeland, N. G., Sisodia, S. S., Rothstein, J. D., Borchelt, D. R., Price, D. L., & Cleveland, D. W. (1997, Feb). ALS-linked SOD1 mutant G85R mediates damage to astrocytes and promotes rapidly progressive disease with SOD1-containing inclusions. *Neuron, 18*(2), 327-338. https://doi.org/10.1016/s0896-6273(00)80272-x

Burke, R. E. (1967, Nov). Motor unit types of cat triceps surae muscle. *J Physiol, 193*(1), 141-160. https://doi.org/10.1113/jphysiol.1967.sp008348

Butt, S. J., Harris-Warrick, R. M., & Kiehn, O. (2002, Nov 15). Firing properties of identified interneuron populations in the mammalian hindlimb central pattern generator. *J Neurosci, 22*(22), 9961-9971. https://doi.org/10.1523/jneurosci.22-22-09961.2002

Butt, S. J., & Kiehn, O. (2003, Jun 19). Functional identification of interneurons responsible for left-right coordination of hindlimbs in mammals. *Neuron, 38*(6), 953-963. https://doi.org/10.1016/s0896-6273(03)00353-2

Cacabelos, D., Ramírez-Núñez, O., Granado-Serrano, A. B., Torres, P., Ayala, V., Moiseeva, V., Povedano, M., Ferrer, I., Pamplona, R., Portero-Otin, M., & Boada, J. (2016, 2016/01/13). Early and gender-specific differences in spinal cord mitochondrial function and oxidative stress markers in a mouse model of ALS. *Acta Neuropathologica Communications, 4*(1), 3. https://doi.org/10.1186/s40478-015-0271-6

Cao, Y. J., Dreixler, J. C., Couey, J. J., & Houamed, K. M. (2002, Aug 2). Modulation of recombinant and native neuronal SK channels by the neuroprotective drug riluzole. *Eur J Pharmacol, 449*(1-2), 47-54. https://doi.org/10.1016/s0014-2999(02)01987-8

Carlin, K. P., Jones, K. E., Jiang, Z., Jordan, L. M., & Brownstone, R. M. (2000, May). Dendritic L-type calcium currents in mouse spinal motoneurons: implications for bistability. *Eur J Neurosci, 12*(5), 1635-1646. https://doi.org/10.1046/j.1460-9568.2000.00055.x

Carp, J. S., & Wolpaw, J. R. (2010). Motor Neurons and Spinal Control of Movement. In *eLS*. https://doi.org/10.1002/9780470015902.a0000156.pub2

Carriedo, S. G., Yin, H. Z., & Weiss, J. H. (1996, Jul 1). Motor neurons are selectively vulnerable to AMPA/kainate receptor-mediated injury in vitro. *J Neurosci, 16*(13), 4069-4079. https://doi.org/10.1523/jneurosci.16-13-04069.1996

Carroll, J. A., & Chesebro, B. (2019, Jan 15). Neuroinflammation, Microglia, and Cell-Association during Prion Disease. *Viruses, 11*(1). https://doi.org/10.3390/v11010065

Celio, M. R. (1990). Calbindin D-28k and parvalbumin in the rat nervous system. *Neuroscience, 35*(2), 375-475. https://doi.org/10.1016/0306-4522(90)90091-h

Chancellor, A. M., Slattery, J. M., Fraser, H., Swingler, R. J., Holloway, S. M., & Warlow, C. P. (1993, Jun). The prognosis of adult-onset motor neuron disease: a prospective study based on the Scottish Motor Neuron Disease Register. *J Neurol, 240*(6), 339-346. https://doi.org/10.1007/bf00839964

Chang, Q., & Martin, L. J. (2011, Feb 23). Glycine receptor channels in spinal motoneurons are abnormal in a transgenic mouse model of amyotrophic lateral sclerosis. *J Neurosci, 31*(8), 2815-2827. https://doi.org/10.1523/jneurosci.2475-10.2011

Chang, Q., & Martin, L. J. (2016, Sep). Voltage-gated calcium channels are abnormal in cultured spinal motoneurons in the G93A-SOD1 transgenic mouse model of ALS. *Neurobiol Dis, 93*, 78-95. https://doi.org/10.1016/j.nbd.2016.04.009

Choi, C. I., Lee, Y. D., Gwag, B. J., Cho, S. I., Kim, S. S., & Suh-Kim, H. (2008, May 15). Effects of estrogen on lifespan and motor functions in female hSOD1 G93A transgenic mice. *J Neurol Sci, 268*(1-2), 40-47. https://doi.org/10.1016/j.jns.2007.10.024

Citri, A., & Malenka, R. C. (2008, Jan). Synaptic plasticity: multiple forms, functions, and mechanisms. *Neuropsychopharmacology, 33*(1), 18-41. https://doi.org/10.1038/sj.npp.1301559

Côté, M. P., Murray, L. M., & Knikou, M. (2018). Spinal Control of Locomotion: Individual Neurons, Their Circuits and Functions. *Front Physiol, 9*, 784. https://doi.org/10.3389/fphys.2018.00784

Dancy, M. T. (2017). *Investigating the Role of an SK Channel Activator on Survival and Motor Function in the SOD1-G93A, ALS Mouse Model* Wright State University]. http://rave.ohiolink.edu/etdc/view?acc_num=wright1493817751768876

Deardorff, A. S., Romer, S. H., Deng, Z., Bullinger, K. L., Nardelli, P., Cope, T. C., & Fyffe, R. E. (2013, Feb 15). Expression of postsynaptic Ca2+-activated K+ (SK) channels at C-bouton synapses in mammalian lumbar -motoneurons. *J Physiol, 591*(4), 875-897. https://doi.org/10.1113/jphysiol.2012.240879

Deardorff, A. S., Romer, S. H., Sonner, P. M., & Fyffe, R. E. (2014). Swimming against the tide: investigations of the C-bouton synapse. *Front Neural Circuits, 8*, 106. https://doi.org/10.3389/fncir.2014.00106

DeJesus-Hernandez, M., Mackenzie, I. R., Boeve, B. F., Boxer, A. L., Baker, M., Rutherford, N. J., Nicholson, A. M., Finch, N. A., Flynn, H., Adamson, J., Kouri, N., Wojtas, A., Sengdy, P., Hsiung, G. Y., Karydas, A., Seeley, W. W., Josephs, K. A., Coppola, G., Geschwind, D. H., Wszolek, Z. K., Feldman, H., Knopman, D. S., Petersen, R. C., Miller, B. L., Dickson, D. W., Boylan, K. B., Graff-Radford, N. R., & Rademakers, R. (2011, Oct 20). Expanded GGGGCC hexanucleotide repeat in noncoding region of C9ORF72 causes chromosome 9p-linked FTD and ALS. *Neuron, 72*(2), 245-256. https://doi.org/10.1016/j.neuron.2011.09.011

Del Signore, S. J., Amante, D. J., Kim, J., Stack, E. C., Goodrich, S., Cormier, K., Smith, K., Cudkowicz, M. E., & Ferrante, R. J. (2009, Apr). Combined riluzole and sodium phenylbutyrate therapy in transgenic amyotrophic lateral sclerosis mice. *Amyotroph Lateral Scler, 10*(2), 85-94. https://doi.org/10.1080/17482960802226148

Delestrée, N., Manuel, M., Iglesias, C., Elbasiouny, S. M., Heckman, C. J., & Zytnicki, D. (2014, Apr 1). Adult spinal motoneurones are not hyperexcitable in a mouse model of inherited amyotrophic lateral sclerosis. *J Physiol, 592*(7), 1687-1703. https://doi.org/10.1113/jphysiol.2013.265843

DeLoach, A., Cozart, M., Kiaei, A., & Kiaei, M. (2015, Oct). A retrospective review of the progress in amyotrophic lateral sclerosis drug discovery over the last decade and a look at the latest strategies. *Expert Opin Drug Discov, 10*(10), 1099-1118. https://doi.org/10.1517/17460441.2015.1067197

Devlin, A. C., Burr, K., Borooah, S., Foster, J. D., Cleary, E. M., Geti, I., Vallier, L., Shaw, C. E., Chandran, S., & Miles, G. B. (2015, Jan 12). Human iPSC-derived motoneurons harbouring TARDBP or C9ORF72 ALS mutations are dysfunctional despite maintaining viability. *Nat Commun, 6*, 5999. https://doi.org/10.1038/ncomms6999

Do-Ha, D., Buskila, Y., & Ooi, L. (2018, Feb). Impairments in Motor Neurons, Interneurons and Astrocytes Contribute to Hyperexcitability in ALS: Underlying Mechanisms and Paths to Therapy. *Mol Neurobiol, 55*(2), 1410-1418. https://doi.org/10.1007/s12035-017-0392-y

Dolga, A. M., Letsche, T., Gold, M., Doti, N., Bacher, M., Chiamvimonvat, N., Dodel, R., & Culmsee, C. (2012, Dec). Activation of KCNN3/SK3/K(Ca)2.3 channels attenuates enhanced calcium influx and inflammatory cytokine production in activated microglia. *Glia, 60*(12), 2050-2064. https://doi.org/10.1002/glia.22419

Dolga, A. M., Netter, M. F., Perocchi, F., Doti, N., Meissner, L., Tobaben, S., Grohm, J., Zischka, H., Plesnila, N., Decher, N., & Culmsee, C. (2013, Apr 12). Mitochondrial small conductance SK2 channels prevent glutamate-induced oxytosis and mitochondrial dysfunction. *J Biol Chem, 288*(15), 10792-10804. https://doi.org/10.1074/jbc.M113.453522

Dukkipati, S. S. (2016). *SK Channel Clustering in SOD1-G93A Motoneurons* Wright State University]. http://rave.ohiolink.edu/etdc/view?acc_num=wright1464713486

Dukkipati, S. S., Garrett, T. L., & Elbasiouny, S. M. (2018, May 1). The vulnerability of spinal motoneurons and soma size plasticity in a mouse model of amyotrophic lateral sclerosis. *J Physiol, 596*(9), 1723-1745. https://doi.org/10.1113/jp275498

Eccles, J. C. (1946, Mar). Synaptic potentials of motoneurones. *J Neurophysiol, 9*, 87-120. https://doi.org/10.1152/jn.1946.9.2.87

Faber, E. S., Delaney, A. J., Power, J. M., Sedlak, P. L., Crane, J. W., & Sah, P. (2008, Oct 22). Modulation of SK channel trafficking by beta adrenoceptors enhances excitatory synaptic transmission and plasticity in the amygdala. *J Neurosci, 28*(43), 10803-10813. https://doi.org/10.1523/jneurosci.1796-08.2008

Faber, E. S., Delaney, A. J., & Sah, P. (2005, May). SK channels regulate excitatory synaptic transmission and plasticity in the lateral amygdala. *Nat Neurosci, 8*(5), 635-641. https://doi.org/10.1038/nn1450

Fellows, S. J., Noth, J., & Schwarz, M. (1998, 10/01). Precision grip and Parkinson's disease. *Brain : a journal of neurology, 121 (Pt 9)*, 1771-1784.

Frey, D., Schneider, C., Xu, L., Borg, J., Spooren, W., & Caroni, P. (2000, Apr 1). Early and selective loss of neuromuscular synapse subtypes with low sprouting competence in motoneuron diseases. *J Neurosci, 20*(7), 2534-2542. https://doi.org/10.1523/jneurosci.20-07-02534.2000

Gardiner, P. F. (1993, Apr). Physiological properties of motoneurons innervating different muscle unit types in rat gastrocnemius. *J Neurophysiol, 69*(4), 1160-1170. https://doi.org/10.1152/jn.1993.69.4.1160

Geevasinga, N., Menon, P., Özdinler, P. H., Kiernan, M. C., & Vucic, S. (2016, Nov). Pathophysiological and diagnostic implications of cortical dysfunction in ALS. *Nat Rev Neurol, 12*(11), 651-661. https://doi.org/10.1038/nrneurol.2016.140

Gold, M. (2013). *Modulation of microglial cells in the Alzheimer-associated neuroinflammation*

Goldberg, J. A., & Wilson, C. J. (2005, Nov 2). Control of spontaneous firing patterns by the selective coupling of calcium currents to calcium-activated potassium currents in striatal cholinergic interneurons. *J Neurosci, 25*(44), 10230-10238. https://doi.org/10.1523/jneurosci.2734-05.2005

Gromicho, M., Oliveira Santos, M., Pinto, A., Pronto-Laborinho, A., & De Carvalho, M. (2017, Aug). Young-onset rapidly progressive ALS associated with heterozygous FUS mutation. *Amyotroph Lateral Scler Frontotemporal Degener, 18*(5-6), 451-453. https://doi.org/10.1080/21678421.2017.1299762

Grunnet, M., Jespersen, T., Angelo, K., Frøkjaer-Jensen, C., Klaerke, D. A., Olesen, S. P., & Jensen, B. S. (2001, Jun). Pharmacological modulation of SK3 channels. *Neuropharmacology, 40*(7), 879-887. https://doi.org/10.1016/s0028-3908(01)00028-4

Gu, M., Zhu, Y., Yin, X., & Zhang, D. M. (2018, Apr 13). Small-conductance Ca(2+)-activated K(+) channels: insights into their roles in cardiovascular disease. *Exp Mol Med, 50*(4), 23. https://doi.org/10.1038/s12276-018-0043-z

Gurney, M. E., Cutting, F. B., Zhai, P., Doble, A., Taylor, C. P., Andrus, P. K., & Hall, E. D. (1996, Feb). Benefit of vitamin E, riluzole, and gabapentin in a transgenic model of familial amyotrophic lateral sclerosis. *Ann Neurol, 39*(2), 147-157. https://doi.org/10.1002/ana.410390203

Gurney, M. E., Fleck, T. J., Himes, C. S., & Hall, E. D. (1998, Jan). Riluzole preserves motor function in a transgenic model of familial amyotrophic lateral sclerosis. *Neurology, 50*(1), 62-66. https://doi.org/10.1212/wnl.50.1.62

Gurney, M. E., Pu, H., Chiu, A. Y., Dal Canto, M. C., Polchow, C. Y., Alexander, D. D., Caliendo, J., Hentati, A., Kwon, Y. W., Deng, H. X., & et al. (1994, Jun 17). Motor neuron degeneration in mice that express a human Cu,Zn superoxide dismutase mutation. *Science, 264*(5166), 1772-1775. https://doi.org/10.1126/science.8209258

Habermann, E. (1984). Apamin. *Pharmacol Ther, 25*(2), 255-270. https://doi.org/10.1016/0163-7258(84)90046-9

Haverkamp, L. J., Appel, V., & Appel, S. H. (1995, Jun). Natural history of amyotrophic lateral sclerosis in a database population. Validation of a scoring system and a model for survival prediction. *Brain, 118 (Pt 3)*, 707-719. https://doi.org/10.1093/brain/118.3.707

Heckman, C. J., Kuo, J. J., & Johnson, M. D. (2004, Aug-Sep). Synaptic integration in motoneurons with hyper-excitable dendrites. *Can J Physiol Pharmacol, 82*(8-9), 549-555. https://doi.org/10.1139/y04-046

Heckman, C. J., & Lee, R. H. (1999). Synaptic integration in bistable motoneurons. *Prog Brain Res, 123*, 49-56. https://doi.org/10.1016/s0079-6123(08)62843-5

Heckman, C. J., Mottram, C., Quinlan, K., Theiss, R., & Schuster, J. (2009, Dec). Motoneuron excitability: the importance of neuromodulatory inputs. *Clin Neurophysiol, 120*(12), 2040-2054. https://doi.org/10.1016/j.clinph.2009.08.009

Hegedus, J., Putman, C. T., & Gordon, T. (2007, Nov). Time course of preferential motor unit loss in the SOD1 G93A mouse model of amyotrophic lateral sclerosis. *Neurobiol Dis, 28*(2), 154-164. https://doi.org/10.1016/j.nbd.2007.07.003

Hegedus, J., Putman, C. T., Tyreman, N., & Gordon, T. (2008, Jul 15). Preferential motor unit loss in the SOD1 G93A transgenic mouse model of amyotrophic lateral sclerosis. *J Physiol, 586*(14), 3337-3351. https://doi.org/10.1113/jphysiol.2007.149286

Herrik, K. F., Redrobe, J. P., Holst, D., Hougaard, C., Sandager-Nielsen, K., Nielsen, A. N., Ji, H., Holst, N. M., Rasmussen, H. B., Nielsen, E., Strøbæk, D., Shepard, P. D., & Christophersen, P. (2012). CyPPA, a Positive SK3/SK2 Modulator, Reduces Activity of Dopaminergic Neurons, Inhibits Dopamine Release, and Counteracts Hyperdopaminergic Behaviors Induced by Methylphenidate. *Front Pharmacol, 3*, 11. https://doi.org/10.3389/fphar.2012.00011

Hirano, A., Donnenfeld, H., Sasaki, S., & Nakano, I. (1984, Sep). Fine structural observations of neurofilamentous changes in amyotrophic lateral sclerosis. *J Neuropathol Exp Neurol, 43*(5), 461-470. https://doi.org/10.1097/00005072-198409000-00001

Hogden, A., Foley, G., Henderson, R. D., James, N., & Aoun, S. M. (2017). Amyotrophic lateral sclerosis: improving care with a multidisciplinary approach. *J Multidiscip Healthc, 10*, 205-215. https://doi.org/10.2147/jmdh.S134992

Honrath, B., Krabbendam, I. E., Ijsebaart, C., Pegoretti, V., Bendridi, N., Rieusset, J., Schmidt, M., Culmsee, C., & Dolga, A. M. (2018, 2018/05/22). SK channel

activation is neuroprotective in conditions of enhanced ER–mitochondrial coupling. *Cell Death & Disease, 9*(6), 593. https://doi.org/10.1038/s41419-018-0590-1

Hougaard, C., Eriksen, B. L., Jørgensen, S., Johansen, T. H., Dyhring, T., Madsen, L. S., Strøbæk, D., & Christophersen, P. (2007). Selective positive modulation of the SK3 and SK2 subtypes of small conductance Ca2+-activated K+ channels. *British Journal of Pharmacology, 151*(5), 655-665. https://doi.org/10.1038/sj.bjp.0707281

Hounsgaard, J., Hultborn, H., Jespersen, B., & Kiehn, O. (1988, Nov). Bistability of alpha-motoneurones in the decerebrate cat and in the acute spinal cat after intravenous 5-hydroxytryptophan. *J Physiol, 405*, 345-367. https://doi.org/10.1113/jphysiol.1988.sp017336

Hounsgaard, J., & Kiehn, O. (1993, Aug). Calcium spikes and calcium plateaux evoked by differential polarization in dendrites of turtle motoneurones in vitro. *J Physiol, 468*, 245-259. https://doi.org/10.1113/jphysiol.1993.sp019769

Hübers, A., Just, W., Rosenbohm, A., Müller, K., Marroquin, N., Goebel, I., Högel, J., Thiele, H., Altmüller, J., Nürnberg, P., Weishaupt, J. H., Kubisch, C., Ludolph, A. C., & Volk, A. E. (2015, Nov). De novo FUS mutations are the most frequent genetic cause in early-onset German ALS patients. *Neurobiol Aging, 36*(11), 3117.e3111-3117.e3116. https://doi.org/10.1016/j.neurobiolaging.2015.08.005

Hugues, M., Schmid, H., & Lazdunski, M. (1982, Aug 31). Identification of a protein component of the Ca2+-dependent K+ channel by affinity labelling with apamin. *Biochem Biophys Res Commun, 107*(4), 1577-1582. https://doi.org/10.1016/s0006-291x(82)80180-0

Huh, S., Heckman, C. J., & Manuel, M. (2021, Feb 25). Time course of alterations in adult spinal motoneuron properties in the SOD1(G93A) mouse model of ALS. *eNeuro*. https://doi.org/10.1523/eneuro.0378-20.2021

Husch, A., Cramer, N., & Harris-Warrick, R. M. (2011, Nov). Long-duration perforated patch recordings from spinal interneurons of adult mice. *J Neurophysiol, 106*(5), 2783-2789. https://doi.org/10.1152/jn.00673.2011

Ikeda, A., Shibasaki, H., Kaji, R., Terada, K., Nagamine, T., Honda, M., Hamano, T., & Kimura, J. (1996, Nov). Abnormal sensorimotor integration in writer's cramp: study of contingent negative variation. *Mov Disord, 11*(6), 683-690. https://doi.org/10.1002/mds.870110614

Ince, P., Stout, N., Shaw, P., Slade, J., Hunziker, W., Heizmann, C. W., & Baimbridge, K. G. (1993, Aug). Parvalbumin and calbindin D-28k in the human motor system

and in motor neuron disease. *Neuropathol Appl Neurobiol, 19*(4), 291-299. https://doi.org/10.1111/j.1365-2990.1993.tb00443.x

Ingre, C., Roos, P. M., Piehl, F., Kamel, F., & Fang, F. (2015). Risk factors for amyotrophic lateral sclerosis. *Clin Epidemiol, 7*, 181-193. https://doi.org/10.2147/clep.S37505

Ishii, T. M., Maylie, J., & Adelman, J. P. (1997, Sep 12). Determinants of apamin and d-tubocurarine block in SK potassium channels. *J Biol Chem, 272*(37), 23195-23200. https://doi.org/10.1074/jbc.272.37.23195

Iwasaki, S., Chihara, Y., Komuta, Y., Ito, K., & Sahara, Y. (2008, Oct). Low-voltage-activated potassium channels underlie the regulation of intrinsic firing properties of rat vestibular ganglion cells. *J Neurophysiol, 100*(4), 2192-2204. https://doi.org/10.1152/jn.01240.2007

Jacobs, B. L., & Fornal, C. A. (1993, Sep). 5-HT and motor control: a hypothesis. *Trends Neurosci, 16*(9), 346-352. https://doi.org/10.1016/0166-2236(93)90090-9

Jaiswal, M. K. (2019, Mar). Riluzole and edaravone: A tale of two amyotrophic lateral sclerosis drugs. *Med Res Rev, 39*(2), 733-748. https://doi.org/10.1002/med.21528

Jensen, D. B., Kadlecova, M., Allodi, I., & Meehan, C. F. (2020, Jul 27). Spinal motoneurones are intrinsically more responsive in the adult G93A SOD1 mouse model of amyotrophic lateral sclerosis. *J Physiol*. https://doi.org/10.1113/jp280097

Jiang, M., Schuster, J. E., Fu, R., Siddique, T., & Heckman, C. J. (2009, Dec 2). Progressive changes in synaptic inputs to motoneurons in adult sacral spinal cord of a mouse model of amyotrophic lateral sclerosis. *J Neurosci, 29*(48), 15031-15038. https://doi.org/10.1523/JNEUROSCI.0574-09.2009

Jiang, M. C., Adimula, A., Birch, D., & Heckman, C. J. (2017, Oct 24). Hyperexcitability in synaptic and firing activities of spinal motoneurons in an adult mouse model of amyotrophic lateral sclerosis. *Neuroscience, 362*, 33-46. https://doi.org/10.1016/j.neuroscience.2017.08.041

Jiang, M. C., Elbasiouny, S. M., Collins, W. F., 3rd, & Heckman, C. J. (2015, Sep). The transformation of synaptic to system plasticity in motor output from the sacral cord of the adult mouse. *J Neurophysiol, 114*(3), 1987-2004. https://doi.org/10.1152/jn.00337.2015

Katz, J. S., Dimachkie, M. M., & Barohn, R. J. (2015, Nov). Amyotrophic Lateral Sclerosis: A Historical Perspective. *Neurol Clin, 33*(4), 727-734. https://doi.org/10.1016/j.ncl.2015.07.013

Khanna, R., Roy, L., Zhu, X., & Schlichter, L. C. (2001, Apr). K+ channels and the microglial respiratory burst. *Am J Physiol Cell Physiol, 280*(4), C796-806. https://doi.org/10.1152/ajpcell.2001.280.4.C796

Khorkova, O., & Golowasch, J. (2007, Aug 8). Neuromodulators, not activity, control coordinated expression of ionic currents. *J Neurosci, 27*(32), 8709-8718. https://doi.org/10.1523/jneurosci.1274-07.2007

Kim, L. H., Sharma, S., Sharples, S. A., Mayr, K. A., Kwok, C. H. T., & Whelan, P. J. (2017). Integration of Descending Command Systems for the Generation of Context-Specific Locomotor Behaviors. *Front Neurosci, 11*, 581. https://doi.org/10.3389/fnins.2017.00581

King, A. E., Woodhouse, A., Kirkcaldie, M. T., & Vickers, J. C. (2016, Jan). Excitotoxicity in ALS: Overstimulation, or overreaction? *Exp Neurol, 275 Pt 1*, 162-171. https://doi.org/10.1016/j.expneurol.2015.09.019

Koch, C. (2004). *Biophysics of Computation: Information Processing in Single Neurons*. Oxford University Press. https://books.google.com/books?id=aeAJCAAAQBAJ

Köhler, M., Hirschberg, B., Bond, C. T., Kinzie, J. M., Marrion, N. V., Maylie, J., & Adelman, J. P. (1996, Sep 20). Small-conductance, calcium-activated potassium channels from mammalian brain. *Science, 273*(5282), 1709-1714. https://doi.org/10.1126/science.273.5282.1709

Kuo, J. J., Schonewille, M., Siddique, T., Schults, A. N., Fu, R., Bär, P. R., Anelli, R., Heckman, C. J., & Kroese, A. B. (2004, Jan). Hyperexcitability of cultured spinal motoneurons from presymptomatic ALS mice. *J Neurophysiol, 91*(1), 571-575. https://doi.org/10.1152/jn.00665.2003

Kuo, J. J., Siddique, T., Fu, R., & Heckman, C. J. (2005, Mar 15). Increased persistent Na(+) current and its effect on excitability in motoneurones cultured from mutant SOD1 mice. *J Physiol, 563*(Pt 3), 843-854. https://doi.org/10.1113/jphysiol.2004.074138

Kurtzke, J. F. (1982). Epidemiology of amyotrophic lateral sclerosis. *Adv Neurol, 36*, 281-302.

Kwak, S., Hideyama, T., Yamashita, T., & Aizawa, H. (2010, Apr). AMPA receptor-mediated neuronal death in sporadic ALS. *Neuropathology, 30*(2), 182-188. https://doi.org/10.1111/j.1440-1789.2009.01090.x

Kwiatkowski, T. J., Jr., Bosco, D. A., Leclerc, A. L., Tamrazian, E., Vanderburg, C. R., Russ, C., Davis, A., Gilchrist, J., Kasarskis, E. J., Munsat, T., Valdmanis, P., Rouleau, G. A., Hosler, B. A., Cortelli, P., de Jong, P. J., Yoshinaga, Y., Haines, J. L., Pericak-Vance, M. A., Yan, J., Ticozzi, N., Siddique, T., McKenna-Yasek,

D., Sapp, P. C., Horvitz, H. R., Landers, J. E., & Brown, R. H., Jr. (2009, Feb 27). Mutations in the FUS/TLS gene on chromosome 16 cause familial amyotrophic lateral sclerosis. *Science, 323*(5918), 1205-1208. https://doi.org/10.1126/science.1166066

Lacomblez, L., Bensimon, G., Leigh, P. N., Guillet, P., & Meininger, V. (1996, May 25). Dose-ranging study of riluzole in amyotrophic lateral sclerosis. Amyotrophic Lateral Sclerosis/Riluzole Study Group II. *Lancet, 347*(9013), 1425-1431. https://doi.org/10.1016/s0140-6736(96)91680-3

Lanuza, G. M., Gosgnach, S., Pierani, A., Jessell, T. M., & Goulding, M. (2004, May 13). Genetic identification of spinal interneurons that coordinate left-right locomotor activity necessary for walking movements. *Neuron, 42*(3), 375-386. https://doi.org/10.1016/s0896-6273(04)00249-1

Lattante, S., Rouleau, G. A., & Kabashi, E. (2013, Jun). TARDBP and FUS mutations associated with amyotrophic lateral sclerosis: summary and update. *Hum Mutat, 34*(6), 812-826. https://doi.org/10.1002/humu.22319

Lee, R. H., & Heckman, C. J. (1998, Aug). Bistability in spinal motoneurons in vivo: systematic variations in persistent inward currents. *J Neurophysiol, 80*(2), 583-593. https://doi.org/10.1152/jn.1998.80.2.583

Lee, R. H., & Heckman, C. J. (1999, Nov). Paradoxical effect of QX-314 on persistent inward currents and bistable behavior in spinal motoneurons in vivo. *J Neurophysiol, 82*(5), 2518-2527. https://doi.org/10.1152/jn.1999.82.5.2518

Leroy, F., Lamotte d'Incamps, B., Imhoff-Manuel, R. D., & Zytnicki, D. (2014, Oct 14). Early intrinsic hyperexcitability does not contribute to motoneuron degeneration in amyotrophic lateral sclerosis. *Elife, 3*. https://doi.org/10.7554/eLife.04046

Lewis, G. N., & Byblow, W. D. (2002). Altered sensorimotor integration in Parkinson's disease. *Brain, 125*(9), 2089-2099. https://doi.org/10.1093/brain/awf200

Li, X., & Bennett, D. J. (2007, May). Apamin-sensitive calcium-activated potassium currents (SK) are activated by persistent calcium currents in rat motoneurons. *J Neurophysiol, 97*(5), 3314-3330. https://doi.org/10.1152/jn.01068.2006

Li, Y., Gorassini, M. A., & Bennett, D. J. (2004, Feb). Role of persistent sodium and calcium currents in motoneuron firing and spasticity in chronic spinal rats. *J Neurophysiol, 91*(2), 767-783. https://doi.org/10.1152/jn.00788.2003

Liang, H., Bácskai, T., Watson, C., & Paxinos, G. (2014, May). Projections from the lateral vestibular nucleus to the spinal cord in the mouse. *Brain Struct Funct, 219*(3), 805-815. https://doi.org/10.1007/s00429-013-0536-4

Liang, H., Watson, C., & Paxinos, G. (2015, Jan 1). Projections from the oral pontine reticular nucleus to the spinal cord of the mouse. *Neurosci Lett, 584*, 113-118. https://doi.org/10.1016/j.neulet.2014.10.025

Liang, H., Watson, C., & Paxinos, G. (2016, Apr). Terminations of reticulospinal fibers originating from the gigantocellular reticular formation in the mouse spinal cord. *Brain Struct Funct, 221*(3), 1623-1633. https://doi.org/10.1007/s00429-015-0993-z

Lin, M. T., Luján, R., Watanabe, M., Adelman, J. P., & Maylie, J. (2008, Feb). SK2 channel plasticity contributes to LTP at Schaffer collateral-CA1 synapses. *Nat Neurosci, 11*(2), 170-177. https://doi.org/10.1038/nn2041

Logroscino, G., Traynor, B. J., Hardiman, O., Chio, A., Couratier, P., Mitchell, J. D., Swingler, R. J., & Beghi, E. (2008, Jan). Descriptive epidemiology of amyotrophic lateral sclerosis: new evidence and unsolved issues. *J Neurol Neurosurg Psychiatry, 79*(1), 6-11. https://doi.org/10.1136/jnnp.2006.104828

Logroscino, G., Traynor, B. J., Hardiman, O., Chiò, A., Mitchell, D., Swingler, R. J., Millul, A., Benn, E., & Beghi, E. (2010, Apr). Incidence of amyotrophic lateral sclerosis in Europe. *J Neurol Neurosurg Psychiatry, 81*(4), 385-390. https://doi.org/10.1136/jnnp.2009.183525

Longinetti, E., & Fang, F. (2019, Oct). Epidemiology of amyotrophic lateral sclerosis: an update of recent literature. *Curr Opin Neurol, 32*(5), 771-776. https://doi.org/10.1097/wco.0000000000000730

Luján, R., Maylie, J., & Adelman, J. P. (2009, Jul). New sites of action for GIRK and SK channels. *Nat Rev Neurosci, 10*(7), 475-480. https://doi.org/10.1038/nrn2668

Madison, D. V., & Nicoll, R. A. (1982, Oct 14). Noradrenaline blocks accommodation of pyramidal cell discharge in the hippocampus. *Nature, 299*(5884), 636-638. https://doi.org/10.1038/299636a0

Magee, J. C. (2000, Dec). Dendritic integration of excitatory synaptic input. *Nat Rev Neurosci, 1*(3), 181-190. https://doi.org/10.1038/35044552

Mahrous, A. A., Mousa, M. H., & Elbasiouny, S. M. (2019). The Mechanistic Basis for Successful Spinal Cord Stimulation to Generate Steady Motor Outputs. *Front Cell Neurosci, 13*, 359. https://doi.org/10.3389/fncel.2019.00359

Mancuso, R., Martínez-Muriana, A., Leiva, T., Gregorio, D., Ariza, L., Morell, M., Esteban-Pérez, J., García-Redondo, A., Calvo, A. C., Atencia-Cibreiro, G., Corfas, G., Osta, R., Bosch, A., & Navarro, X. (2016, Nov). Neuregulin-1 promotes functional improvement by enhancing collateral sprouting in

SOD1(G93A) ALS mice and after partial muscle denervation. *Neurobiol Dis, 95*, 168-178. https://doi.org/10.1016/j.nbd.2016.07.023

Manuel, M. (2021, Jan-Feb). Suboptimal Discontinuous Current-Clamp Switching Rates Lead to Deceptive Mouse Neuronal Firing. *eNeuro, 8*(1). https://doi.org/10.1523/eneuro.0461-20.2020

Manuel, M., Meunier, C., Donnet, M., & Zytnicki, D. (2006, Nov 1). The afterhyperpolarization conductance exerts the same control over the gain and variability of motoneurone firing in anaesthetized cats. *J Physiol, 576*(Pt 3), 873-886. https://doi.org/10.1113/jphysiol.2006.117002

Marchand-Pauvert, V., Peyre, I., Lackmy-Vallee, A., Querin, G., Bede, P., Lacomblez, L., Debs, R., & Pradat, P.-F. (2019). Absence of hyperexcitability of spinal motoneurons in patients with amyotrophic lateral sclerosis. *The Journal of Physiology, 597*(22), 5445-5467. https://doi.org/https://doi.org/10.1113/JP278117

Martin, E., Cazenave, W., Cattaert, D., & Branchereau, P. (2013, Jun). Embryonic alteration of motoneuronal morphology induces hyperexcitability in the mouse model of amyotrophic lateral sclerosis. *Neurobiol Dis, 54*, 116-126. https://doi.org/10.1016/j.nbd.2013.02.011

Martin, L. J., & Chang, Q. (2012, Feb). Inhibitory synaptic regulation of motoneurons: a new target of disease mechanisms in amyotrophic lateral sclerosis. *Mol Neurobiol, 45*(1), 30-42. https://doi.org/10.1007/s12035-011-8217-x

Martínez-Silva, M. L., Imhoff-Manuel, R. D., Sharma, A., Heckman, C. J., Shneider, N. A., Roselli, F., Zytnicki, D., & Manuel, M. (2018, Mar 27). Hypoexcitability precedes denervation in the large fast-contracting motor units in two unrelated mouse models of ALS. *Elife, 7*. https://doi.org/10.7554/eLife.30955

McGown, A., McDearmid, J. R., Panagiotaki, N., Tong, H., Al Mashhadi, S., Redhead, N., Lyon, A. N., Beattie, C. E., Shaw, P. J., & Ramesh, T. M. (2013, Feb). Early interneuron dysfunction in ALS: insights from a mutant sod1 zebrafish model. *Ann Neurol, 73*(2), 246-258. https://doi.org/10.1002/ana.23780

Meech, R. W. (1978). Calcium-dependent potassium activation in nervous tissues. *Annu Rev Biophys Bioeng, 7*, 1-18. https://doi.org/10.1146/annurev.bb.07.060178.000245

Mehta, P., Kaye, W., Raymond, J., Punjani, R., Larson, T., Cohen, J., Muravov, O., & Horton, K. (2018, Nov 23). Prevalence of Amyotrophic Lateral Sclerosis - United States, 2015. *MMWR Morb Mortal Wkly Rep, 67*(46), 1285-1289. https://doi.org/10.15585/mmwr.mm6746a1

Mejzini, R., Flynn, L. L., Pitout, I. L., Fletcher, S., Wilton, S. D., & Akkari, P. A. (2019). ALS Genetics, Mechanisms, and Therapeutics: Where Are We Now? *Front Neurosci, 13*, 1310. https://doi.org/10.3389/fnins.2019.01310

Miller, R. G., Mitchell, J. D., & Moore, D. H. (2012, Mar 14). Riluzole for amyotrophic lateral sclerosis (ALS)/motor neuron disease (MND). *Cochrane Database Syst Rev, 2012*(3), Cd001447. https://doi.org/10.1002/14651858.CD001447.pub3

Mitchell, C., & Lee, R. (2012). Dynamic Meta-Analysis as a Therapeutic Prediction Tool for Amyotrophic Lateral Sclerosis. In. https://doi.org/10.5772/32384

Mitchell, J. D., Callagher, P., Gardham, J., Mitchell, C., Dixon, M., Addison-Jones, R., Bennett, W., & O'Brien, M. R. (2010, Dec). Timelines in the diagnostic evaluation of people with suspected amyotrophic lateral sclerosis (ALS)/motor neuron disease (MND)--a 20-year review: can we do better? *Amyotroph Lateral Scler, 11*(6), 537-541. https://doi.org/10.3109/17482968.2010.495158

Mitsumoto, H., Brooks, B. R., & Silani, V. (2014, Nov). Clinical trials in amyotrophic lateral sclerosis: why so many negative trials and how can trials be improved? *Lancet Neurol, 13*(11), 1127-1138. https://doi.org/10.1016/s1474-4422(14)70129-2

Morgan, S., & Orrell, R. W. (2016, Sep). Pathogenesis of amyotrophic lateral sclerosis. *Br Med Bull, 119*(1), 87-98. https://doi.org/10.1093/bmb/ldw026

Murphy, M. M. (2020). *Investigating the Effects of CyPPA on Small-Conductance Calcium-Activated Potassium Channels in SOD1G93A Transgenic Mouse Model* Wright State University]. http://rave.ohiolink.edu/etdc/view?acc_num=wright1589929963490428

Nanou, E., Alpert, M. H., Alford, S., & El Manira, A. (2013, Jun). Differential regulation of synaptic transmission by pre- and postsynaptic SK channels in the spinal locomotor network. *J Neurophysiol, 109*(12), 3051-3059. https://doi.org/10.1152/jn.00067.2013

Naujock, M., Stanslowsky, N., Bufler, S., Naumann, M., Reinhardt, P., Sterneckert, J., Kefalakes, E., Kassebaum, C., Bursch, F., Lojewski, X., Storch, A., Frickenhaus, M., Boeckers, T. M., Putz, S., Demestre, M., Liebau, S., Klingenstein, M., Ludolph, A. C., Dengler, R., Kim, K. S., Hermann, A., Wegner, F., & Petri, S. (2016, Jun). 4-Aminopyridine Induced Activity Rescues Hypoexcitable Motor Neurons from Amyotrophic Lateral Sclerosis Patient-Derived Induced Pluripotent Stem Cells. *Stem Cells, 34*(6), 1563-1575. https://doi.org/10.1002/stem.2354

Neumann, M., Sampathu, D. M., Kwong, L. K., Truax, A. C., Micsenyi, M. C., Chou, T. T., Bruce, J., Schuck, T., Grossman, M., Clark, C. M., McCluskey, L. F., Miller,

B. L., Masliah, E., Mackenzie, I. R., Feldman, H., Feiden, W., Kretzschmar, H. A., Trojanowski, J. Q., & Lee, V. M. (2006, Oct 6). Ubiquitinated TDP-43 in frontotemporal lobar degeneration and amyotrophic lateral sclerosis. *Science, 314*(5796), 130-133. https://doi.org/10.1126/science.1134108

Ngo-Anh, T. J., Bloodgood, B. L., Lin, M., Sabatini, B. L., Maylie, J., & Adelman, J. P. (2005, May). SK channels and NMDA receptors form a Ca2+-mediated feedback loop in dendritic spines. *Nat Neurosci, 8*(5), 642-649. https://doi.org/10.1038/nn1449

Nielsen, J. B. (2004, May). Sensorimotor integration at spinal level as a basis for muscle coordination during voluntary movement in humans. *J Appl Physiol (1985), 96*(5), 1961-1967. https://doi.org/10.1152/japplphysiol.01073.2003

Noh, T. K., Bang, S. H., Lee, Y. J., Cho, H. I., Jung, M. Y., Kim, I., Leem, C. H., & Chang, S. E. (2019, Feb 25). The ion channel activator CyPPA inhibits melanogenesis via the GSK3β/β-catenin pathway. *Chem Biol Interact, 300*, 1-7. https://doi.org/10.1016/j.cbi.2018.12.014

Norris, F., Shepherd, R., Denys, E., U, K., Mukai, E., Elias, L., Holden, D., & Norris, H. (1993, Aug). Onset, natural history and outcome in idiopathic adult motor neuron disease. *J Neurol Sci, 118*(1), 48-55. https://doi.org/10.1016/0022-510x(93)90245-t

Paganoni, S., Macklin, E. A., Lee, A., Murphy, A., Chang, J., Zipf, A., Cudkowicz, M., & Atassi, N. (2014, Sep). Diagnostic timelines and delays in diagnosing amyotrophic lateral sclerosis (ALS). *Amyotroph Lateral Scler Frontotemporal Degener, 15*(5-6), 453-456. https://doi.org/10.3109/21678421.2014.903974

PARALS. (2001, Jan 23). Incidence of ALS in Italy: evidence for a uniform frequency in Western countries. *Neurology, 56*(2), 239-244. https://doi.org/10.1212/wnl.56.2.239

Petrov, D., Mansfield, C., Moussy, A., & Hermine, O. (2017). ALS Clinical Trials Review: 20 Years of Failure. Are We Any Closer to Registering a New Treatment? *Front Aging Neurosci, 9*, 68. https://doi.org/10.3389/fnagi.2017.00068

Pieri, M., Albo, F., Gaetti, C., Spalloni, A., Bengtson, C. P., Longone, P., Cavalcanti, S., & Zona, C. (2003, Nov 20). Altered excitability of motor neurons in a transgenic mouse model of familial amyotrophic lateral sclerosis. *Neurosci Lett, 351*(3), 153-156. https://doi.org/10.1016/j.neulet.2003.07.010

Pieri, M., Caioli, S., Canu, N., Mercuri, N. B., Guatteo, E., & Zona, C. (2013, Sep). Over-expression of N-type calcium channels in cortical neurons from a mouse model of

Amyotrophic Lateral Sclerosis. *Exp Neurol, 247*, 349-358. https://doi.org/10.1016/j.expneurol.2012.11.002

Pineda, R. H., Knoeckel, C. S., Taylor, A. D., Estrada-Bernal, A., & Ribera, A. B. (2008, Oct). Kv1 potassium channel complexes in vivo require Kvbeta2 subunits in dorsal spinal neurons. *J Neurophysiol, 100*(4), 2125-2136. https://doi.org/10.1152/jn.90667.2008

Powers, R. K., & Binder, M. D. (2001). Input-output functions of mammalian motoneurons. *Rev Physiol Biochem Pharmacol, 143*, 137-263. https://doi.org/10.1007/BFb0115594

Primot, A., Mogha, A., Corre, S., Roberts, K., Debbache, J., Adamski, H., Dreno, B., Khammari, A., Lesimple, T., Mereau, A., Goding, C. R., & Galibert, M.-D. (2010). ERK-regulated differential expression of the Mitf 6a/b splicing isoforms in melanoma. *Pigment Cell & Melanoma Research, 23*(1), 93-102. https://doi.org/10.1111/j.1755-148X.2009.00652.x

Pun, S., Santos, A. F., Saxena, S., Xu, L., & Caroni, P. (2006, Mar). Selective vulnerability and pruning of phasic motoneuron axons in motoneuron disease alleviated by CNTF. *Nat Neurosci, 9*(3), 408-419. https://doi.org/10.1038/nn1653

Quinlan, K. A., Schuster, J. E., Fu, R., Siddique, T., & Heckman, C. J. (2011, May 1). Altered postnatal maturation of electrical properties in spinal motoneurons in a mouse model of amyotrophic lateral sclerosis. *J Physiol, 589*(Pt 9), 2245-2260. https://doi.org/10.1113/jphysiol.2010.200659

Quinn, L., Reilmann, R., Marder, K., & Gordon, A. M. (2001, May). Altered movement trajectories and force control during object transport in Huntington's disease. *Mov Disord, 16*(3), 469-480. https://doi.org/10.1002/mds.1108

Rall, W. (1969, Dec). Time constants and electrotonic length of membrane cylinders and neurons. *Biophys J, 9*(12), 1483-1508. https://doi.org/10.1016/s0006-3495(69)86467-2

Ransom, B. R., Barker, J. L., & Nelson, P. G. (1975, Jul 31). Two mechanisms for poststimulus hyperpolarisations in cultured mammalian neurones. *Nature, 256*(5516), 424-425. https://doi.org/10.1038/256424a0

Regehr, W. G. (2012, Jul 1). Short-term presynaptic plasticity. *Cold Spring Harb Perspect Biol, 4*(7), a005702. https://doi.org/10.1101/cshperspect.a005702

Rekling, J. C., Funk, G. D., Bayliss, D. A., Dong, X. W., & Feldman, J. L. (2000, Apr). Synaptic control of motoneuronal excitability. *Physiol Rev, 80*(2), 767-852. https://doi.org/10.1152/physrev.2000.80.2.767

Renton, A. E., Majounie, E., Waite, A., Simón-Sánchez, J., Rollinson, S., Gibbs, J. R., Schymick, J. C., Laaksovirta, H., van Swieten, J. C., Myllykangas, L., Kalimo, H., Paetau, A., Abramzon, Y., Remes, A. M., Kaganovich, A., Scholz, S. W., Duckworth, J., Ding, J., Harmer, D. W., Hernandez, D. G., Johnson, J. O., Mok, K., Ryten, M., Trabzuni, D., Guerreiro, R. J., Orrell, R. W., Neal, J., Murray, A., Pearson, J., Jansen, I. E., Sondervan, D., Seelaar, H., Blake, D., Young, K., Halliwell, N., Callister, J. B., Toulson, G., Richardson, A., Gerhard, A., Snowden, J., Mann, D., Neary, D., Nalls, M. A., Peuralinna, T., Jansson, L., Isoviita, V. M., Kaivorinne, A. L., Hölttä-Vuori, M., Ikonen, E., Sulkava, R., Benatar, M., Wuu, J., Chiò, A., Restagno, G., Borghero, G., Sabatelli, M., Heckerman, D., Rogaeva, E., Zinman, L., Rothstein, J. D., Sendtner, M., Drepper, C., Eichler, E. E., Alkan, C., Abdullaev, Z., Pack, S. D., Dutra, A., Pak, E., Hardy, J., Singleton, A., Williams, N. M., Heutink, P., Pickering-Brown, S., Morris, H. R., Tienari, P. J., & Traynor, B. J. (2011, Oct 20). A hexanucleotide repeat expansion in C9ORF72 is the cause of chromosome 9p21-linked ALS-FTD. *Neuron, 72*(2), 257-268. https://doi.org/10.1016/j.neuron.2011.09.010

Richter, M., Nickel, C., Apel, L., Kaas, A., Dodel, R., Culmsee, C., & Dolga, A. M. (2015, Feb). SK channel activation modulates mitochondrial respiration and attenuates neuronal HT-22 cell damage induced by H2O2. *Neurochem Int, 81*, 63-75. https://doi.org/10.1016/j.neuint.2014.12.007

Richter, M., Vidovic, N., Honrath, B., Mahavadi, P., Dodel, R., Dolga, A. M., & Culmsee, C. (2016, May). Activation of SK2 channels preserves ER Ca^{2+} homeostasis and protects against ER stress-induced cell death. *Cell Death Differ, 23*(5), 814-827. https://doi.org/10.1038/cdd.2015.146

Rickards, C., & Cody, F. W. (1997, Jun). Proprioceptive control of wrist movements in Parkinson's disease. Reduced muscle vibration-induced errors. *Brain, 120 (Pt 6)*, 977-990. https://doi.org/10.1093/brain/120.6.977

Riddle, C. N., Edgley, S. A., & Baker, S. N. (2009, Apr 15). Direct and indirect connections with upper limb motoneurons from the primate reticulospinal tract. *J Neurosci, 29*(15), 4993-4999. https://doi.org/10.1523/jneurosci.3720-08.2009

Rodríguez-Gómez, J. A., Kavanagh, E., Engskog-Vlachos, P., Engskog, M. K. R., Herrera, A. J., Espinosa-Oliva, A. M., Joseph, B., Hajji, N., Venero, J. L., & Burguillos, M. A. (2020, Jul 17). Microglia: Agents of the CNS Pro-Inflammatory Response. *Cells, 9*(7). https://doi.org/10.3390/cells9071717

Rossignol, S., Dubuc, R., & Gossard, J. P. (2006, Jan). Dynamic sensorimotor interactions in locomotion. *Physiol Rev, 86*(1), 89-154. https://doi.org/10.1152/physrev.00028.2005

Rothstein, J. D. (2017, Nov 2). Edaravone: A new drug approved for ALS. *Cell, 171*(4), 725. https://doi.org/10.1016/j.cell.2017.10.011

Rothstein, J. D., Jin, L., Dykes-Hoberg, M., & Kuncl, R. W. (1993, Jul 15). Chronic inhibition of glutamate uptake produces a model of slow neurotoxicity. *Proc Natl Acad Sci U S A, 90*(14), 6591-6595. https://doi.org/10.1073/pnas.90.14.6591

Rothstein, J. D., Martin, L. J., & Kuncl, R. W. (1992, May 28). Decreased glutamate transport by the brain and spinal cord in amyotrophic lateral sclerosis. *N Engl J Med, 326*(22), 1464-1468. https://doi.org/10.1056/nejm199205283262204

Rothstein, J. D., Tsai, G., Kuncl, R. W., Clawson, L., Cornblath, D. R., Drachman, D. B., Pestronk, A., Stauch, B. L., & Coyle, J. T. (1990, Jul). Abnormal excitatory amino acid metabolism in amyotrophic lateral sclerosis. *Ann Neurol, 28*(1), 18-25. https://doi.org/10.1002/ana.410280106

Rothstein, J. D., Van Kammen, M., Levey, A. I., Martin, L. J., & Kuncl, R. W. (1995, Jul). Selective loss of glial glutamate transporter GLT-1 in amyotrophic lateral sclerosis. *Ann Neurol, 38*(1), 73-84. https://doi.org/10.1002/ana.410380114

Rouleau, G. A., Clark, A. W., Rooke, K., Pramatarova, A., Krizus, A., Suchowersky, O., Julien, J. P., & Figlewicz, D. (1996, Jan). SOD1 mutation is associated with accumulation of neurofilaments in amyotrophic lateral sclerosis. *Ann Neurol, 39*(1), 128-131. https://doi.org/10.1002/ana.410390119

Rowland, L. P., & Shneider, N. A. (2001, May 31). Amyotrophic lateral sclerosis. *N Engl J Med, 344*(22), 1688-1700. https://doi.org/10.1056/nejm200105313442207

Saba, L., Viscomi, M. T., Caioli, S., Pignataro, A., Bisicchia, E., Pieri, M., Molinari, M., Ammassari-Teule, M., & Zona, C. (2015). Altered Functionality, Morphology, and Vesicular Glutamate Transporter Expression of Cortical Motor Neurons from a Presymptomatic Mouse Model of Amyotrophic Lateral Sclerosis. *Cerebral Cortex, 26*(4), 1512-1528. https://doi.org/10.1093/cercor/bhu317

Sah, P. (1996, Apr). Ca(2+)-activated K+ currents in neurones: types, physiological roles and modulation. *Trends Neurosci, 19*(4), 150-154. https://doi.org/10.1016/s0166-2236(96)80026-9

Sah, P., & McLachlan, E. M. (1992, Nov). Potassium currents contributing to action potential repolarization and the afterhyperpolarization in rat vagal motoneurons. *J Neurophysiol, 68*(5), 1834-1841. https://doi.org/10.1152/jn.1992.68.5.1834

Sangari, S., Giron, A., Marrelec, G., Pradat, P. F., & Marchand-Pauvert, V. (2018, Apr). Abnormal cortical brain integration of somatosensory afferents in ALS. *Clin Neurophysiol, 129*(4), 874-884. https://doi.org/10.1016/j.clinph.2017.12.008

Sawada, H. (2017, May). Clinical efficacy of edaravone for the treatment of amyotrophic lateral sclerosis. *Expert Opin Pharmacother, 18*(7), 735-738. https://doi.org/10.1080/14656566.2017.1319937

Saxena, S., Roselli, F., Singh, K., Leptien, K., Julien, J. P., Gros-Louis, F., & Caroni, P. (2013, Oct 2). Neuroprotection through excitability and mTOR required in ALS motoneurons to delay disease and extend survival. *Neuron, 80*(1), 80-96. https://doi.org/10.1016/j.neuron.2013.07.027

Schipper, L. J., Raaphorst, J., Aronica, E., Baas, F., de Haan, R., de Visser, M., & Troost, D. (2016, Oct). Prevalence of brain and spinal cord inclusions, including dipeptide repeat proteins, in patients with the C9ORF72 hexanucleotide repeat expansion: a systematic neuropathological review. *Neuropathol Appl Neurobiol, 42*(6), 547-560. https://doi.org/10.1111/nan.12284

Schlichter, L. C., Kaushal, V., Moxon-Emre, I., Sivagnanam, V., & Vincent, C. (2010, Jan 14). The Ca2+ activated SK3 channel is expressed in microglia in the rat striatum and contributes to microglia-mediated neurotoxicity in vitro. *J Neuroinflammation, 7*, 4. https://doi.org/10.1186/1742-2094-7-4

Schulz, D. J., Goaillard, J. M., & Marder, E. (2006, Mar). Variable channel expression in identified single and electrically coupled neurons in different animals. *Nat Neurosci, 9*(3), 356-362. https://doi.org/10.1038/nn1639

Schwarz, M., Fellows, S. J., Schaffrath, C., & Noth, J. (2001, Jan). Deficits in sensorimotor control during precise hand movements in Huntington's disease. *Clin Neurophysiol, 112*(1), 95-106. https://doi.org/10.1016/s1388-2457(00)00497-1

Schwindt, P. C., Spain, W. J., Foehring, R. C., Chubb, M. C., & Crill, W. E. (1988, Feb). Slow conductances in neurons from cat sensorimotor cortex in vitro and their role in slow excitability changes. *J Neurophysiol, 59*(2), 450-467. https://doi.org/10.1152/jn.1988.59.2.450

Serrien, D. J., Burgunder, J. M., & Wiesendanger, M. (2000, Sep). Disturbed sensorimotor processing during control of precision grip in patients with writer's cramp. *Mov Disord, 15*(5), 965-972. https://doi.org/10.1002/1531-8257(200009)15:5<965::aid-mds1030>3.0.co;2-0

Shah, M., & Haylett, D. G. (2000, Feb). The pharmacology of hSK1 Ca2+-activated K+ channels expressed in mammalian cell lines. *Br J Pharmacol, 129*(4), 627-630. https://doi.org/10.1038/sj.bjp.0703111

Shaw, P. J., & Ince, P. G. (1997, May). Glutamate, excitotoxicity and amyotrophic lateral sclerosis. *J Neurol, 244 Suppl 2*, S3-14. https://doi.org/10.1007/bf03160574

Shibata, N., Nagai, R., Uchida, K., Horiuchi, S., Yamada, S., Hirano, A., Kawaguchi, M., Yamamoto, T., Sasaki, S., & Kobayashi, M. (2001, Oct 26). Morphological evidence for lipid peroxidation and protein glycoxidation in spinal cords from sporadic amyotrophic lateral sclerosis patients. *Brain Res, 917*(1), 97-104. https://doi.org/10.1016/s0006-8993(01)02926-2

Shoenfeld, L., Westenbroek, R. E., Fisher, E., Quinlan, K. A., Tysseling, V. M., Powers, R. K., Heckman, C. J., & Binder, M. D. (2014, Aug 1). Soma size and Cav1.3 channel expression in vulnerable and resistant motoneuron populations of the SOD1G93A mouse model of ALS. *Physiol Rep, 2*(8). https://doi.org/10.14814/phy2.12113

Spalloni, A., Nutini, M., & Longone, P. (2013, Feb). Role of the N-methyl-d-aspartate receptors complex in amyotrophic lateral sclerosis. *Biochim Biophys Acta, 1832*(2), 312-322. https://doi.org/10.1016/j.bbadis.2012.11.013

Spruston, N. (2008, Mar). Pyramidal neurons: dendritic structure and synaptic integration. *Nat Rev Neurosci, 9*(3), 206-221. https://doi.org/10.1038/nrn2286

Stein, R. B., & Capaday, C. (1988, Jul). The modulation of human reflexes during functional motor tasks. *Trends Neurosci, 11*(7), 328-332. https://doi.org/10.1016/0166-2236(88)90097-5

Stowe, D. F., Gadicherla, A. K., Zhou, Y., Aldakkak, M., Cheng, Q., Kwok, W. M., Jiang, M. T., Heisner, J. S., Yang, M., & Camara, A. K. (2013, Feb). Protection against cardiac injury by small Ca(2+)-sensitive K(+) channels identified in guinea pig cardiac inner mitochondrial membrane. *Biochim Biophys Acta, 1828*(2), 427-442. https://doi.org/10.1016/j.bbamem.2012.08.031

Strøbaek, D., Jørgensen, T. D., Christophersen, P., Ahring, P. K., & Olesen, S. P. (2000, Mar). Pharmacological characterization of small-conductance Ca(2+)-activated K(+) channels stably expressed in HEK 293 cells. *Br J Pharmacol, 129*(5), 991-999. https://doi.org/10.1038/sj.bjp.0703120

Swash, M. (2018, Apr). Sensorimotor integration is problematic in amyotrophic lateral sclerosis. *Clin Neurophysiol, 129*(4), 849-850. https://doi.org/10.1016/j.clinph.2018.01.005

Swensen, A. M., & Bean, B. P. (2005, Apr 6). Robustness of burst firing in dissociated purkinje neurons with acute or long-term reductions in sodium conductance. *J Neurosci, 25*(14), 3509-3520. https://doi.org/10.1523/jneurosci.3929-04.2005

Talbot, K. (2009, Oct). Motor neuron disease: the bare essentials. *Pract Neurol, 9*(5), 303-309. https://doi.org/10.1136/jnnp.2009.188151

Talbot, K. (2014, Jan). Amyotrophic lateral sclerosis: cell vulnerability or system vulnerability? *J Anat, 224*(1), 45-51. https://doi.org/10.1111/joa.12107

Taylor, J. P., Brown, R. H., Jr., & Cleveland, D. W. (2016, Nov 10). Decoding ALS: from genes to mechanism. *Nature, 539*(7628), 197-206. https://doi.org/10.1038/nature20413

Tortarolo, M., Grignaschi, G., Calvaresi, N., Zennaro, E., Spaltro, G., Colovic, M., Fracasso, C., Guiso, G., Elger, B., Schneider, H., Seilheimer, B., Caccia, S., & Bendotti, C. (2006, Jan). Glutamate AMPA receptors change in motor neurons of SOD1G93A transgenic mice and their inhibition by a noncompetitive antagonist ameliorates the progression of amytrophic lateral sclerosis-like disease. *J Neurosci Res, 83*(1), 134-146. https://doi.org/10.1002/jnr.20715

Turrigiano, G., LeMasson, G., & Marder, E. (1995, May). Selective regulation of current densities underlies spontaneous changes in the activity of cultured neurons. *J Neurosci, 15*(5 Pt 1), 3640-3652. https://doi.org/10.1523/jneurosci.15-05-03640.1995

Van Den Bosch, L., Van Damme, P., Bogaert, E., & Robberecht, W. (2006, Nov-Dec). The role of excitotoxicity in the pathogenesis of amyotrophic lateral sclerosis. *Biochim Biophys Acta, 1762*(11-12), 1068-1082. https://doi.org/10.1016/j.bbadis.2006.05.002

Van Den Bosch, L., Vandenberghe, W., Klaassen, H., Van Houtte, E., & Robberecht, W. (2000, Nov 1). Ca(2+)-permeable AMPA receptors and selective vulnerability of motor neurons. *J Neurol Sci, 180*(1-2), 29-34. https://doi.org/10.1016/s0022-510x(00)00414-7

van Zundert, B., Peuscher, M. H., Hynynen, M., Chen, A., Neve, R. L., Brown, R. H., Jr., Constantine-Paton, M., & Bellingham, M. C. (2008, Oct 22). Neonatal neuronal circuitry shows hyperexcitable disturbance in a mouse model of the adult-onset neurodegenerative disease amyotrophic lateral sclerosis. *J Neurosci, 28*(43), 10864-10874. https://doi.org/10.1523/jneurosci.1340-08.2008

Vance, C., Rogelj, B., Hortobágyi, T., De Vos, K. J., Nishimura, A. L., Sreedharan, J., Hu, X., Smith, B., Ruddy, D., Wright, P., Ganesalingam, J., Williams, K. L., Tripathi, V., Al-Saraj, S., Al-Chalabi, A., Leigh, P. N., Blair, I. P., Nicholson, G., de Belleroche, J., Gallo, J. M., Miller, C. C., & Shaw, C. E. (2009, Feb 27). Mutations in FUS, an RNA processing protein, cause familial amyotrophic lateral sclerosis type 6. *Science, 323*(5918), 1208-1211. https://doi.org/10.1126/science.1165942

Veldink, J. H., Bär, P. R., Joosten, E. A., Otten, M., Wokke, J. H., & van den Berg, L. H. (2003, Nov). Sexual differences in onset of disease and response to exercise in a

transgenic model of ALS. *Neuromuscul Disord, 13*(9), 737-743. https://doi.org/10.1016/s0960-8966(03)00104-4

Viana, F., Bayliss, D. A., & Berger, A. J. (1993, Jun). Multiple potassium conductances and their role in action potential repolarization and repetitive firing behavior of neonatal rat hypoglossal motoneurons. *J Neurophysiol, 69*(6), 2150-2163. https://doi.org/10.1152/jn.1993.69.6.2150

Wikström, M. A., & El Manira, A. (1998, Apr). Calcium influx through N- and P/Q-type channels activate apamin-sensitive calcium-dependent potassium channels generating the late afterhyperpolarization in lamprey spinal neurons. *Eur J Neurosci, 10*(4), 1528-1532. https://doi.org/10.1046/j.1460-9568.1998.00194.x

Witham, C. L., Fisher, K. M., Edgley, S. A., & Baker, S. N. (2016, Mar 2). Corticospinal Inputs to Primate Motoneurons Innervating the Forelimb from Two Divisions of Primary Motor Cortex and Area 3a. *J Neurosci, 36*(9), 2605-2616. https://doi.org/10.1523/jneurosci.4055-15.2016

Wolpaw, J. R., & Tennissen, A. M. (2001). Activity-dependent spinal cord plasticity in health and disease. *Annu Rev Neurosci, 24*, 807-843. https://doi.org/10.1146/annurev.neuro.24.1.807

Wootz, H., Fitzsimons-Kantamneni, E., Larhammar, M., Rotterman, T. M., Enjin, A., Patra, K., André, E., Van Zundert, B., Kullander, K., & Alvarez, F. J. (2013, May 1). Alterations in the motor neuron-renshaw cell circuit in the Sod1(G93A) mouse model. *J Comp Neurol, 521*(7), 1449-1469. https://doi.org/10.1002/cne.23266

Yamashita, S., & Ando, Y. (2015). Genotype-phenotype relationship in hereditary amyotrophic lateral sclerosis. *Transl Neurodegener, 4*, 13. https://doi.org/10.1186/s40035-015-0036-y

Zarei, S., Carr, K., Reiley, L., Diaz, K., Guerra, O., Altamirano, P. F., Pagani, W., Lodin, D., Orozco, G., & Chinea, A. (2015). A comprehensive review of amyotrophic lateral sclerosis. *Surg Neurol Int, 6*, 171. https://doi.org/10.4103/2152-7806.169561

Zhang, L., & Krnjević, K. (1987, Feb 10). Apamin depresses selectively the after-hyperpolarization of cat spinal motoneurons. *Neurosci Lett, 74*(1), 58-62. https://doi.org/10.1016/0304-3940(87)90051-6

Zhang, L., & McBain, C. J. (1995, Nov 1). Potassium conductances underlying repolarization and after-hyperpolarization in rat CA1 hippocampal interneurones. *J Physiol, 488 (Pt 3)*(Pt 3), 661-672. https://doi.org/10.1113/jphysiol.1995.sp020998

Zhang, W., Fan, B., Agarwal, D., Li, T., & Yu, Y. (2019, 2019/01/01). Axonal sodium and potassium conductance density determines spiking dynamical properties of regular- and fast-spiking neurons. *Nonlinear Dynamics, 95*(2), 1035-1052. https://doi.org/10.1007/s11071-018-4613-3

Zou, Z. Y., Cui, L. Y., Sun, Q., Li, X. G., Liu, M. S., Xu, Y., Zhou, Y., & Yang, X. Z. (2013, Apr). De novo FUS gene mutations are associated with juvenile-onset sporadic amyotrophic lateral sclerosis in China. *Neurobiol Aging, 34*(4), 1312.e1311-1318. https://doi.org/10.1016/j.neurobiolaging.2012.09.005

Zou, Z. Y., Zhou, Z. R., Che, C. H., Liu, C. Y., He, R. L., & Huang, H. P. (2017, Jul). Genetic epidemiology of amyotrophic lateral sclerosis: a systematic review and meta-analysis. *J Neurol Neurosurg Psychiatry, 88*(7), 540-549. https://doi.org/10.1136/jnnp-2016-315018

Zucker, R. S., & Regehr, W. G. (2002). Short-term synaptic plasticity. *Annu Rev Physiol, 64*, 355-405. https://doi.org/10.1146/annurev.physiol.64.092501.114547